Coordination Chemistry Reviews, 95 (1989) 41–107
Elsevier Science Publishers B.V., Amsterdam – Printed in The Netherlands

EARLY–LATE HETEROBIMETALLICS

DOUGLAS W. STEPHAN

Department of Chemistry and Biochemistry, University of Windsor, Windsor, Ont. N9B 3P4 (Canada)

(Received 6 September 1988)

CONTENTS

1. INTRODUCTION

The past few years have witnessed an ever-increasing interest in the chemistry of compounds that contain two or more metal centers. A wide variety of transition metal cluster compounds have been studied because of the presumed analogy of their chemistry to that of heterogeneous catalyst surfaces. The possibility of new reactivity patterns has spawned interest in related heteronuclear clusters. The chemistry of such clusters has been reviewed [1–3]. In the late 1970s, a flurry of interest in homonuclear bimetallic transition metal complexes arose from their potential for applications in catalysis. In particular, the suggestion that two metal centers could act in a cooperative fashion to activate organic substrates seemed reasonable.

More recently, considerable interest has focused on the synthesis and chemistry of complexes containing widely divergent transition metal centers [4–6]. Among the reasons for interest in such species is the possibility that new reactivity patterns will emerge which are substantially different from those of bimetallic complexes containing identical or closely related metals.

0010-8545/89/$23.45

Early–late heterobimetallic (ELHB) complexes offer the potential of cooperative activation of small molecular substrates such as carbon monoxide. A situation might be envisioned in which the Lewis acidic, early, oxophilic, transition metal interacts with the oxygen terminus of a substrate molecule bound to a proximate late metal center. The resulting enhancement of activation, combined with the ability of late metal centers to bind and activate hydrogen, offers the potential for applications in homogeneous catalytic processes.

A second reason for interest in ELHB complexes arises from the observation of strong metal–support interactions (SMSI) seen in some heterogeneous catalytic systems [7]. In systems where electron-rich metals are dispersed on Lewis acidic supports, there is recent evidence of enhanced activity and/or selectivity. In particular, TiO_2 can greatly affect the chemisorption properties and activity of a supported metal catalyst, depending on the conditions under which the metal–titania composite is prepared. The support material may play a direct role in catalytic processes, although the nature of this role is not well understood. Proposed explanations for the observed effects involve the encapsulation of the late metal by the support or direct electronic communication between the constituent metals.

With these two reasons for interest in homogeneous organometallic ELHB complexes, some of the objectives that have been addressed to date include (1) the development of rational synthetic approaches for the preparation of complexes containing widely divergent transition metals, (2) the examination of metal–metal interactions in ELHB complexes and their relation to SMSI, and (3) the study of reactivity of ELHB systems related to postulated Fischer–Tropsch intermediates or to potential catalytic applications. This review describes the progress that has been achieved. The chemistry presented is limited by restricting the discussion to those organometallic ELHB compounds in which the early transition metal is one of titanium, zirconium, hafnium, vanadium, niobium or tantalum. Several references to ELHB species where thorium is the early metal are also relevant and will be included.

Within this restricted area, a wide variety of ELHB complexes is known. We have segregated the discussion according to the type of ligands linking the disparate metal centers. These include carbonyl, carbon, hydrido, halide, amido and phosphido, selenolato and thiolato and chalcogenide-atom bridged complexes, as well as distal and metal–metal-bonded species. Each of these classes of ELHB complexes will be described and their relation to the major objectives will be discussed. Complexes of each class are tabulated at the end of the relevant section.

Other investigations of ELHB compounds have been concerned with complex heteropolyanions [8–18], their organometallic derivatives [19–29], extended solid state polymers [30–35], and model compounds relevant to biological systems [36–43]. Such species are not relevant to the above objectives and thus discussion of such ELHB species is not included.

2. CARBONYL-BRIDGED ELHB COMPLEXES

The activation of CO continues to be a motivating force in studies of ELHB complexes. To this end, a number of groups have studied the reaction of late metal carbonyl species with early metal complexes. In 1976, Schmid et al. [44] described the reaction of $Co_2(CO)_8$ and Cp_2TiCl_2 ($Cp = C_5H_5$). The product, $Cp_2(Cl)Ti(\mu\text{-}OC)Co_3(CO)_9$ **2.8**, was crystallographically characterized (Fig. 1). The lengthening of the μ-CO distance to 1.22 Å was expected as a result of the interaction with the Lewis acidic titanium center. The related complexes $(C_5H_4Me_3)_2(CO)M(\mu\text{-}OC)Co_3(CO)_9$ (M = Nb **2.40**, Ta **2.42**) [45] and $(C_5H_4R)_2V(\mu\text{-}OC)Co_3(CO)_9$ ($R = CMe_3$ **2.35**, CO_2Me **2.36**) [46] have also been prepared in similar reactions of $(C_5H_4Me)MH_3$ (M = Ta, Nb) and $(C_5H_4R)_2V$ respectively with excess $Co_2(CO)_8$.

Stoichiometric reactions of $[OCCo_3(CO)_9]^-$ with Cp_2MCl_2 led to high yields and a generalized synthetic route to products of the form $Cp_2(Cl)M(\mu\text{-}OC)Co_3(CO)_9$ (M = Ti **2.8**, Zr **2.27**, Hf **2.32**) and $Cp_2M(\mu\text{-}OC)Co_3(CO)_9)_2$ (M = Ti **2.9**, Zr **2.28**, Hf **2.33**) [47]. Structural studies of **2.27**, **2.28**, **2.32** and **2.33** confirmed that binding of the carbonyl to the early metal is through the oxygen atom. Reactions of **2.8**, **2.27** or **2.32** with NaOH resulted in the formation of the oxo-bridged species $O(Cp_2M((\mu\text{-}OC)Co_3(CO)_9)_2)_2$ (M = Ti **2.10**, Zr **2.29**, Hf **2.34**).

A related reaction of $CpTiCl_3$ with $Na[Co(CO)_4]$ led to the unique species $CpTi((\mu\text{-}OC)Co_3(CO)_9)_2(Co(CO)_4)$ **2.11** [48]. Structural characterization of this species confirmed that $OCCo_3(CO)_9$ groups are bound to titanium through the triply bridging CO oxygen atom. In addition, a $Co(CO)_4$ moiety is bound through a direct Ti–Co bond (2.614 Å).

Recently, Gambarotta et al. [49] have isolated and structurally characterized the product of the reaction of $CpCo(C_2H_4)_2$ and $Cp_2Ti(CO)_2$ (eqn. (1)):

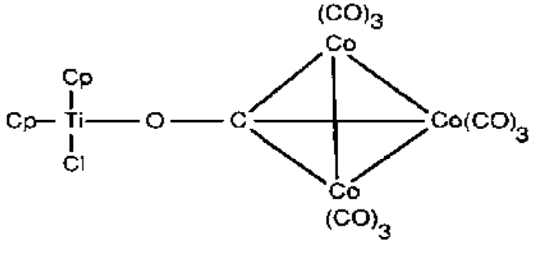

Fig. 1. Structure of **2.8**.

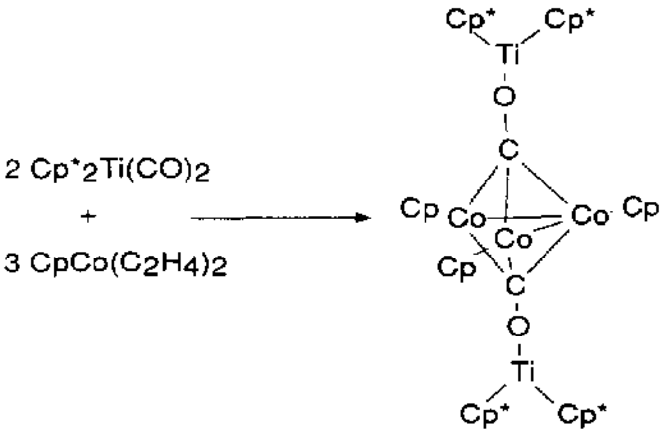

(1)

The Ti(II) species acts as a one-electron reductant and thus the product $(Cp_2Ti)_2(\mu\text{-}OC)_2Co_3Cp_3$ **2.12** results. The magnetic moment of this species reflects the presence of two uncoupled Ti(III) centers. The carbonyl stretching frequency (1300 cm^{-1}) and CO bond distance (1.30(1) Å) are consistent with reduction of the CO bond order.

Carbonyl-bridged complexes containing niobium have been prepared by reaction of a niobium hydride species with a metal carbonyl. For example, reactions of Cp_2NbH_3 with $Co_2(CO)_8$ or $Mn_2(CO)_{10}$ led to the formation of the ELHB species $Cp_2(CO)Nb(\mu\text{-}OC)Co(CO)_3$ **2.41** [50] and $Cp_2(CO)Nb(\mu\text{-}OC)Mn(CO)_4$ **2.39** [51] respectively. In addition to the metal–metal bonds, these complexes contain semibridging carbonyls (Fig. 2). Both the IR and structural data indicate that these bridging carbonyl moieties are not as significantly activated as the isocarbonyls seen in previously described systems.

The reaction of Cp_2NbBH_4 with $CpM(CO)_3Me$ led to the formation of the species $Cp_2Nb(\mu\text{-}CO)_2M(CO)Cp$ (M = Mo **2.37**, W **2.38**) (Fig. 3) [52]. In

Fig. 2. ORTEP drawing of **2.41**, Reproduced with permission from ref. 50. Copyright 1979 American Chemical Society.

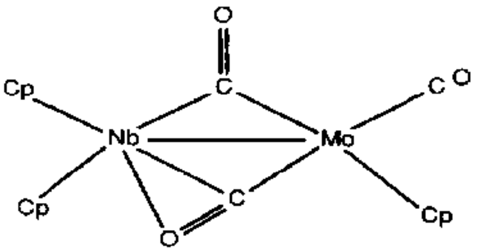

Fig. 3. Structure of **2.37**.

contrast to **2.39** and **2.41**, these complexes contain both a semibridging and an η^1,η^2-CO. In the structural study of **2.37**, π bonding of the latter carbonyl to niobium is clear from the Nb–C (2.22(1) Å) and Nb–O (2.26(1) Å) distances. Significant activation of the η^1,η^2-CO is suggested by the CO bond distance of 1.22(1) Å and the low carbonyl stretching frequency (1560 cm^{-1}).

The titanium complex, $\mathrm{Cp}_2^*(\mathrm{Me})\mathrm{Ti}(\mu\text{-OC})\mathrm{Mo(CO)}_2\mathrm{Cp}$ ($\mathrm{Cp}^* = \mathrm{C_5Me_5}$) **2.1**, was prepared by Hamilton, Jr., et al. [53] via the reaction of $\mathrm{Cp}^*(\mathrm{C_5Me_4CH_2})\mathrm{TiMe}$ and $\mathrm{CpMo(CO)_3H}$. The nature of the bridging isocarbonyl group was confirmed crystallographically (Fig. 4). The lengthening of the CO bond to 1.212(5) Å is expected upon interaction with the Lewis acidic titanium center. The carbonyl stretching frequency of 1623 cm^{-1} reflects the activation of the bridging carbonyl.

In the related reactions of $\mathrm{Cp}_2^*\mathrm{Ti(COR)}$ (R = Me, *neo*-$\mathrm{C_5H_{11}}$) with $[\mathrm{CpMo(CO)_3}]_2$, the products are proposed to be the acyl analogs of **2.1**, i.e. $\mathrm{Cp}_2^*(\eta^2\text{-OCR})\mathrm{Ti}(\mu\text{-OC})\mathrm{Mo(CO)}_2\mathrm{Cp}$ (R = Me **2.2**, *neo*-$\mathrm{C_5H_{11}}$ **2.3**) [54]. These products decompose at 25 °C via ring expansion of Cp* to give substituted

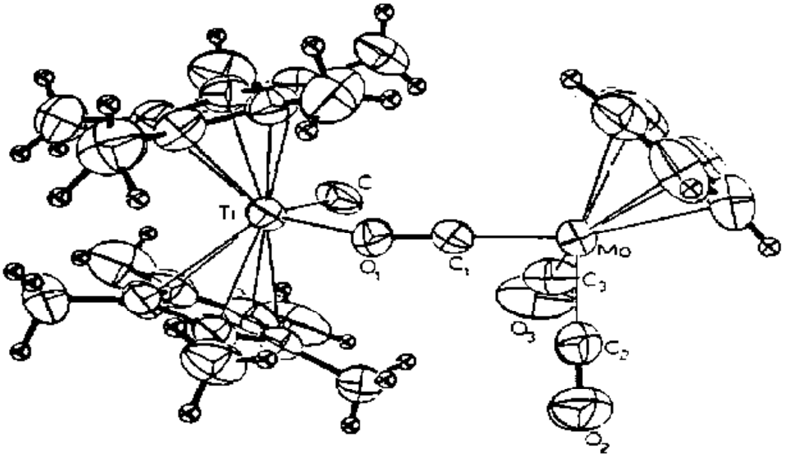

Fig. 4. ORTEP drawing of **2.1**. Reproduced with permission from ref. 53. Copyright 1981 American Chemical Society.

pentamethylbenzenes. The mechanism of decomposition is proposed to involve reaction of the electrophilic acyl carbon atom with the electron-rich Cp*, followed by acyl O–C bond scission. The structure of the organometallic byproduct is proposed to be $[Cp^*Ti(O)]_2[(\mu\text{-}OC)Mo(CO)_2Cp]_2$ **2.4**.

A related Ti(III) complex was prepared by reaction of the Ti(II) species $Cp_2Ti(CO)_2$ with $CpMo(CO)_2{\equiv}Mo(CO)_2Cp$ [55]. The product, $Cp_2(THF)Ti(\mu\text{-}OC)Mo(CO)_2Cp$ **2.5**, was crystallographically studied and found to be similar in structure to **2.1**, with a bridging carbonyl C–O distance of 1.201(8) Å. Although the mechanism of formation is not known, a mechanism involving formation of "Cp_2Ti" as an intermediate was postulated. Interestingly, if a similar reaction between $Cp_2Ti(CO)_2$ and $(C_5H_4Me)Mo(CO)_2{\equiv}Mo(CO)_2(C_5H_4Me)$ was performed in a non-coordinating solvent, the product isolated was not the analog of **2.5** but $[Cp_2Ti(\mu\text{-}OC)Mo(CO)_2(C_5H_4Me)]_2$ **2.6** [56]. The X-ray structure of this complex confirmed the formulation as a dimer containing a 12-membered $\{Ti–O–C–Mo–C–O\}_2$ ring (Fig. 5). Upon dissolution in tetrahydrofuran (THF), the dimeric structure is cleaved. The complex, **2.6**, was found to react with H_2 in a reversible reaction, yielding monometallic titanium and an Mo–hydrido species (eqn. (2)):

$$\begin{tikzcd}[Cp2Ti(OC)2Mo(CO)Cp]2 \arrow[d, shift left, "+ H2"] \\ 2\ [Cp2TiH]_x + 2\ CpMo(CO)3H \arrow[u, shift left, "- H2"]\end{tikzcd} \qquad (2)$$

Another compound that was found to contain a similar 12-membered ring was reported by Sartain and Selegue [57]. The complex $[(NEt_2)_2(NEt_2H)_2Zr((\mu\text{-}OC)_2Mo(CO)Cp)(\mu\text{-}OC)Mo(CO)_2Cp)]_2$ **2.15** was derived from the reaction of $Zr(NEt_2)_4$ and $CpMo(CO)_3H$. The structural data show that the C–O distance in the terminal $(\mu\text{-}OC)Mo(CO)_2Cp$ groups is 1.23(1) Å, while the isocarbonyls in the 12-membered ring are inequivalent, with CO bond

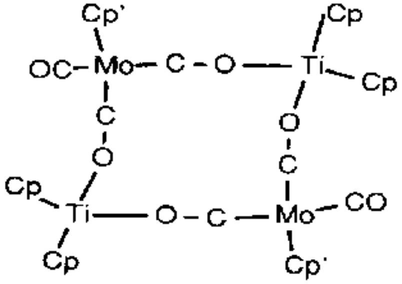

Fig. 5. Structure of **2.6**.

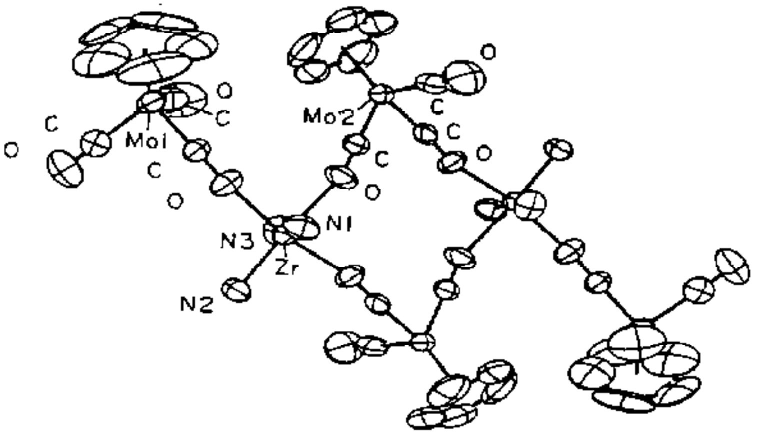

Fig. 6. ORTEP drawing of **2.15**. Reproduced with permission from ref. 57. Copyright 1984 American Chemical Society.

distances of 1.15(2) and 1.22(1) Å (Fig. 6). The differences in the C–O and the relevant Zr–O distances indicate the range of donor ability for CO oxygen atoms from ketone-like to oxycarbyne.

The species derived from the reaction of $Cp^*_2Ti(\textit{neo}\text{-}C_5H_{11})$ and $CpMo(CO)_2{\equiv}Mo(CO)_2Cp$ was formulated as containing Ti(III) centers [58]. The product, $(Cp^*_2Ti(\mu\text{-}OC)Mo(CO)_2Cp)_2$ **2.7**, is novel in that the Ti–O–C fragments are linear (Fig. 7). The substantial activation of the bridging CO bond evident (CO 1.271(7) Å, ν_{CO} 1351 cm^{-1}) in this complex, in addition to its paramagnetism, resulted in a description of this compound in terms of Ti(III) and Mo(0) centers. Molecular orbital calculations support this view [58].

In a report by some French researchers, the product of the reaction of Cp_2ZrMe_2 with $CpMo(CO)_3H$ was formulated as containing a Zr–Mo bond [59]. However, Norton and coworkers subsequently determined that this was not the case, but rather that the reaction gave the Cp_2Zr analog of **2.1** [60–62]. The product, $Cp_2(Me)Zr(\mu\text{-}OC)Mo(CO)_2Cp$ **2.16**, was formulated as containing a $\mu\text{-}\eta^1,\eta^2$-OC group by analogy to the Nb–Mo species **2.37**

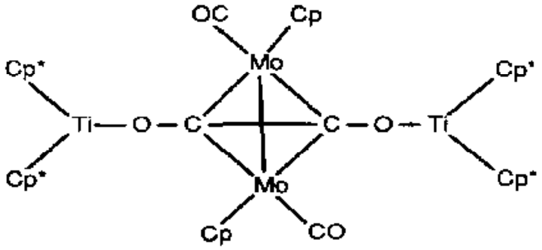

Fig. 7. Structure of 2.7.

[60]. A subsequent crystallographic study [61] showed that this was not the case. In fact, the structure is very similar to that of **2.1**, with a μ-CO O-bonded to zirconium and C-bonded to molybdenum. The C–O bond in the μ-CO moiety was 1.236(5) Å, significantly longer than a typical terminal CO distance. This result was indeed consistent with the low ν_{CO} assigned to the μ-CO (1545 cm^{-1}). The metal atoms in **2.16** were found to be almost 5 Å apart, thus supporting an ion-paired resonance form.

The complex **2.16** reacts with CO, affording the acetyl complex $Cp_2(\eta^2$-$OCMe)Zr(\mu$-$OC)Mo(CO)_2Cp$ **2.17** [62]. This complex was also prepared directly from $Cp_2Zr(\eta^2$-$OCMe)Me$ and $CpMo(CO)_3H$. Reaction of **2.16** with a proton source led to monomeric acidolysis products (eqn. (3)):

$$\mathrm{Cp_2Zr(OCMe)(OCMo(CO)_2Cp)} \xrightarrow{\mathrm{CF_3CO_2H}} \mathrm{Cp_2Zr(O_2CCF_3)_2 + MeCHO + CpMo(CO)_3H} \qquad (3)$$

Structural data for **2.17** reveal that it too contains a μ-O–C-type bridging carbonyl group (Fig. 8). Again, the C–O distance (1.209(4) Å) and the ν_{CO} (1600 cm^{-1}) are consistent with significant CO bond order reduction. The structural data also support an ion-paired formulation as was made for **2.16**.

On standing at 40 °C for 3 days, **2.17** loses CO, yielding the species $Cp_2Zr(\mu$-$OCMe)(\mu$-$OC)Mo(CO)Cp$ **2.18** (Fig. 9). The nature of the two bridging moieties was established by X-ray crystallography. Although the Zr–Mo distance of 3.3 Å is long, bonding modes considering the inclusion of an Mo–Zr bond have been considered. Interestingly, the C–O distance in the η^1,η^2-CO (1.241(4) Å) is even longer than the C–O distances found for the ion-paired species **2.17** and **2.18**. Thus a π-type interaction of a coordinated CO with zirconium is apparently capable of considerable bond order reduction.

The preparations of the chromium and tungsten analogs of the carbonyl-bridged ELHB complexes **2.16** and **2.17** have been described [61]. Although no structural data are available for these complexes, the spectroscopic data

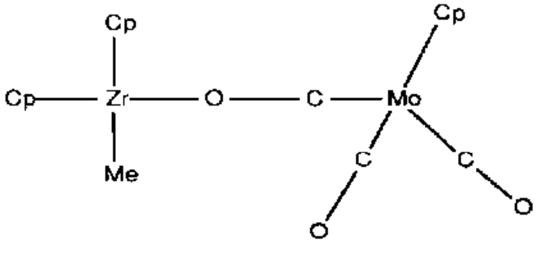

Fig. 8. Structure of **2.16**.

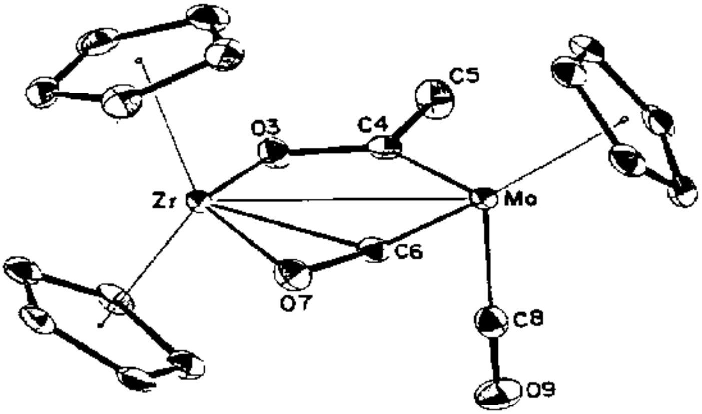

Fig. 9. ORTEP drawing of **2.18**. Reproduced with permission from ref. 60. Copyright 1981 American Chemical Society.

suggest structures similar to those described for the molybdenum compounds.

Kinetic and mechanistic studies showed that the formation of **2.18** proceeds by nucleophilic attack of the acetyl carbon by the molybdenum of **2.17** [63]. Similar nucleophilic attack, by added Cp_2ZrMe_2, yielded the trinuclear species $(Cp_2Zr(\mu\text{-}OCMe_2)Zr(Me)Cp_2)(\mu\text{-}OC)Mo(CO)_2Cp$ **2.19** (eqn. (4)). Reaction of this species containing the bridging ketone moiety with HCl yielded isopropanol (eqn. (4)):

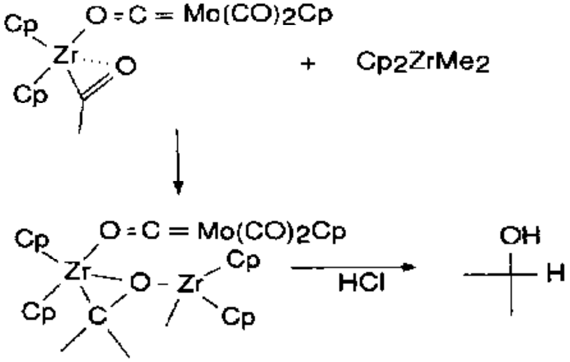

(4)

Similar chemistry was observed for the tungsten analogs.

Barger and Bercaw [64] have prepared a Zr–Co ELHB complex via the reaction of $Cp^*_2ZrH_2$ or $[Cp^*_2ZrN_2]_2N_2$ with $CpCo(CO)_2$. Crystallographic study of the product, $Cp^*_2Zr(\mu\text{-}CO)_2CoCp$ **2.30**, showed a Co–Zr bond (2.926(1) Å) bridged by both η^1- and η^1,η^2-carbonyl groups (Fig. 10). Attempts to study the interchange of these two bonding modes via ^{13}C NMR were thwarted by the quadrupole of ^{59}Co; however, a variable-temperature ^{13}C NMR study was carried out on the rhodium analog of **2.30** (i.e. $Cp^*_2Zr(\mu\text{-}CO)_2RhCp$ **2.31**) [65]. The activation energy for the fluxional

TABLE 1

Carbonyl-bridged ELHB complexes

M–M′	Number	Complex	μ-C–O (Å)	$\nu_{\mu\text{-CO}}$ ($\mathrm{cm^{-1}}$)	Ref.
Ti–Mo	**2.1**	$Cp^*_2(Me)Ti(\mu\text{-}OC)Mo(CO)_2Cp$	1.212(5)	1623	53
	2.2	$Cp^*_2(\eta^2\text{-}OCMe)Ti(\mu\text{-}OC)Mo(CO)_2Cp$		1700	54
	2.3	$Cp^*_2(\eta^2\text{-}OC\mathit{neo}\text{-}C_5H_{11})Ti(\mu\text{-}OC)\text{-}Mo(CO)_2Cp$		1700	54
	2.4	$[Cp^*TiO]_2[(\mu\text{-}OC)Mo(CO)_2Cp]_2$		1563	54
	2.5	$Cp_2(THF)Ti(\mu\text{-}OC)Mo(CO)_2Cp$	1.201(8)	1650	55
	2.6	$[Cp_2Ti(\mu\text{-}OC)Mo(CO)_2(C_5H_4Me)]_2$	1.208(7)	1710	56
	2.7	$(Cp^*_2Ti(\mu\text{-}OC)Mo(CO)Cp)_2$	1.271(7)		58
Ti–Co	**2.8**	$Cp_2(Cl)Ti(\mu\text{-}OC)Co_3(CO)_9$	1.22	1401	44 47
	2.9	$Cp_2Ti((\mu\text{-}OC)Co_3(CO)_9)_2$		1403	47
	2.10	$O(Cp_2Ti((\mu\text{-}OC)Co_3(CO)_9)_2)_2$		1413	47
	2.11	$CpTi((\mu\text{-}OC)Co_3(CO)_9)_2(Co(CO)_4)$	1.315 1.306		48
	2.12	$(Cp_2Ti)_2(\mu\text{-}OC)_2Co_3Cp_3$	1.36(2) 1.29(2)	1300	49
Zr–Cr	**2.13**	$Cp_2(Me)Zr(\mu\text{-}OC)Cr(CO)_2Cp$		1540	61
	2.14	$Cp_2(\eta^2\text{-}OCMe)Zr(\mu\text{-}OC)Cr(CO)_2Cp$		1595	61
Zr–Mo	**2.15**	$[(NEt_2)_2(NEt_2H)_2Zr((\mu\text{-}OC)_2\text{-}Mo(CO)Cp)_2]_2$	1.15(2) 1.22(1)	1580	57
	2.16	$Cp_2(Me)Zr(\mu\text{-}OC)Mo(CO)_2Cp$	1.236(5)	1545	59, 61
	2.17	$Cp_2(\eta^2\text{-}OCMe)Zr(\mu\text{-}OC)Mo(CO)_2Cp$	1.207(5) 1.211(5)	1600	60, 62
	2.18	$Cp_2Zr(\mu\text{-}OCMe)(\mu\text{-}OC)Mo(CO)Cp$	1.241(4)	1534	60
	2.19	$(Cp_2Zr(\mu\text{-}OCMe_2)Zr(Me)Cp_2)(\mu\text{-}OC)\text{-}Mo(CO)_2Cp$	1.218(5)		63
	2.20	$Cp^*_2Zr(\mu\text{-}OC)Mo(CO)_2Cp)_2$			65
Zr–W	**2.21**	$Cp_2(Me)Zr(\mu\text{-}OC)W(CO)_2Cp$		1544	61
	2.22	$Cp_2(\eta^2\text{-}OCMe)Zr(\mu\text{-}OC)W(CO)_2Cp$		1593	61
	2.23	$Cp_2Zr(\mu\text{-}OCMe)(\mu\text{-}OC)W(CO)Cp$		1536	61
Zr–Fe	**2.24**	$Cp^*_2Zr(\mu\text{-}O_2C_2)Fe_2(CO)_2Cp_2$	1.32(2)	1260	66
	2.25	$Cp^*_2Zr(\mu\text{-}O_2C_2)Fe_2(CO)_2(C_5H_4Me)_2$		1287	66
Zr–Ru	**2.26**	$Cp^*_2Zr(\mu\text{-}OC)_2RuHCp$		1706, 1671	65
Zr–Co	**2.27**	$Cp_2(Cl)Zr(\mu\text{-}OC)Co_3(CO)_9$	1.276(6)	1373	47
	2.28	$Cp_2Zr((\mu\text{-}OC)Co_3(CO)_9)_2$	1.30(2) 1.27(2)	1372	47
	2.29	$O(Cp_2Zr((\mu\text{-}OC)Co_3(CO)_9)_2)_2$		1377	47
	2.30	$Cp^*_2Zr(\mu\text{-}OC)_2CoCp$	1.200(9) 1.18(1)	1683 1737	65

TABLE 1 (continued)

M–M′	Number	Complex	μ-C–O (Å)	$\nu_{\mu\text{-CO}}$ (cm^{-1})	Ref.
Zr–Rh	**2.31**	$Cp^*_2Zr(\mu\text{-}OC)_2RhCp$		1752, 1696	65
Hf–Co	**2.32**	$Cp_2(Cl)Hf(\mu\text{-}CO)Co_3(CO)_9$	1.32(3)	1373	47
	2.33	$Cp_2Hf((\mu\text{-}OC)Co_3(CO)_9)_2$	1.35(4) 1.33(4)	1378	47
	2.34	$O(Cp_2Hf((\mu\text{-}OC)Co_3(CO)_9)_2)_2$		1379	47
V–Co	**2.35**	$(C_5H_4CMe_3)_2V(\mu\text{-}OC)Co_3(CO)_9$			46
	2.36	$(C_5H_4CO_2Me)_2V(\mu\text{-}OC)Co_3(CO)_9$			46
Nb–Mo	**2.37**	$Cp_2Nb(\mu\text{-}OC)_2Mo(CO)Cp$	1.22(1)	1560	52
Nb–W	**2.38**	$Cp_2Nb(\mu\text{-}OC)_2W(CO)Cp$		1560	52
Nb–Mn	**2.39**	$Cp_2(CO)Nb(\mu\text{-}OC)Mn(CO)_4$	1.156(6)	1842	52
Nb–Co	**2.40**	$(C_5H_4CMe_3)_2(CO)Nb(\mu\text{-}OC)Co_3(CO)_9$		1483	45
	2.41	$Cp_2(CO)Nb(\mu\text{-}OC)Co(CO)_3$	1.165(4)	1850	50
Ta–Co	**2.42**	$(C_5H_4CMe_3)_2(CO)Ta(\mu\text{-}OC)Co_3(CO)_9$		1463	45

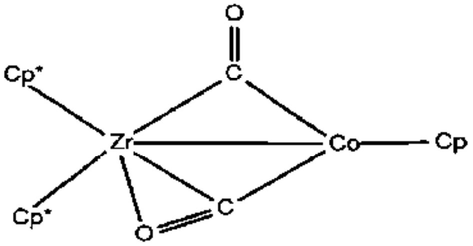

Fig. 10. Structure of **2.30**.

process was found to be, at the upper limit, 8 kcal mol^{-1}. Thus the interchange of the two carbonyl bonding modes is indeed energetically facile.

In a related system, Berry and Bercaw [66] have shown that reaction of $[Cp^*_2ZrN_2]_2N_2$ and $[CpFe(CO)_2]_2$ proceeds through a reductive coupling of the carbonyl ligands to give $Cp^*_2Zr(\mu^2\text{-}O_2C_2)Fe_2(CO)_2Cp_2$ **2.24**. The formation of **2.24** is apparently reversible, as the $[CpFe(CO)_2]_2$ fragment exchanges with $[(C_5H_4Me)_2Fe(CO)_2]_2$. In addition, treatment of **2.24** with ^{13}CO affords $Cp^*_2Zr(^{13}CO)_2$. Thus an equilibrium between **2.24** and the Zr(II) complex was postulated (eqn. 5):

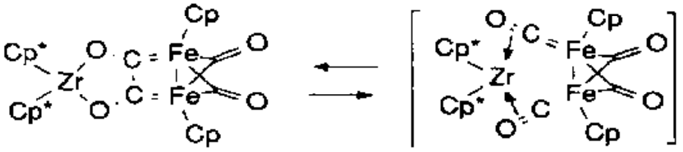

(5)

3. OTHER CARBON-ATOM-BASED BRIDGED ELHB COMPLEXES

In expanding the work on carbene chemistry, Fischer and coworkers [67,68] have described the formation of the first oxytitanocene carbene complexes. Reaction of $[(CO)_5Cr(COR)]Li$ with Cp_2TiCl_2 afforded the ELHB species $Cp_2(Cl)Ti(\mu\text{-}OCR)Cr(CO)_5$ (R = Me **3.1**, Ph **3.2**, NMe_2 **3.3**) and $Cp_2Ti((\mu\text{-}OCMe)Cr(CO)_5)_2$ **3.4**. The related oxytitanium ELHB carbene complexes $(Me_2N)_3Ti(\mu\text{-}OCNMe_2)ML_x$ (ML_x = $Mo(CO)_5$ **3.6**, $W(CO)_5$ **3.8**, $Fe(CO)_4$ **3.16**, $Ni(CO)_3$ **3.21**) were prepared by Petz [69] via reaction of $Ti(NMe_2)_4$ with metal carbonyls. These reactions demonstrated formation of carbene-bridged ELHB species via insertion of a metal carbonyl moiety into a Ti–N bond.

Erker and coworkers [70–73] have prepared ELHB complexes by insertion of metal carbonyls into an early metal complex. Using metal carbonyls as ketone analogs, in reactions with *cis/trans* diene complexes of zirconium and hafnium, new metallated carbene ELHB species have been prepared. For example, the reaction of $Cp_2Zr(C_4H_6)$ with metal carbonyls afforded the formation of the following metallated oxycarbene complexes: $Cp_2Zr(\mu\text{-}OCCH_2CHCHCH_2)ML_x$ (ML_x = $Cr(CO)_5$ **3.24**, $Mo(CO)_5$ **3.26**, $W(CO)_5$

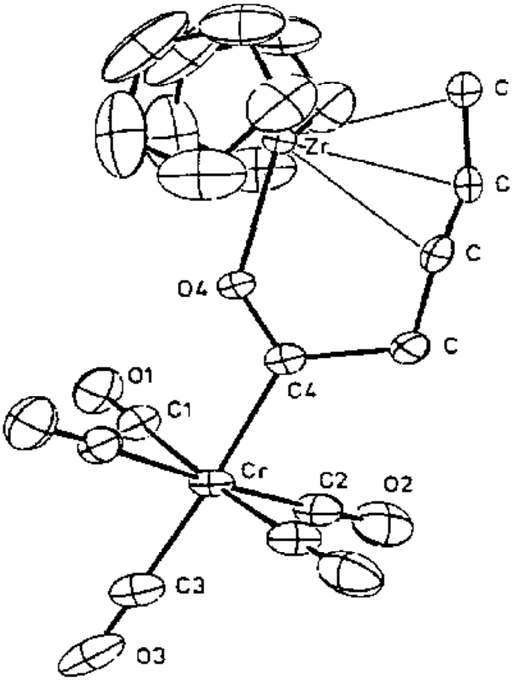

Fig. 11. ORTEP drawing of **3.24**. Reproduced with permission from ref. 70. Copyright 1984 American Chemical Society.

3.30, $Fe(CO)_4$ **3.42**, $Fe(CO)_3PPh_3$ **3.43**, $Co(CO)(C_5H_4Cl)$ **3.50**, $Co(CO)Cp$ **3.51**) (eqn. (6)):

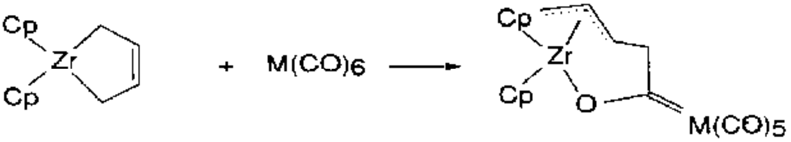

(6)

For **3.24**, **3.50** and **3.51**, the structures were confirmed by X-ray crystallography (Fig. 11). Studies involving the reactions of the analogous hafnium diene complexes showed selective consumption of the *trans*-butadiene complex, implying an electrophilic ring-closure of an (η^2-olefin)(η^2-carbonyl)MCp_2-type intermediate.

Erker et al. [74] have extended this chemistry. The reaction of Cp_2Zr(aryne) with $M(CO)_6$ was found to give products of the form $Cp_2Zr(\mu\text{-}OCC_6H_4)M(CO)_5$ (M = Mo **3.27**, W **3.31**). The Zr–W compound **3.31** was crystallographically characterized. On the basis of the structure of the product and on the results of substitution experiments, an aryne–carbonyl zirconocene intermediate was postulated (eqn. (7)):

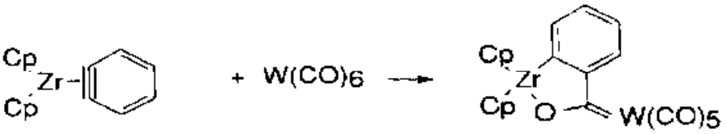

(7)

Controlled hydrolysis of **3.27** or **3.31** with $CuSO_4 \cdot 5H_2O$ afforded species of the form $O(Cp_2Zr(\mu\text{-}OCPh)M(CO)_5)_2$ (M = Mo **3.28**, W **3.33**) [75]. The Zr–Mo species **3.28** was shown by X-ray diffraction to contain two Mo–zirconoxycarbene subunits joined by the Zr–O–Zr linkage (eqn. (8)):

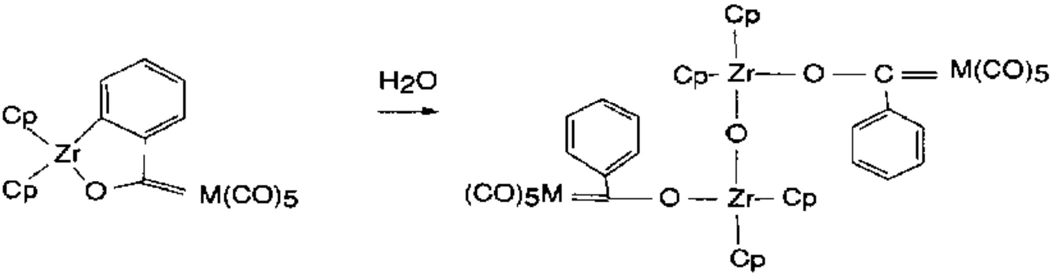

(8)

Other metallated oxycarbene ELHB complexes have been prepared by Takaya and coworkers [76] by employing reactions very reminiscent of zirconocene–aryne/metal carbonyl reactions described by Erker et al. Reaction of $Cp^*_2Ti(C_2H_4)$ with metal carbonyls afforded the products $Cp^*_2Ti(\mu\text{-}OCCH_2CH_2)ML_x$ ($ML_x = Cr(CO)_5$ **3.5**, $Mo(CO)_5$ **3.7**, $W(CO)_5$ **3.9**, Mn$_2$(CO)$_9$ **3.14**, Re$_2$(CO)$_9$ **3.15**) (eqn. (9)):

(9)

These species were found to be generally unstable in solution above −20 °C. Species **3.15** was isolated, and the structural study confirmed the formation of the titanoxycarbene–Rh carbonyl species. Thermolysis of these complexes led to the unusual fission of a C–C bond, yielding ethylene and the metal carbonyl.

Casey et al. [77] reported the formation of the zirconoxycarbene complex Cp$_2$(CO)Zr(μ-OCCH$_2$CH$_2$C$_5$H$_4$)Ru(CO) **3.46** from the reaction of CO with Cp$_2$Zr(μ-CH$_2$CH$_2$C$_5$H$_4$)Ru(CO)$_2$ **9.40** (see Section 9). The structure of **3.46** has been confirmed crystallographically (Fig. 12). In a similar vein, reaction of H$_2$–CO with Cp$_2$(CO)Zr(μ-C$_5$H$_4$)Ru(CO)$_2$ **9.38** yielded the zirconoxycarbene complex (CO)Cp$_2$Zr(μ-OCH)Ru(CO)Cp **3.47**. The mechanism of formation is thought to proceed through a hydrogenolysis intermediate Cp$_2$(H)ZrRu(CO)$_2$Cp. Insertion of CO into the Zr–H bond and a subsequent formyl migration are the suggested steps leading to **3.47** (eqn. (10)):

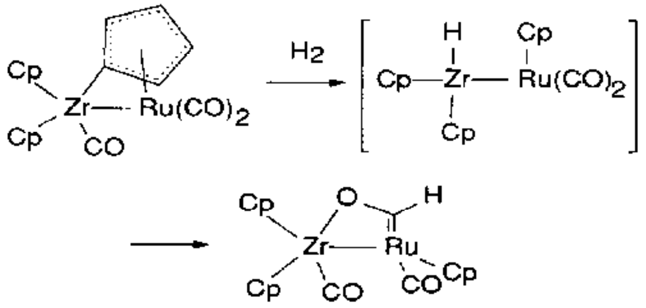

(10)

Interest in CO reduction has led to investigation of the reaction of metal carbonyl species with metal hydrides. Bercaw and coworkers [78] have described the reaction of Cp$_2$W(CO) and Cp$^*_2$ZrH$_2$. The resulting product, Cp$^*_2$(H)Zr(μ-OCH)WCp$_2$ **3.34** (Fig. 13), has been structurally characterized. This zirconoxycarbene complex of tungsten was shown to react with H$_2$ at 170 °C over 48 h to yield Cp$_2$WH$_2$ and Cp$^*_2$ZrH(OMe). Reaction of the analogous chromium and molybdenum complexes with Cp$^*_2$ZrH$_2$ gave the chromium and molybdenum analogs of **3.34**. Similar reactions of Cp$^*_2$ZrHX with CpM(CO)$_2$ gave Cp$^*_2$(X)Zr(μ-OCH)M(CO)Cp (M = Co, X = Cl **3.48**, F **3.49**; M = Rh, X = Cl **3.52**, F **3.53**) [65]. Related reactions of Cp$^*_2$ZrH$_2$ with CpM(PMe$_3$)(CO)H did not occur; however, in the presence of excess phosphine, the complexes Cp$^*_2$(H)Zr(μ-OCH$_2$)M(PMe$_3$)$_2$Cp (M = Fe **3.41**, Ru **3.45**) were formed. The formation of the reduced bridge complexes was

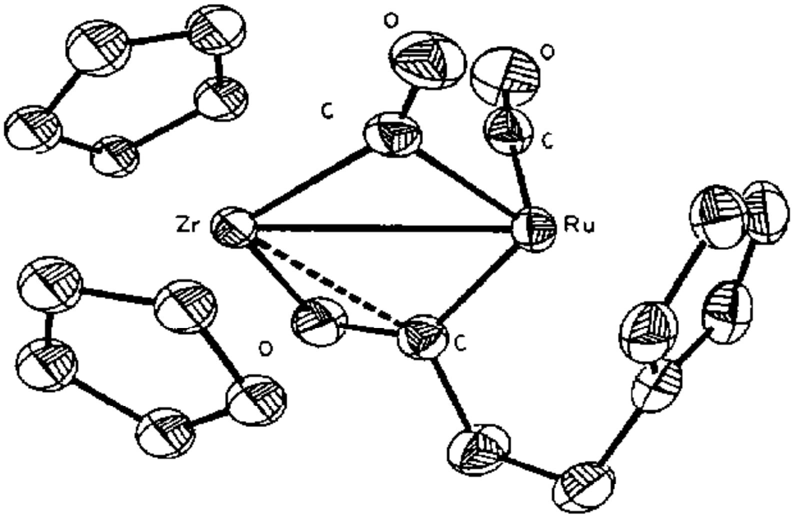

Fig. 12. ORTEP drawing of **3.46**. Reproduced with permission from ref. 77. Copyright 1986 American Chemical Society.

explained in terms of equilibria involving zirconoxycarbene-bridged species [65].

Marsella and Caulton [79] have studied related reactions of $Cp_2ZrX(\eta^2\text{-}OCMe)$ with Cp_2MoH_2 in which reduction of the acyl to ethoxide is rapidly effected, yielding $Cp_2ZrX(OEt)$ and "Cp_2Mo". The molybdenum species were trapped as Cp_2MoL (L = CO, NCMe) by addition of the ligand L. Deuteration experiments showed no evidence of hydrogen scrambling. A similar reaction of $Cp_2ZrMe(\eta^2\text{-}OCMe)$ with Cp_2ReH yielded the ELHB species $Cp_2ZrMe(\mu\text{-}OCHMe)ReCp_2$ **3.38**. The implication of an OCHMe-bridged species as an intermediate in the reduction of the acyl ligand to ethoxide is further supported by the spectroscopic observation of the species $Cp_2(Me)Zr(\mu\text{-}OCHMe)W(H)Cp_2$ **3.35**. Interestingly, the phenyl analog of **3.35**, i.e. $Cp_2(Ph)Zr(\mu\text{-}OCHPh)W(H)Cp_2$ **3.36**, has been shown to undergo thermolysis to yield $(Cp_2ZrPh)_2O$ and $Cp_2W(CHPh)$ [80]. This reaction represents one way of accomplishing the poorly understood C–O bond scission step in Fischer–Tropsch hydrocarbon synthesis.

Ho et al. [81] have described other reactions of $Cp_2ZrMe(\eta^2\text{-}OCMe)$. The zirconaenolate anion, $[Cp_2ZrMe(\eta^2\text{-}OCCH_2)]^-$, was formed via reaction of $Cp_2ZrMe(\eta^2\text{-}OCMe)$ with $NaN(SiMe_3)_2$. This species reacts with a number

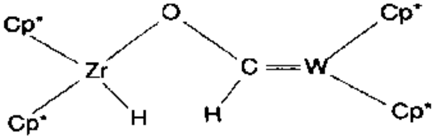

Fig. 13. Structure of **3.34**.

of reagents, including $(Me_3P)_2PtMeCl$, to yield the heterobimetallic ketone complex $Cp_2(Me)Zr(\mu\text{-}OCCH_2)PtMe(PMe_3)_2$ **3.54** (eqn. (11)):

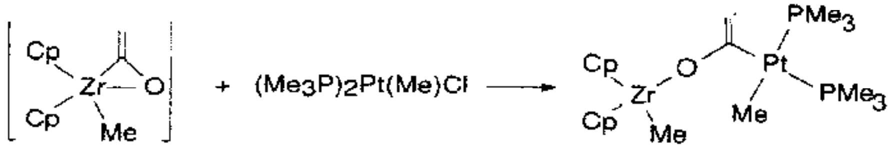

(11)

In related reactions of the organometallic enolate $[CpFe(CO)(PPh_3)\text{-}CCH_2O]^-$, Weinstock et al. [82] have demonstrated that selective trapping of the enol or keto forms is possible by use of the oxophilic Cp_2ZrCl_2, affording the ELHB species $Cp_2(Cl)Zr(\mu\text{-}OCCH_2)Fe(CO)(PPh_3)Cp$ **3.44** (Fig. 14). The formulation of **3.44** was confirmed crystallographically.

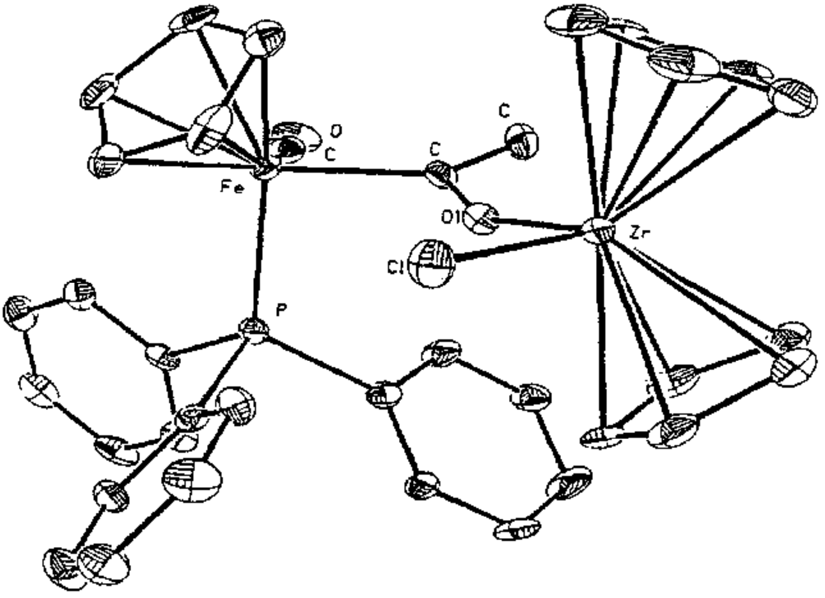

Fig. 14. ORTEP drawing of **3.44**. Reproduced with permission from ref. 82. Copyright 1986 American Chemical Society.

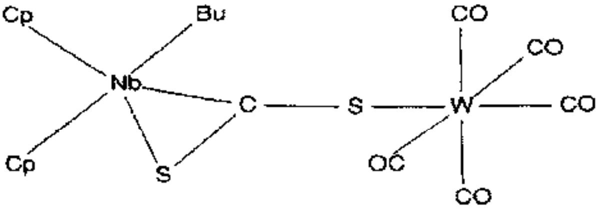

Fig. 15. Structure of **3.62**.

Tso and Cutler [83] have reported the formation of $Cp_2(Cl)Zr(\mu\text{-}O_2C)Re(CO)(NO)Cp$ **3.39** by reaction of $CpRe(CO)(NO)(CO_2H)$ with $Cp_2ZrMeCl$. Subsequent reaction of the bridging carbon dioxide complex **3.39** with Cp_2ZrHCl yielded the bridging formaldehyde complex $Cp_2(Cl)Zr(\mu\text{-}OCH_2)Re(CO)(NO)Cp$ **3.40** and $(Cp_2ZrCl)_2O$. Complex **3.40** was also prepared via reaction of $CpRe(CO)(NO)(CH_2OH)$ with $Cp_2ZrMeCl$. These results demonstrate that heterobimetallic reduction of CO_2 is viable.

Complexes in which CS_2 bridges the two constituent metals have been reported by Amaudrut et al. [84]. Reaction of $Cp_2Nb(Bu)(CS_2)$ with metal carbonyl species yielded the complexes $Cp_2(Bu)Nb(\mu\text{-}CS_2)ML_x$ (ML_x = $Cr(CO)_5$ **3.60**, $Mo(CO)_5$ **3.61**, $W(CO)_5$ **3.62**, $Mn(CO)_2(C_5H_4Me)$ **3.63**, $Fe(CO)_4$ **3.64**). Structural characterization of **3.62** showed that the $W(CO)_5$ fragment binds to one sulfur while the niobium is π bound to the C=S terminus (Fig. 15).

Carbene-bridged (i.e. $\mu\text{-}CR_2$) ELHB complexes were postulated as intermediates in reactions involving neopentylidene ligand transfer from $Ta(CHCMe_3)Cl_3L_2$ to $WO(OCCMe_3)_4$; however, these complexes were not isolated [85]. Stone and his group have developed a general method for the preparation of carbyne-bridged ELHB complexes. In the initial report [86] of such a system, the carbyne complex $CpW(CC_6H_4Me)(CO)_2$ was reacted with $Cp_2M(CO)_2$ (M = Ti, Zr). The products which have the form $Cp_2M(\mu\text{-}CC_6H_4Me)(\mu\text{-}OC)W(CO)Cp$ (M = Ti **3.10**, Zr **3.37**) (Fig. 16) are the metalloanalogs of alkyne addition to the titanocene or zirconocene moieties. The crystallographic study of **3.10** confirmed that the tungsten to bridging carbyne carbon distance reflects a bond order of two, while the Ti–W distance of 2.977(4) Å confirmed the presence of an M–M′ bond. The carbon and oxygen of the bridging carbonyl group are about equidistant from the titanium (Ti–C 2.20(3) Å, Ti–O 2.27(2) Å), while the W–C distance is 1.90(1) Å, thus confirming the η^1,η^2 nature of the bridging CO. The Lewis acidity of the titanium acts to activate the CO group. This is reflected in both the C–O distance (1.21(4) Å) and the ν_{CO} (1638 cm^{-1}).

The related reactions of the appropriate tungsten carbyne complexes with

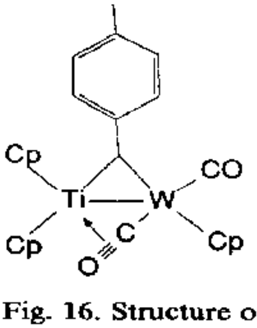

Fig. 16. Structure of **3.10**.

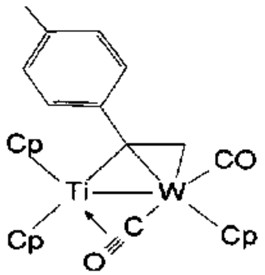

Fig. 17. Structure of **3.13**.

Cp_2V yielded the vanadium analogs of **3.10** and **3.37**. $Cp_2V(\mu\text{-}CR)(\mu\text{-}OC)W(CO)Cp$ (R = Me **3.58**, C_6H_4Me **3.59**) [87]. A structural study of the paramagnetic species **3.59** showed that the structure is similar to that of **3.10** with a bridging carbyne unit and a metal–metal bond (V–W 2.994(3) Å). However, the bridging carbonyl group was found not to be η^1,η^2 in nature, as was the case in **3.10**. The V–C distance of 2.63(3) Å and the ν_{CO} of 1758 cm^{-1} implied only a weak interaction of the Cp_2V fragment with the tungsten carbyne. This was further reflected in the observation of ca. 4% dissociation of **3.59** in solution into its monometallic constituents.

Stone and his group [88,89] studied the reaction of $Cp_2Ti(\mu\text{-}CH_2)(\mu\text{-}Cl)AlMe_2$ with the carbyne complex $CpW(CR)(CO)_2$. The products, $Cp_2Ti(\mu\text{-}C(R)CH_2)(\mu\text{-}OC)W(CO)Cp$ (R = Me **3.12**, C_6H_4Me **3.13**) (Fig. 17), are structurally similar to **3.10**. A crystallographic study of **3.13** revealed the presence of a Ti–W bond (3.082(2) Å) and an η^1,η^2 CO moiety (Ti–C 2.222(4) Å, Ti–O 2.285(3) Å). In addition, the methylene carbon originally bonded to the titanium has migrated to the tungsten and thus formed a metallocyclopropene.

Recently, Dutch workers [90] have prepared a tantalum alkylidyne complex which is stabilized by interaction with $ZnCl_2$. In the structure proposed, the alkylidyne and halide ligands bridge the tantalum and zinc atoms. This complex, $[Cl_2(MeOCH_2CH_2OMe)Ta(\mu\text{-}CCMe_3)(\mu\text{-}CCMe_3)(\mu\text{-}Cl)]_2Zn$ **3.65**, reacts with acetylenes to give substituted cyclopentadienyl derivatives of tantalum and ejects the $ZnCl_2$ moiety [91].

Mackenzie et al. have utilized the reactive titanium species Cp_2TiCH_2 to form a number of methylene-bridged ELHB complexes (eqn. (12)) [92]:

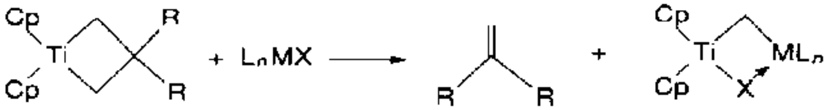

(12)

Reaction of $Cp_2Ti(\mu\text{-}CH_2)(\mu\text{-}Cl)Rh(COD)$ **3.17**, with MeLi yielded $Cp_2Ti(\mu\text{-}CH_2)(\mu\text{-}Me)Rh(COD)$ **3.19** [93]. Crystallographic characterization of **3.19** revealed an agostic interaction between the titanium and a CH bond of the

TABLE 2

Other carbon-based bridged ELHB complexes

M–M′	Number	Complex	Ref.
Ti–Cr	**3.1**	$Cp_2(Cl)Ti(\mu\text{-}OCMe)Cr(CO)_5$	67
	3.2	$Cp_2(Cl)Ti(\mu\text{-}OCPh)Cr(CO)_5$	68
	3.3	$Cp_2(Cl)Ti(\mu\text{-}OCNMe_2)Cr(CO)_5$	68
	3.4	$Cp_2Ti(\mu\text{-}OCMe)Cr(CO)_5)_2$	67
	3.5	$Cp^*_2Ti(\mu\text{-}OCCH_2CH_2)Cr(CO)_5$	76
Ti–Mo	**3.6**	$(Me_2N)_3Ti(\mu\text{-}OCNMe_2)Mo(CO)_5$	69
	3.7	$Cp^*_2Ti(\mu\text{-}OCCH_2CH_2)Mo(CO)_5$	76
Ti–W	**3.8**	$(Me_2N)_3Ti(\mu\text{-}OCNMe_2)W(CO)_5$	69
	3.9	$Cp^*_2Ti(\mu\text{-}OCCH_2CH_2)W(CO)_5$	76
	3.10	$Cp_2Ti(\mu\text{-}CC_6H_4Me)(\mu\text{-}OC)W(CO)Cp$	86
	3.11	$Cp_2Ti(\mu\text{-}CMe)(\mu\text{-}OC)W(CO)Cp$	88
	3.12	$Cp_2Ti(\mu\text{-}C(Me)CH_2)(\mu\text{-}OC)W(CO)Cp$	88
	3.13	$Cp_2Ti(\mu\text{-}C(C_6H_4Me)CH_2)(\mu\text{-}OC)W(CO)Cp$	88, 89
Ti–Mn	**3.14**	$Cp^*_2Ti(\mu\text{-}OCCH_2CH_2)Mn_2(CO)_9$	76
Ti–Re	**3.15**	$Cp^*_2Ti(\mu\text{-}OCCH_2CH_2)Re_2(CO)_9$	76
Ti–Fe	**3.16**	$(Me_2N)_3Ti(\mu\text{-}OCNMe_2)Fe(CO)_4$	69
Ti–Rh	**3.17**	$Cp_2Ti(\mu\text{-}CH_2)(\mu\text{-}Cl)Rh(COD)$	92
	3.18	$Cp_2Ti(\mu\text{-}CH_2)(\mu\text{-}OMe)Rh(COD)$	92
	3.19	$Cp_2Ti(\mu\text{-}CH_2)(\mu\text{-}Me)Rh(COD)$	93
Ti–Ir	**3.20**	$Cp_2Ti(\mu\text{-}CH_2)(\mu\text{-}Cl)Ir(COD)$	92
Ti–Ni	**3.21**	$(Me_2N)_3Ti(\mu\text{-}OCNMe_2)Ni(CO)_3$	69
Ti–Pd	**3.22**	$Cp_2Ti(\mu\text{-}CH_2)(\mu\text{-}Cl)Pd(CH_2CHCH_2)$	92
Ti–Pt	**3.23**	$Cp_2Ti(\mu\text{-}CH_2)(\mu\text{-}Cl)Pt(Me)PMe_3$	92
Zr–Cr	**3.24**	$Cp_2Zr(\mu\text{-}OCCH_2CHCHCH_2)Cr(CO)_5$	70
	3.25	$Cp^*_2(H)Zr(\mu\text{-}OCH)CrCp_2$	78
Zr–Mo	**3.26**	$Cp_2Zr(\mu\text{-}OCCH_2CHCHCH_2)Mo(CO)_5$	70
	3.27	$Cp_2Zr(\mu\text{-}OCC_6H_4)Mo(CO)_5$	75
	3.28	$O(Cp_2Zr(\mu\text{-}OCPh)Mo(CO)_5)_2$	75
	3.29	$Cp^*_2(H)Zr(\mu\text{-}OCH)MoCp_2$	78
Zr–W	**3.30**	$Cp_2Zr(\mu\text{-}OCCH_2CHCHCH_2)W(CO)_5$	70
	3.31	$Cp_2Zr(\mu\text{-}OCC_6H_4)W(CO)_5$	74
	3.32	$Cp_2Zr(\mu\text{-}OCC_6H_3Me)W(CO)_5$	74
	3.33	$O(Cp_2Zr(\mu\text{-}OCPh)W(CO)_5)_2$	75
	3.34	$Cp^*_2(H)Zr(\mu\text{-}OCH)WCp_2$	78
	3.35	$Cp^*_2(Me)Zr(\mu\text{-}OCHMe)W(H)Cp_2$	78
	3.36	$Cp_2(Ph)Zr(\mu\text{-}OCHPh)W(H)Cp_2$	80
	3.37	$Cp_2Zr(\mu\text{-}CC_6H_4Me)(\mu\text{-}OC)W(CO)Cp$	86
Zr–Re	**3.38**	$Cp_2(Me)Zr(\mu\text{-}OCHMe)ReCp_2$	79
	3.39	$Cp_2(Cl)Zr(\mu\text{-}O_2C)Re(CO)(NO)Cp$	83
	3.40	$Cp_2(Cl)Zr(\mu\text{-}OCH_2)Re(CO)(NO)Cp$	83
Zr–Fe	**3.41**	$Cp^*_2(H)Zr(\mu\text{-}OCH_2)Fe(PMe_3)_2Cp$	65
	3.42	$Cp_2Zr(\mu\text{-}OCCH_2CHCHCH_2)Fe(CO)_4$	71
	3.43	$Cp_2Zr(\mu\text{-}OCCH_2CHCHCH_2)Fe(CO)_3PPh_3$	71
	3.44	$Cp_2(Cl)Zr(\mu\text{-}OCCH_2)Fe(CO)(PPh_3)Cp$	82

TABLE 2 (continued)

M–M′	Number	Complex	Ref.
Zr–Ru	**3.45**	$Cp_2^*(H)Zr(\mu\text{-}OCH_2)Ru(PMe_3)_2Cp$	65
	3.46	$Cp_2(CO)Zr(\mu\text{-}OCCH_2CH_2C_5H_4)Ru(CO)$	77
	3.47	$Cp_2(CO)Zr(\mu\text{-}OCH)Ru(CO)Cp$	77
Zr–CO	**3.48**	$Cp_2^*(Cl)Zr(\mu\text{-}OCH)Co(CO)Cp$	65
	3.49	$Cp_2^*(F)Zr(\mu\text{-}OCH)Co(CO)Cp$	65
	3.50	$Cp_2Zr(\mu\text{-}OCCH_2CHCHCH_2)Co(CO)(C_5H_4Cl)$	72
	3.51	$Cp_2Zr(\mu\text{-}OCCH_2CHCHCH_2)Co(CO)Cp$	73
Zr–Rh	**3.52**	$Cp_2^*(Cl)Zr(\mu\text{-}OCH)Rh(CO)Cp$	65
	3.53	$Cp_2^*(F)Zr(\mu\text{-}OCH)Rh(CO)Cp$	65
Zr–Pt	**3.54**	$Cp_2(Me)Zr(\mu\text{-}OCCH_2)PtMe(PMe_3)_2$	81
Hf–Cr	**3.55**	$Cp_2Hf(\mu\text{-}OCCH_2CHCHCH_2)Cr(CO)_5$	70
Hf–Mo	**3.56**	$Cp_2Hf(\mu\text{-}OCCH_2CHCHCH_2)Mo(CO)_5$	70
Hf–W	**3.57**	$Cp_2Hf(\mu\text{-}OCCH_2CHCHCH_2)W(CO)_5$	70, 71
V–M	**3.58**	$Cp_2V(\mu\text{-}CMe)(\mu\text{-}OC)W(CO)Cp$	87
	3.59	$Cp_2V(\mu\text{-}CC_6H_4Me)(\mu\text{-}OC)W(CO)Cp$	87
Nb–Cr	**3.60**	$Cp_2(Bu)Nb(\mu\text{-}CS_2)Cr(CO)_5$	84
Nb–Mo	**3.61**	$Cp_2(Bu)Nb(\mu\text{-}CS_2)Mo(CO)_5$	84
Nb–W	**3.62**	$Cp_2(Bu)Nb(\mu\text{-}CS_2)W(CO)_5$	84
Nb–Mn	**3.63**	$Cp_2(Bu)Nb(\mu\text{-}CS_2)Mn(CO)_2(C_5H_4Me)$	84
Nb–Fe	**3.64**	$Cp_2(Bu)Nb(\mu\text{-}CS_2)Fe(CO)_4$	84
Ta–Zn	**3.65**	$[Cl_2(MeOCH_2CH_2OMe)Ta(\mu\text{-}CCMe_3)(\mu\text{-}Cl)]_2Zn$	90, 91
Th–Cr	**3.66**	$Cp_2^*Th(OCCH_2CHCHCH_2)Cr(CO)_5$	71

bridging methyl group (Fig. 18). NMR data showed that the agostic interaction is fluxional at 25 °C. Low temperature studies showed distinct ^{13}C–^{1}H coupling constants for the agostic and terminal hydrogen atoms of the methyl group. Hydrogen transfer processes between the μ-CH_2 and the μ-Me groups were also observed by NMR ($t_{1/2} = 15$ days at 65 °C); however, the role of the agostic interaction in these hydrogen atom transfers is not understood.

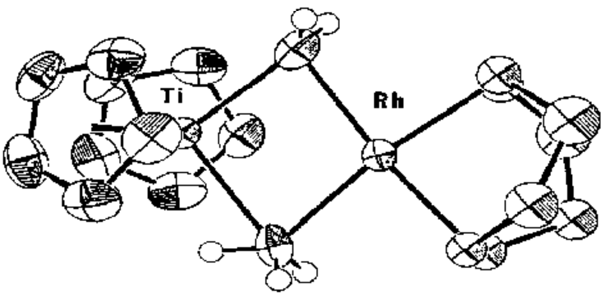

Fig. 18. ORTEP drawing of **3.19**. Reproduced with permission from ref. 93. Copyright 1986 American Chemical Society.

4. HYDRIDO-BRIDGED ELHB COMPLEX

The potential use of heterobimetallic complexes in reduction processes depends on the ability to incorporate hydrogen, presumably as hydride ligands. Thus interest has developed in hydrido-bridged ELHB complexes. In 1978 and 1979 Labinger and coworkers [94,95] reported the characterization of the species $Cp_2(CO)Nb(\mu\text{-}H)Fe(CO)_4$ **4.17**. The most notable feature of this species, prepared by reaction of Cp_2NbH_3 and $Fe(CO)_5$, is the length of the Nb–Fe bond (3.324(1) Å) (Fig. 19). It was suggested that the presence of the bridging hydride results in the apparently long M–M′ bond. ^1H NMR studies of **4.17** revealed "thermal decoupling" of the hydride signal at −6.4 ppm, owing to the quadrupole on the ^{93}Nb nucleus. ^1H and ^{13}C NMR spectra of **4.17** showed two signals attributable to the Cp groups, yet the carbonyl region showed only a single resonance in the ^{13}C NMR spectrum, implying rapid exchange of the carbonyls on the ion. The inequivalence of the Cp groups was not fully explained; however, it was suggested that a species in which a terminal hydride on niobium existed was also present in solution.

A similar hydride-bridged Nb–Ni ELHB complex has been reported by Russian workers [96]. Reaction of $Cp_2Nb(BH_4)$ with $Ni(CO)_4$ led to the formation of $Cp_2(CO)Nb(\mu\text{-}H)Ni(CO)_3$ **4.18** (eqn. (13)):

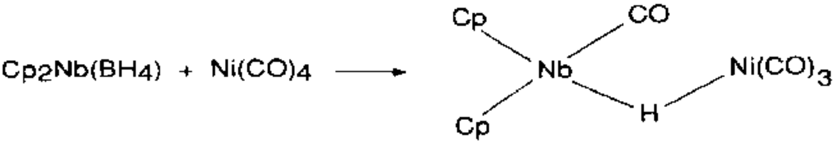

(13)

The Nb–Ni distance of 3.218(1) Å in **4.18** is longer than the sum of the covalent radii of niobium and nickel and the geometry about the nickel is

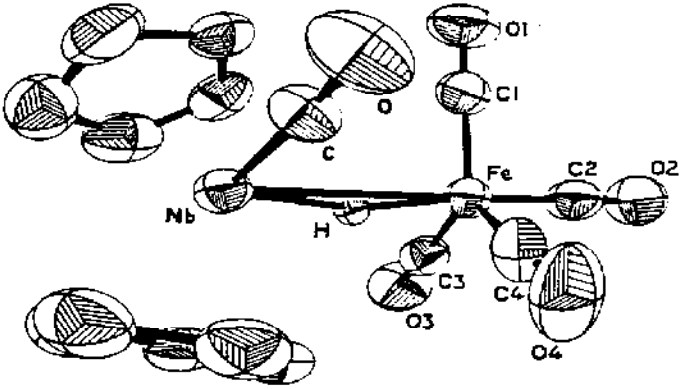

Fig. 19. ORTEP drawing of **4.17**. Reproduced with permission from ref. 94. Copyright 1978 American Chemical Society.

essentially that of a tetrahedral coordination sphere consisting of the three carbonyls and the hydride. Thus the metal–metal interaction was deemed to be non-bonding.

In the related reaction of Cp_2NbH_3 with $Cr(CO)_6$ in benzene, only the monometallic species $Cp_2Nb(CO)H$ was formed [97]. However, when this reaction was performed under H_2, selective formation of ethane was observed. The use of $CO-H_2$ did not afford catalytic CO reduction, presumably as a result of the tendency to form the unreactive monometallic complex $Cp_2Nb(CO)H$. If the reaction was done in THF the ELHB species $Cp_2(CO)Nb(\mu\text{-}H)Cr(CO)_5$ **4.7** is formed. The formulation of **4.7** was recently confirmed crystallographically [98]. The analogous reaction with $M(CO)_6$ did not yield either ethane or $Cp_2Nb(CO)H$; rather ELHB products formulated as $Cp_2(CO)Nb(\mu\text{-}H)M(CO)_5$ (M = Mo **4.10**, W **4.13**) were formed. Full characterization of these species has not been reported.

Similar reactions involving Cp_2NbH_3 and $Mn_2(CO)_{10}$ led not to ELHB complexes, but rather to the ionic product $[(Cp_2(CO)Nb)_2(\mu\text{-}H)]^+[Mn(CO)_5]^-$ [98,99]. In contrast, the reaction of the analogous tantalum species is reported to form $Cp_2(CO)Ta(\mu\text{-}H)Mn_2(CO)_9$ **4.27**, a species isoelectronic and structurally similar to $HRe_3(CO)_{14}$ [100,101]. The related complexes $Cp'_2(CO)Ta(\mu\text{-}H)ML_x$ ($Cp' = Cp$, $ML_x = Cr(CO)_5$ **4.21**, $Mo(CO)_5$ **4.23**, $W(CO)_5$ **4.25**, $CpMn(CO)_2$ **4.28**; $Cp' = C_5H_4CMe_3$, $ML_x = Cr(CO)_5$ **4.22**, $Mo(CO)_5$ **4.24**, $W(CO)_5$ **4.26**, $CpMn(CO)_2$ **4.29**) have been prepared via direct reaction of $Cp'_2Ta(CO)H$ with $(THF)ML_x$ [101]. The reactions of $Cp_2Nb(BH_4)$ and $M(CO)_6$ led to the formation of the related species $(Cp_2(CO)Nb(\mu\text{-}H))_2M(CO)_4$ (M = Mo **4.9**, W **4.12**) (Fig. 20) [96]. A crystallographic study showed that the geometry about the molybdenum in **4.9** is essentially that of a *cis*-substituted octahedron (four carbonyls and two hydrides). The Mo–Nb distances of 3.579(1) and 3.565(1) Å in **4.9**, imply the absence of any Nb–Mo bonding interaction.

Recently, Oltmanns and Rehder [102] have reported the formation of the related hydrido-bridged ELHB salts $[(Ph_2P)_2N]^+[Cp(CO)_3Nb(\mu\text{-}H)ML_x]^-$ ($ML_x = Cr(CO)_5$ **4.8**, $Mo(CO)_5$ **4.11**, $W(CO)_5$ **4.14**, $Mn(CO)_2Cp$ **4.15**, $Mn(CO)_2(C_5H_4Me)$ **4.16**) via reaction of $[(Ph_2P)_2N][CpNb(CO)_3H]$ with

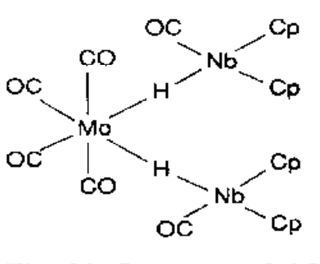

Fig. 20. Structure of **4.9**.

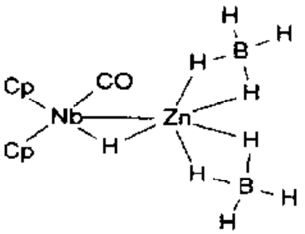

Fig. 21. Structure of **4.20**.

(THF)ML_x. In these reactions, formation of some of the hydrido-bridged homobimetallic anions, $[(L_xM)_2(\mu\text{-H})]^-$, was also observed.

Tebbe [103] described the synthesis of the complex $(Cp_2Nb(\mu\text{-H})_2)_2Zn$ **4.19** via reaction of Cp_2NbH_3 with Et_2Zn. The proposed structure was one in which a central zinc atom was tetrahedrally coordinated to four bridging Nb–H moieties. The analogous tantalum reactions did not evolve ethane; rather, an equilibrium between Cp_2TaH_3 and $Cp_2Ta(\mu\text{-H})_3ZnEt_2$ **4.30** was observed.

The complex $Cp_2(CO)Nb(\mu\text{-H})Zn(BH_4)_2$ **4.20** (Fig. 21) was prepared by reaction of $NbCl_5$ with NaCp, zinc dust and $NaBH_4$ under an atmosphere of CO [104]. Structural characterization of **4.20** showed the Nb–H–Zn angle to be 107.0(1)°, while the Nb–Zn distance is 2.829(1) Å. Both of these parameters are substantially smaller than the corresponding values observed in **4.17**. Thus the authors concluded that the structural and spectroscopic data supported the notion of a direct Zn–Nb bonding interaction.

Caulton and coworkers [105] have characterized the species $[(Ph_2MeP)_2V(\mu\text{-H})_2Zn(BH_4)]_2$ **4.6**. The Zn–V distance in this hydrido-bridged species is longer than the sum of the covalent radii of vanadium and zinc and thus the molecule is described in terms of a $V_2H_4(PMePh_2)_4^{2-}$ anion and two $Zn(BH_4)^+$ cations.

More recently, Caulton and coworkers [106] have studied the reaction of the hydride species $K[OsH_3(PPhMe_2)_3]$ and $K[ReH_6(PPhMe_2)_3]$ with the zirconium compounds $Cp_2Zr(X)Cl$ (eqns. (14) and (15)):

$$\begin{array}{l} \mathrm{K[OsH_3(PMe_2Ph)_3] + Cp_2Zr(X)Cl} \\ \qquad\qquad \downarrow \\ \mathrm{Cp_2Zr(X)[OsH_3(PMe_2Ph)_3] + KCl} \end{array} \tag{14}$$

$$\begin{array}{l} \mathrm{K[ReH_6(PMePh_2)_2] + Cp_2Zr(X)Cl} \\ \qquad\qquad \downarrow \\ \mathrm{Cp_2Zr(X)[ReH_6(PMePh_2)_2] + KCl} \end{array} \tag{15}$$

TABLE 3

Hydrido-bridged ELHB complexes

M–M′	Number	Complex	M–M′ distance (Å)	Ref.
Zr–Re	**4.1**	$Cp_2(Me)rReH_6(PMe_2Ph)_2$		106
	4.2	$Cp_2(H)ZrReH_6(PMe_2Ph)_2$		106
	4.3	$Cp_2(iPrO)ZrReH_6(PMe_2Ph)_2$		106
Zr–Os	**4.4**	$Cp_2(Cl)Zr(\mu\text{-}H)_3Os(PMe_2Ph)_3$	2.805(1)	106
	4.5	$Cp_2(H)Zr(\mu\text{-}H)_3Os(PMe_2Ph)_3$		106
V–Zn	**4.6**	$[(PhMe_2P)_2V(\mu\text{-}H)_2Zn(BH_4)]_2$		105
Nb–Cr	**4.7**	$Cp_2(CO)Nb(\mu\text{-}H)Cr(CO)_5$	3.453(2)	98
	4.8	$[Cp(CO)_3Nb(\mu\text{-}H)Cr(CO)_5]^-$		102
Nb–Mo	**4.9**	$(Cp_2(CO)Nb(\mu\text{-}H))_2Mo(CO)_4$	3.579(2) 3.565(2)	96
	4.10	$Cp_2(CO)Nb(\mu\text{-}H)Mo(CO)_5$		97, 98
	4.11	$[Cp(CO)_3Nb(\mu\text{-}H)Mo(CO)_5]^-$		102
Nb–W	**4.12**	$(Cp_2(CO)Nb(\mu\text{-}H))_2W(CO)_4$		96
	4.13	$Cp_2(CO)Nb(\mu\text{-}H)W(CO)_5$		98
	4.14	$[Cp(CO)_3Nb(\mu\text{-}H)W(CO)_5]^-$		102
Nb–Mn	**4.15**	$[Cp(CO)_3Nb(\mu\text{-}H)Mn(CO)_2Cp]^-$		102
	4.16	$[Cp(CO)_3Nb(\mu\text{-}H)Mn(CO)_2(C_5H_4Me)]^-$		102
Nb–Fe	**4.17**	$Cp_2(CO)Nb(\mu\text{-}H)Fe(CO)_4$	3.324(1)	94, 95
Nb–Ni	**4.18**	$Cp_2(CO)Nb(\mu\text{-}H)Ni(CO)_3$	3.218(1)	96
Nb–Zn	**4.19**	$(Cp_2Nb(\mu\text{-}H)_2)_2Zn$		101
	4.20	$Cp_2(CO)Nb(\mu\text{-}H)Zn(BH_4)_2$	2.829(2)	104
Ta–Cr	**4.21**	$Cp_2(CO)Ta(\mu\text{-}H)Cr(CO)_5$		101
	4.22	$(C_5H_4CMe_3)_2(CO)Ta(\mu\text{-}H)Cr(CO)_5$		101
Ta–Mo	**4.23**	$Cp_2(CO)Ta(\mu\text{-}H)Mo(CO)_5$		101
	4.24	$(C_5H_4CMe_3)_2(CO)Ta(\mu\text{-}H)Cr(CO)_5$		101
Ta–W	**4.25**	$Cp_2(CO)Ta(\mu\text{-}H)W(CO)_5$		101
	4.26	$(C_5H_4CMe_3)_2(CO)Ta(\mu\text{-}H)W(CO)_5$		101
Ta–Mn	**4.27**	$Cp_2(CO)Ta(\mu\text{-}H)Mn_2(CO)_9$	3.441(11)	98–100
	4.28	$Cp_2(CO)Ta(\mu\text{-}H)Mn(CO)_2Cp$		101
	4.29	$(C_5H_4CMe_3)_2(CO)Ta(\mu\text{-}H)Mo(CO)_2Cp$		101
Ta–Zn	**4.30**	$Cp_2Ta(\mu\text{-}H)_3ZnEt_2$		103

The osmium-containing products have the form $Cp_2(X)Zr(\mu\text{-}H)_3Os(PMe_2Ph)_3$ ($X = Cl$ **4.4**, H **4.5**), while the rhenium species were formulated as $Cp_2(X)ZrReH_6(PMe_2Ph)_2$ ($X = Me$ **4.1**, H **4.2**, iPrO **4.3**). NMR data for these complexes are consistent with three bridging hydrides in both **4.4** and **4.5**. All rhenium-bound hydrides in **4.1**–**4.3** are equivalent in the ^1H NMR spectra up to $-85\,^\circ C$. In **4.4** and **4.5**, no exchange of the zirconium-bound hydride with the other hydrides in the complexes occurred on the NMR time scale. An X-ray study of **4.4** confirmed the structural formulation.

5. HALIDE-BRIDGED ELHB COMPLEXES

A number of complexes generated by zinc reduction of an early metal species are formally bimetallics; however, the zinc or other late metal reductant is present only as a component of the counter-ion. Such species are not described here. In a few cases, halide-bridged ELHB complexes are formed, and studies have focused on their structure and magnetic properties. Reduction of Cp_2TiCl_2 with zinc, in benzene, yields $[Cp_2Ti(\mu\text{-}Cl)_2]_2Zn \cdot 2C_6H_6$ **5.2**. The crystal structure of this complex has been studied by several groups [107–109]. This compound was found to be a linear trimetallic with each metal adopting a pseudotetrahedral coordination sphere. The complex $[Cp_2Ti(\mu\text{-}Cl)_2]_2Mn(THF)_2$ **5.1** is also a linear trimetallic in which the central metal atom, manganese, adopts a pseudooctahedral coordination sphere. Detailed physical studies of **5.2**, $[Cp_2Ti(\mu\text{-}Br)_2]_2Zn$ **5.3** and **5.1** have examined the process of magnetic exchange between the Ti(III) centers in these linear trimetallic compounds [110,111]. Electron nuclear double resonance (ENDOR) and ESR studies showed that dissolution of **5.2** and **5.3** in THF promotes rupture of the trimetallic and formation of $[Cp_2Ti(THF)]^+$ [112].

No other organometallic halide-bridged ELHB complexes are known; however, in studying zinc reductions of vanadium chlorides, Caulton and coworkers [113] found a number of synthetic routes to $(THF)_4V(\mu\text{-}Cl)_2ZnCl_2$. This halide-bridged ELHB complex was shown to be a homogeneous catalyst precursor for the polymerization of ethylene. The role of the zinc is still unclear and the formulation of the catalytic species has not been established; however, organometallic intermediates are implied.

TABLE 4

Halide-bridged ELHB complexes

M–M′	Number	Complex	Ref.
Ti–Mn	**5.1**	$[Cp_2Ti(\mu\text{-}Cl)_2]_2Mn(THF)_2$	110, 111
Ti–Zn	**5.2**	$[Cp_2Ti(\mu\text{-}Cl)_2]_2Zn$	107–109, 112
	5.3	$[Cp_2Ti(\mu\text{-}Br)_2]_2Zn$	112

6. AMIDO- AND PHOSPHIDO-BRIDGED ELHB COMPLEXES

Phosphido-bridged ELHB complexes were first reported by Stelzer and coworkers in 1975 [114,115]. Metallation of phosphine complexes of the form $(RR'HP)_2Mo(CO)_4$, with an alkyl lithium, led to the formation of $(LiRR'P)_2Mo(CO)_4$. These species react with a variety of halides including Cp_2MCl_2, yielding several ELHB complexes of the form $Cp_2M(\mu\text{-}$

PRR$'$)$_2$Mo(CO)$_4$ [114,115]. For the complexes Cp$_2$M(μ-PHPh)$_2$Mo(CO)$_4$ (M = Ti **6.3**, Zr **6.13**) and Cp$_2$M(μ-PPh(SiMe$_3$))$_2$Mo(CO)$_4$ (M = Ti **6.4**, Zr **6.14**), the chirality at the phosphorus atoms gives rise to diastereoisomers. This is reflected by the presence of two singlets in the ^{31}P{^{1}H} NMR spectrum corresponding to the *meso* and the racemic forms. In addition, the ^{1}H NMR spectrum is consistent with inequivalent Cp groups in the *meso* form and equivalent Cp moieties in the racemic compound.

An earlier report by Bradley and Kasenally [116], in 1968, described the formation of the related amido-bridged ELHB complexes CpTi(μ-NMe$_2$)$_3$M(CO)$_3$ (M = Cr **6.2**, Mo **6.6**, W **6.7**) from the photochemical reaction of CpTi(NMe)$_3$ with M(CO)$_6$. Although the formulations of these complexes have not been confirmed crystallographically, IR data suggest dative M–M$'$ bonding. This remains the only report of amido-bridged ELHB species.

It was not until 1985 that further exploration of phosphido-bridged ELHB complexes resumed. Geoffroy and coworkers [117] expanded on Stelzer's approach and described a series of reactions involving the dianions [(R$_2$P)$_2$ML$_x$]$^{2-}$ and Cp$_2$MCl$_2$. The products were the diphosphido-bridged complexes Cp$_2$M(μ-PR$_2$)$_2$M$'$L$_x$ (M = Ti, R = Ph, M$'$L$_x$ = Fe(CO)$_3$ **6.1**, W(CO)$_4$ **6.8**; M = Zr, M$'$L$_x$ = Fe(CO)$_3$ **6.10**, Mo(CO)$_4$ **6.11**, W(CO)$_4$ **6.15**; R = cyclohexyl (Cy), M$'$L$_x$ = Fe(CO)$_3$ **6.9**). Similar complexes were prepared by the research groups of Baker [118], Stephan [119] and Wade [120] employing an alternative synthetic route. These groups described reactions of the metalloligands Cp$_2$M(PR$_2$)$_2$ (M = Zr, Hf; R = Et, Ph, Cy) with later

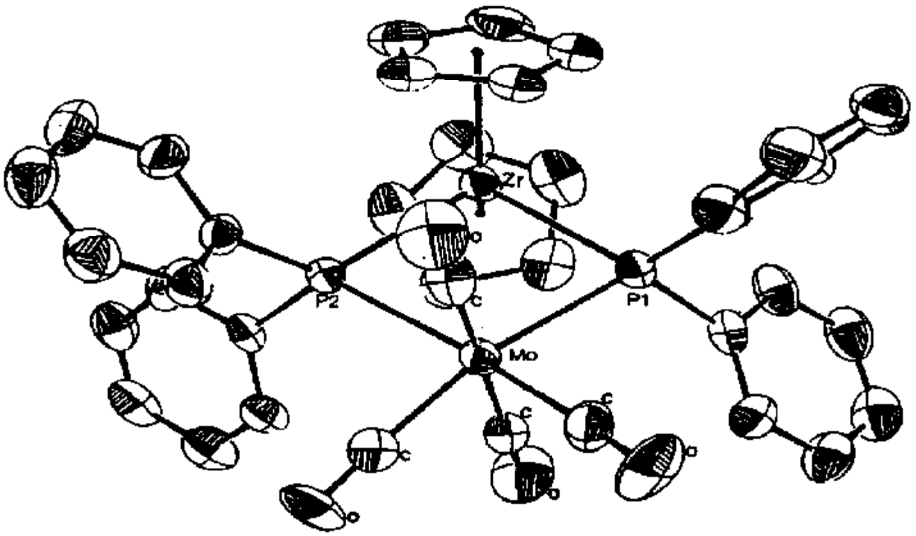

Fig. 22. ORTEP drawing of **6.11**. Reproduced with permission from ref. 119. Copyright 1985 American Chemical Society.

metal complexes containing easily replaceable ligands. In the reaction of $Cp_2Hf(PEt_2)_2$ with $Fe_2(CO)_9$, Baker et al. [118] showed that the initial product formed is one in which a single phosphide bridges iron and hafnium, thus yielding $Cp_2(PEt_2)Hf(\mu\text{-}PEt_2)Fe(CO)_4$ **6.40**. Thermal reaction of **6.40** led to displacement of a second CO on the ion by the terminal phosphide on hafnium, giving $Cp_2Hf(\mu\text{-}PEt_2)_2Fe(CO)_3$ **6.39**.

Structural characterizations of **6.11** (Fig. 22), **6.15** and **6.41** have been reported [117–120]. In addition, the Zr–Re ELHB species, $Cp_2Zr(\mu\text{-}PPh_2)_2ReH(CO)_3$ **6.16**, has been recently prepared and structurally characterized [121]. The MP_2M' cores are essentially planar, and although the angles about the MP_2M' core may indicate the possibility of metal–metal interactions, the metal–metal separations of 3.299(1) Å, 3.289(1) Å, 3.275(1) Å and 3.400(1) Å in **6.11**, **6.15**, **6.16** and **6.41** respectively suggest that if any direct metal–metal interactions are present, they are certainly weak.

Reaction of the early metal diphosphides to displace ethylene from $(C_2H_4)_2Rh(indenyl)$ led to the ELHB complexes $Cp_2M(\mu\text{-}PR_2)_2Rh(indenyl)$ (M = Zr, R = Ph **6.17**, Et **6.18**; M = Hf, R = Ph **6.43**, Et **6.44** [122]. A crystallographic study of **6.17** shows a Zr–Rh distance of 3.088(1) Å. In addition, the indenyl ligand shows a pronounced "slip–fold" distortion relative to a planar η^5-indenyl ligand. Variable-temperature ^1H NMR studies revealed that the indenyl ring is involved in a hindered rotation about the Zr–Rh vector. At the low temperature limit, the ^1H NMR spectrum of these compounds shows two phenyl and Cp environments, as expected from the solid state structure. At the high temperature end, averaging of the signals is seen and is attributed to rapid rotation of the indenyl group. The energy of activation for this hindered indenyl rotation ranged from 13.9 to 15.0 kcal mol^{-1} for the four compounds studied. The magnitudes of the observed barriers were attributed to the slip–fold distortion of the indenyl ring.

Reactions of $Cp_2Zr(PPh_2)_2$ with zerovalent complexes of nickel, palladium and platinum led to a variety of ELHB species [123,124]. For example, reactions of the zirconocene diphosphide with $M(PPh_3)_4$ led to the ELHB species $Cp_2Zr(\mu\text{-}PPh_2)_2MPPh_3$ (M = Ni **6.28**, Pd **6.30**, Pt **6.31**) (eqn. (16)):

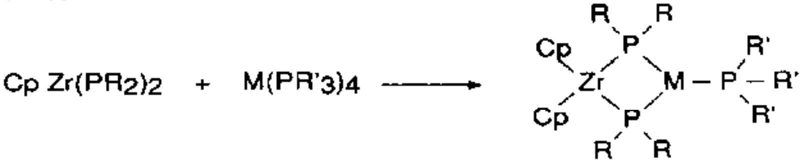

(16)

Similar reactions involving $(Ph_3P)_2Ni(CO)_2$ led to the formation of $Cp_2Zr(\mu\text{-}PPh_2)_2Ni(CO)_2$ **6.29**.

The complex **6.31** reacts with basic phosphines to yield related ELHB complexes in which the more basic phosphines replace the PPh_3 on platinum.

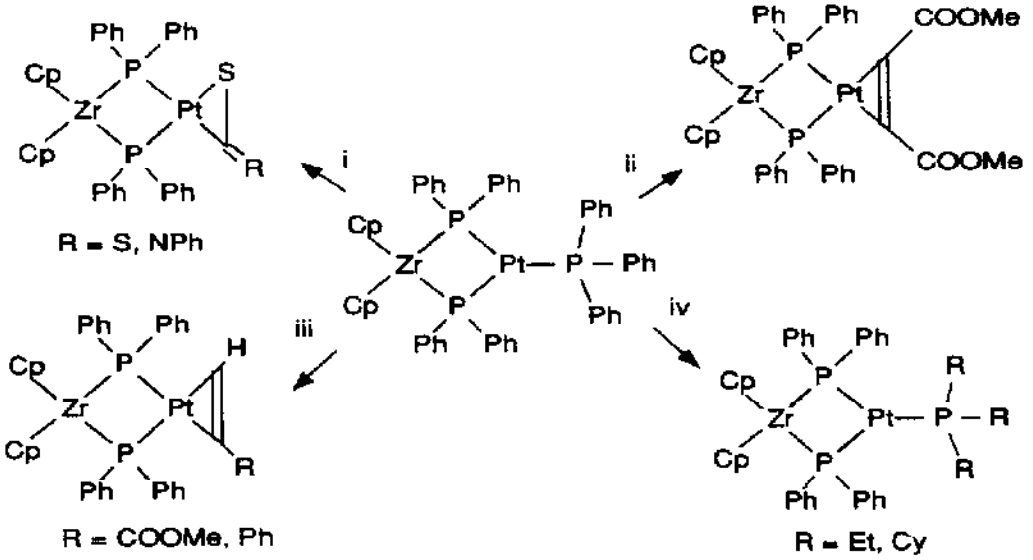

Fig. 23. Reactions of **6.31**: i = SCNPh or CS_2; ii = $MeO_2CC{\equiv}CCO_2Me$; iii = $HC{\equiv}CPh$ or $HC{\equiv}CCO_2Me$ with MeI (loss of PPh_3MeI); iv = PEt_3 or PCy_3.

In addition to phosphine substitution reactions, **6.31** also reacts with a variety of heteroallenes and acetylenes [124]. Activated acetylenes, as well as CS_2 and isothiocyanates, undergo facile reaction with **6.31** to replace the phosphine on platinum (Fig. 23). Reaction with less activated acetylenes results in equilibria between **6.31** and the acetylene-substituted product. These equilibria can be forced to the side of the acetylene product by using MeI as a phosphine scavenger [124].

Structural studies [125] of the related species $Cp_2Hf(\mu\text{-}PPh_2)_2PdPPh_3$ **6.49** have been performed by Baker and coworkers. The non-planar nature of the HfP_2Pd core as well as the Hf–Pd distance of 2.896(1) Å have been interpreted in terms of a Pd(d^{10})-to-Hf(d^0) dative bond.

The preparation of the ELHB complexes $Cp_2M(\mu\text{-}PR_2)_2M'H(CO)(PPh_3)$ (M = Zr, M′ = Rh, R = Ph **6.20**, Cy **6.21**, M′ = Ir, R = Ph **6.26**, Cy **6.27**; M = Hf, M′ = Rh, R = Ph **6.47**, Cy **6.48**) is achieved by reaction of the early metal diphosphides with the late metal carbonyl hydrido species $M'H(CO)(PPh_3)_3$ [126]. The complex **6.20** undergoes phosphine and CO substitution reactions to yield $Cp_2Zr(\mu\text{-}PPh_2)_2RhH(CO)(L)$ (L = PCy_3 **6.22**, PEt_3 **6.23**, CO **6.24**). Treatment of **6.20** with base results in deprotonation and yields the d^{10}–d^0 ELHB anion $[Cp_2Zr(\mu\text{-}PPh_2)_2Rh(CO)PPh_3]^-$ **6.25** [126]. In addition, **6.20** acts as a catalyst precursor for the catalytic hydroformylation of 1-hexene. The rate of catalysis is considerably slower than that of known monometallic rhodium catalysts; however, use of the ELHB catalyst precursor leads to a dramatic increase in selectivity for the terminal

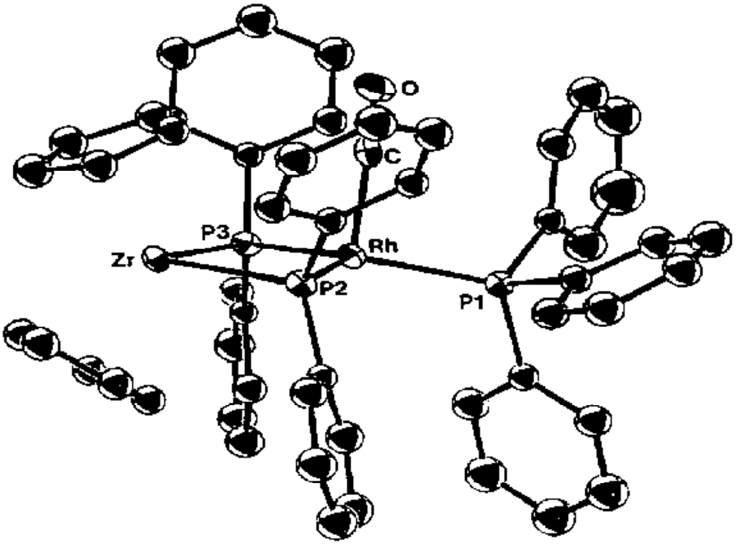

Fig. 24. ORTEP drawing of **6.20**. Reproduced with permission from ref. 127. Copyright 1988 American Chemical Society.

aldehyde product. Although a heterobimetallic species has been implicated as the actual catalyst, this has not been unequivocally confirmed.

Structural studies of $Cp_2M(\mu\text{-}PPh_2)_2RhH(CO)(PPh_3)$ (M = Zr **6.20**, Hf **6.46**) indicate that these compounds are isostructural [127]. The MP_2Rh cores are not planar, but rather are of a "butterfly" shape, with a dihedral angle between the MP_2 and P_2Rh planes of about 10°. The M–P–Rh angles range from 72.4° to 73.2°, while the M–Rh distances are 2.980(1) Å and 2.964(1) Å for **6.20** and **6.46** respectively. The structural data were interpreted in terms of a bonding mode involving a dative interaction between the d^8 rhodium center and the d^0 early metal (Fig. 24).

Related to the above complexes are several others that contain thorium and a late transition metal. $Cp_2^*Th(\mu\text{-}PPh_2)_2Ni(CO)_2$ **6.50** [128] was prepared from the reaction of $Cp_2^*Th(PPh_2)_2$, $Ni(COD)_2$ (COD = C_8H_{12}) and CO. This complex was found to have a Th–Ni distance of 3.206(2) Å which is ca. 0.5 Å less than the expected non-bonding distance. In addition, the geometry of the ThP_2Ni core suggests a direct metal–metal interaction. This postulate was later supported by the results of extended Hückel molecular orbital calculations performed for the model compound $Cp_2Th(\mu\text{-}PH_2)_2Ni(CO)_2$ [129]. The related complex, $Cp_2^*Th(\mu\text{-}PPh_2)_2PtPMe_3$ **6.51**, was prepared via reaction of $Cp_2^*Th(PPh_2)_2$ with $Pt(COD)_2$ and PMe_3 [130]. A structural study of **6.51** shows a dihedral angle of 45.2° between the ThP_2 and PtP_3 planes. The Th–P–Pt angles were found to be 69.1(1)° and 67.8(1)°, with a Th–Pt distance of 2.984(1) Å (Fig. 25). These data suggest a

TABLE 5

Amido- and phosphido-bridged ELHB complexes

M–M′	Number	Complex	M–M′ distance (Å)	Ref.
Ti–Fe	**6.1**	$Cp_2Ti(\mu\text{-}PPh_2)_2Fe(CO)_3$		117
Ti–Cr	**6.2**	$CpTi(\mu\text{-}NMe_2)_3Cr(CO)_3$		116
Ti–Mo	**6.3**	$Cp_2Ti(\mu\text{-}PHPh)_2Mo(CO)_4$		114
	6.4	$Cp_2Ti(\mu\text{-}PPh(SiMe_3))_2Mo(CO)_4$		114
	6.5	$Cp_2Ti(\mu\text{-}PMe)_2Mo(CO)_4$		115
	6.6	$CpTi(\mu\text{-}NMe_2)_3Mo(CO)_3$		116
Ti–W	**6.7**	$CpTi(\mu\text{-}NMe_2)_3W(CO)_3$		116
	6.8	$Cp_2Ti(\mu\text{-}PPh_2)_2W(CO)_4$		117
Zr–Fe	**6.9**	$Cp_2Zr(\mu\text{-}PCy_2)_2Fe(CO)_3$		117
	6.10	$Cp_2Zr(\mu\text{-}PPh_2)_2Fe(CO)_3$		117
Zr–Mo	**6.11**	$Cp_2Zr(\mu\text{-}PPh_2)_2Mo(CO)_4$	3.299 (1)	119, 120
	6.12	$Cp_2Zr(\mu\text{-}PMe_2)_2Mo(CO)_4$		115
	6.13	$Cp_2Zr(\mu\text{-}PHPh)_2Mo(CO)_4$		114
	6.14	$Cp_2Zr(\mu\text{-}PPh(SiMe_3))_2Mo(CO)_4$		114
Zr–W	**6.15**	$Cp_2Zr(\mu\text{-}PPh_2)_2W(CO)_4$	3.289 (1)	117
Zr–Re	**6.16**	$Cp_2Zr(\mu\text{-}PPh_2)_2ReH(CO)_3$	3.275 (1)	121
Zr–Rh	**6.17**	$Cp_2Zr(\mu\text{-}PPh_2)_2Rh(indenyl)$		122
	6.18	$Cp_2Zr(\mu\text{-}PEt_2)_2Rh(indenyl)$	3.088 (1)	122
	6.19	$[Cp_2Zr(\mu\text{-}PEt_2)_2Rh(indenyl)Me]I$		122
	6.20	$Cp_2Zr(\mu\text{-}PPh_2)_2RhH(CO)PPh_3$	2.980 (1)	127
	6.21	$Cp_2Zr(\mu\text{-}PCy_2)_2RhH(CO)PPh_3$		127
	6.22	$Cp_2Zr(\mu\text{-}PPh_2)_2RhH(CO)PCy_3$		127
	6.23	$Cp_2Zr(\mu\text{-}PPh_2)_2RhH(CO)PEt_3$		127
	6.24	$Cp_2Zr(\mu\text{-}PPh_2)_2RhH(CO)_2$		127
	6.25	$[Cp_2Zr(\mu\text{-}PPh_2)_2Rh(CO)PPh_3]^-$		126
Zr–Ir	**6.26**	$Cp_2Zr(\mu\text{-}PPh_2)_2IrH(CO)PPh_3$		127
	6.27	$Cp_2Zr(\mu\text{-}PCy_2)_2IrH(CO)PPh_3$		127
Zr–Ni	**6.28**	$Cp_2Zr(\mu\text{-}PPh_2)_2NiPPh_3$		123, 124
	6.29	$Cp_2Zr(\mu\text{-}PPh_2)_2Ni(CO)_2$		123
Zr–Pd	**6.30**	$Cp_2Zr(\mu\text{-}PPh_2)_2PdPPh_3$		123, 124
Zr–Pt	**6.31**	$Cp_2Zr(\mu\text{-}PPh_2)_2PtPPh_3$		123, 124
	6.23	$Cp_2Zr(\mu\text{-}PPh_2)_2PtPCy_3$		124
	6.33	$Cp_2Zr(\mu\text{-}PPh_2)_2PtPEt_3$		124
	6.34	$Cp_2Zr(\mu\text{-}PPh_2)_2Pt(CS_2)$		124
	6.35	$Cp_2Zr(\mu\text{-}PPh_2)_2Pt(SCNPh)$		124
	6.36	$Cp_2Zr(\mu\text{-}PPh_2)_2Pt(MeO_2CCCCO_2Me)$		123, 124
	6.37	$Cp_2Zr(\mu\text{-}PPh_2)_2Pt(MeO_2CCCH)$		124
	6.38	$Cp_2Zr(\mu\text{-}PPh_2)_2Pt(PhCCH)$		124
Hf–Fe	**6.39**	$Cp_2Hf(\mu\text{-}PEt_2)_2Fe(CO)_3$		118
	6.40	$Cp_2(PEt_2)Hf(\mu\text{-}PEt_2)Fe(CO)_4$		118
Hf–Mo	**6.41**	$Cp_2Hf(\mu\text{-}PEt_2)_2Mo(CO)_4$	3.400 (1)	118
Hf–Pd	**6.42**	$Cp_2Hf(\mu\text{-}PEt_2)_2Ni(CO)_2$		118
Hf–Rh	**6.43**	$Cp_2Hf(\mu\text{-}PPh_2)_2Rh(indenyl)$		122
	6.44	$Cp_2Hf(\mu\text{-}PEt_2)_2Rh(indenyl)$		122

TABLE 5 (continued)

M–M′	Number	Complex	M–M′ distance (Å)	Ref.
Hf–Rh	**6.45**	$[Cp_2Hf(\mu\text{-}PEt_2)_2Rh(indenyl)Me]I$		122
	6.46	$Cp_2Hf(\mu\text{-}PPh_2)_2RhH(CO)PPh_3$	2.964 (1)	127
	6.47	$Cp_2Hf(\mu\text{-}PCy_2)_2RhH(CO)PPh_3$		127
Hf–Ir	**6.48**	$Cp_2Hf(\mu\text{-}PPh_2)_2IrH(CO)PPh_3$		127
Hf–Pd	**6.49**	$Cp_2Hf(\mu\text{-}PPh_2)_2PdPPh_3$	2.896 (1)	125
Th–Ni	**6.50**	$Cp^*_2Th(\mu\text{-}PPh_2)_2Ni(CO)_2$	3.206 (1)	128
Th–Pt	**6.51**	$Cp^*_2Th(\mu\text{-}PPh_2)_2PtPMe_3$	2.984 (1)	130

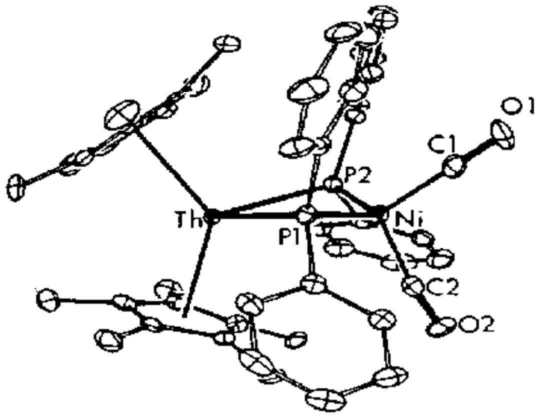

Fig. 25. ORTEP drawing of **6.51**. Reproduced with permission from ref. 128. Copyright 1985 American Chemical Society.

bond. Molecular orbital calculations are consistent with a donor–acceptor or dative bond in which electron density from the filled d^{10} shell on platinum is donated to the empty *d* shell on thorium.

7. SELENOLATO- AND THIOLATO-BRIDGED ELHB COMPLEXES

The first report of thiolato-bridged ELHB complexes appeared almost 30 years ago when Joshi et al. communicated the preliminary characterization of the products of the reaction of $Cp_2Ti(SMe)_2$ with $(NBD)Mo(CO)_4$ (NBD $= C_7H_8$) and $[(COD)CuCl]_2$ [131]. The formulations as the thiolato-bridged ELHB complexes $Cp_2Ti(\mu\text{-}SMe)_2Mo(CO)_4$ **7.3** and $[Cp_2Ti(\mu\text{-}SMe)_2CuCl]_2$ **7.26** respectively were based solely on the elemental analyses and IR data. Kopf and Rathlein [132] reported that the photolysis of $Mo(CO)_6$ in the

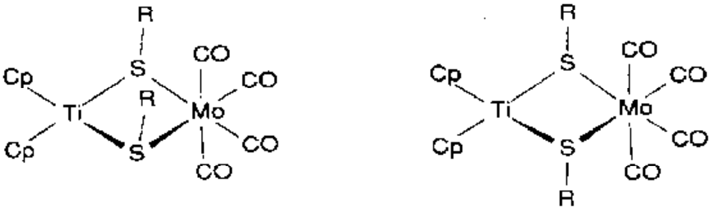

Fig. 26. *Cisoid* and *transoid* conformers of $Cp_2Ti(\mu\text{-}SR)_2Mo(CO)_4$.

presence of $Cp_2Ti(XPh)_2$ led to the formation of $Cp_2Ti(\mu\text{-}XPh)_2Mo(CO)_4$ (X = S **7.5**, Se **7.6**). The related species $Cp_2Ti(\mu\text{-}SMe)_2M(CO)_4$ (M = Cr **7.1**, Mo **7.3**, W **7.11**), $Cp_2Ti(\mu\text{-}SPh)_2W(CO)_4$ **7.13** and **7.5** were also prepared by the thermal reaction of the appropriate $Cp_2Ti(SR)_2$ with $(NBD)M(CO)_4$ [133].

These thiolato-bridged complexes exist in two isomeric forms in solution, a *cisoid* and a *transoid* conformer (Fig. 26) [134,135]. For the related complex, $Cp_2Ti(\mu\text{-}SH)_2Mo(CO)_4$ **7.7** [134], variable-temperature ^1H NMR data show that the thermodynamically favored conformer is the *cisoid* form. The equilibrium constant at 298 K was found to be 0.6. The activation energy for the isomerization process was calculated to be 76 kJ mol^{-1} for the complex $Cp_2Ti(\mu\text{-}SH)_2W(CO)_4$ **7.14**. The mechanism for this isomerization was proposed to involve pyramidal inversion at sulfur. In addition, the observation of a rate enhancement in the presence of base was indicative of a facile base-catalyzed pathway.

Low energy bands in the UV–visible spectra of the compounds **7.1**, **7.3**, **7.5**, **7.11** and **7.13** were assigned to transitions involving both of the metal atoms and suggest some degree of metal–metal bonding [136]. IR and ^1H NMR spectra of **7.1**, **7.3** and **7.11** were consistent with the postulate of metal–metal bonding [133]. The possibility of a dative donation from the d^6 metal center to the d^0 titanium center was subsequently supported by the X-ray crystallographic study of **7.3** [135,137]. The Ti–Mo distance of 3.32 Å is approximately 0.7 Å shorter than the metal–metal distances seen in the thiolato-bridged complexes $Cp_2W(\mu\text{-}SPh)_2M(CO)_4$ (M = Cr, Mo, W). Thus the bonding in these ELHB species was described in terms of contributions from the two resonance forms (Fig. 27). The existence of a direct metal–metal interaction, rather than a relay of electron density through the sulfur

Fig. 27. Bonding in dithiolato-bridged ELHB complexes.

d-orbitals, was favored on the basis of spectroscopic and structural data. In particular, the S–Ti–S angle in **7.3** is widened to 99.9° compared with the analogous angle in Cp_2TiS_5 (94.6°), while the the acuteness of the angle at the bridging atoms was cited as evidence for a direct metal–metal interaction.

Cyclic voltammetric studies [138] of the complexes **7.5** and **7.13**, as well as of the compounds $Cp_2Ti(\mu\text{-SEt})_2M(CO)_4$ (M = Cr **7.2**, Mo **7.4**, W **7.12**) display quasi-reversible electrochemistry at both the Ti(IV) and M(0) sites. The waves at negative potentials vs. the standard calomel electrode (SCE) were assigned to the Ti(IV)/Ti(III) redox couple. The redox processes at positive potentials were assigned to the oxidation of the M(0). Attempts to perform bulk reductions or oxidations led to decomposition of the ELHB complexes. Although speculation regarding the observed trends in the values of the redox potential involved the presence of donor–acceptor M(0)–Ti(IV) bonds, such a rationale was not fully supported by the data.

The chemistry of the complex $Cp_2Ti(\mu\text{-SH})_2Mo(CO)_4$ **7.7** was investigated by Ruffing and Rauchfuss [134]. Treatment of **7.7** with strong base leads to the formation of the blue dianion $[Cp_2Ti(\mu\text{-S})_2Mo(CO)_4]^{2-}$ **7.8** (Fig. 28). This species reacts with MeI to yield the methanethiolato-bridged species **7.3**. Reaction of **7.7** with $CH_2{=}CHCO_2Me$ results in the formation of $Cp_2Ti(\mu\text{-SCH}_2CH_2CO_2Me)_2Mo(CO)_4$ **7.9** (Fig. 29). Reactions of **7.7** with S_8, Cp_2TiS_5 and Ph_2E_2 (E = S, Se) lead to degradation of the ELHB complex to various titanium species.

The related ELHB complex, $Cp_2Nb(\mu\text{-SMe})_2Mo(CO)_4$ **7.41**, can be prepared via the reaction of $Cp_2Nb(SMe)_2$ with $(NBD)Mo(CO)_4$ [139]. The resulting paramagnetic ELHB complex is unstable, but it does exhibit the expected ten-line EPR spectrum (^{93}Nb $I = 9/2$). In a related study, the reactions of $Cp_2Nb(SMe)_2$ with $NiCl_2$ or $(PhCN)_2MCl_2$ (M = Pd, Pt) were found to yield the trimetallic species of the form $[(Cp_2Nb(\mu\text{-SMe})_2)_2M]^{2+}$ (M = Ni **7.48**, Pd **7.49**, Pt **7.50**). Complex **7.48** was structurally characterized [140,141]. Similarly, reaction of $Cp_2Ta(SMe)_2$ with $(PhCN)_2PtCl_2$ yielded

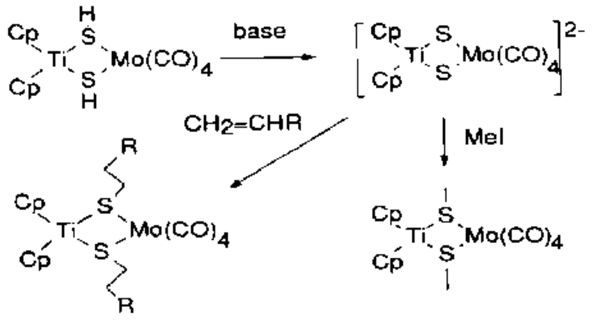

Fig. 28. Reactions of 7.7.

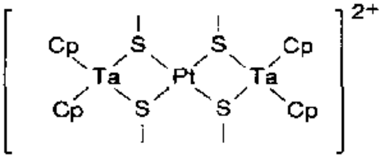

Fig. 29. Structure of **7.51**.

the trimetallic species $[(Cp_2Ta(\mu\text{-}SMe)_2)_2Pt][PF_6]_2$ **7.51** [142]. A structural study of **7.51** shows the platinum coordination sphere to be essentially tetrahedral, indicative of a formally Pt(0) oxidation state (Fig. 29). Metal–metal bonding was suggested on the basis of the Ta–Pt distance (2.788(1) Å) and Ta–S–Pt angles (ca. 70°).

The complexes $Cp_2Ti(\mu\text{-}ER)_2Fe(NO)_2$ (ER = SMe **7.15**, SPh **7.16**, SeMe **7.17**, SePh **7.18**, TePh **7.19**) and $Cp_2Nb(\mu\text{-}EPh)_2ML_x$ (ML_x = Fe(CO)(NO), E = S **7.42**, Se **7.43**, Te **7.44**; $ML_x = Co(CO)_2$, E = S **7.45**, Se **7.46**, Te **7.47**) were prepared via reaction of $Cp_2M(ER)_2$ with $Hg[Fe(CO)_3(NO)]_2$ or $Hg[Co(CO)_4]_2$ [143]. The niobium complexes are diamagnetic, suggesting that, in addition to the bridging organochalcogen groups, there are also Nb–M (M = Fe or Co) bonds in these complexes.

The ELHB complexes $[Cp_2Ti(\mu\text{-}SR)_2NiCp]BF_4$ (R = Me **7.20**, Ph **7.21**) can be prepared from the reaction of the triple-decker sandwich complex, $[Ni_2Cp_3]BF_4$, with $Cp_2Ti(SR)_2$ [144]. Attempts to prepare the analogous V(IV) species led only to monometallic species in which anion exchange had occurred. The Ti–Ni ELHB complexes **7.20** and **7.21** exhibit temperature-dependent ^1H NMR spectra which were interpreted in terms of the isomerization of the *cisoid/transoid* species. The mechanism suggested was pyramidal inversion at sulfur.

The Ti–Cu complexes $[Cp_2Ti(SR)_2CuX]_n$ (X = Cl, R = Me **7.26**, Ph **7.27**; X = Br, R = Me **7.28**, Ph **7.29**) were first reported by Braterman and Wilson in 1971 [145]. These insoluble complexes were prepared by reaction of $Cp_2Ti(SR)_2$ and $[(COD)CuX]_2$. Characterization of these complexes was limited; however, low energy bands in the diffuse reflectance spectra suggested Cu(I)–Ti(IV) dative bonding.

White and Stephan [146] have described the synthesis and structure of the Ti–Cu complex $[Cp_2Ti(\mu\text{-}SCH_2CH_2PPh_2)_2Cu][BF_4]$ **7.30**. This compound was prepared by reaction of the metalloligand $Cp_2Ti(SCH_2CH_2PPh_2)_2$ with $[Cu(MeCN)_4]BF_4$. The resulting Ti–Cu complex exhibits a reversible wave in the cyclic voltammogram, which corresponds formally to a Ti(IV)/Ti(III) redox couple. The corresponding reduction of the metalloligand is not reversible, and thus the electrochemical behavior of the ELHB species **7.30** is attributed to the rigidity of the bimetallic. The green–black complex **7.30** exhibits low energy absorptions in the UV–visible spectrum, similar to those seen for the polymeric Ti–Cu species described by Braterman and Wilson, thus suggesting a Cu–Ti dative interaction. The X-ray study of this species offers structural data in support of this postulate (Fig. 30). The angles at the sulfur atoms which bridge the pseudotetrahedral coordination spheres of the titanium and copper atoms (i.e. the Ti–S–Cu angles) are 78.0(1)°. The S–Ti–S and S–Cu–S angles are 97.5(1)° and 106.4(1)° respectively, with a Ti ··· Cu separation of 3.024(1) Å. These data are consistent with a Cu(I) d^{10} to Ti(IV) d^0 dative interaction.

More recently, Wark and Stephan [147] have described a series of related Ti–Cu species of the form $[Cp_2Ti(\mu\text{-}SEt)_2CuL]^+$ (L = PPh_3 **7.31**, PCy_3 **7.32**, PEt_3 **7.33**, $P(CH_2Ph)_3$ (PBz_3) **7.34**, $PhPCH_2CH_2PPh_2$ (diphos) **7.35**, C_5H_5N (py) **7.36**). These complexes were prepared via reaction of $Cp_2Ti(SEt)_2$ with $[Cu(MeCN)_4]PF_6$ in the presence of the appropriate ligand. Similar to the Ti–M (M = Cr **7.1**, Mo **7.3**, W **7.11**) thiolato-bridged complexes, these Ti–Cu species also exist in two conformations corresponding to the two isomers in which the ethyl substituents are either *cisoid* or *transoid* in disposition. The activation energy for the isomerization process for **7.32** was found to be about 72 kcal mol^{-1} with the *cisoid* conformer favored at low temperatures. This may reflect the minimization of steric interactions be-

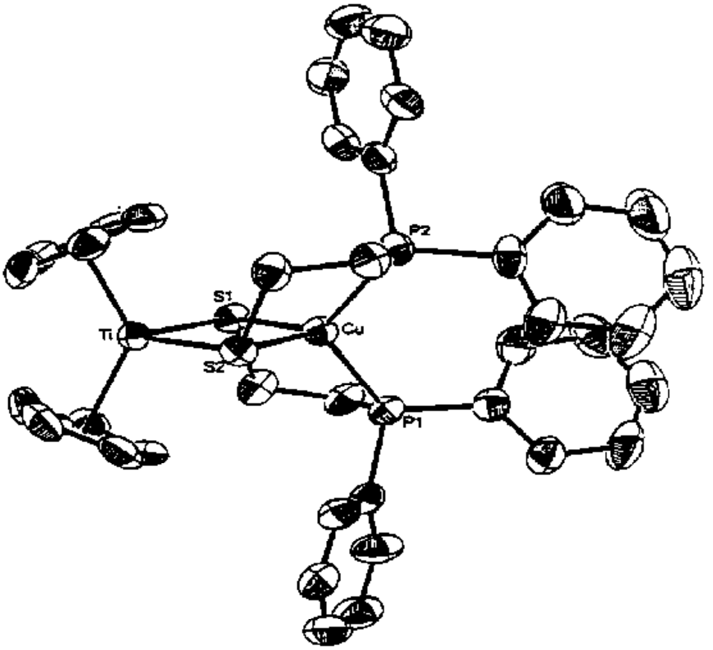

Fig. 30. ORTEP drawing of **7.30**. Reproduced with permission from ref. 146. Copyright 1985 American Chemical Society.

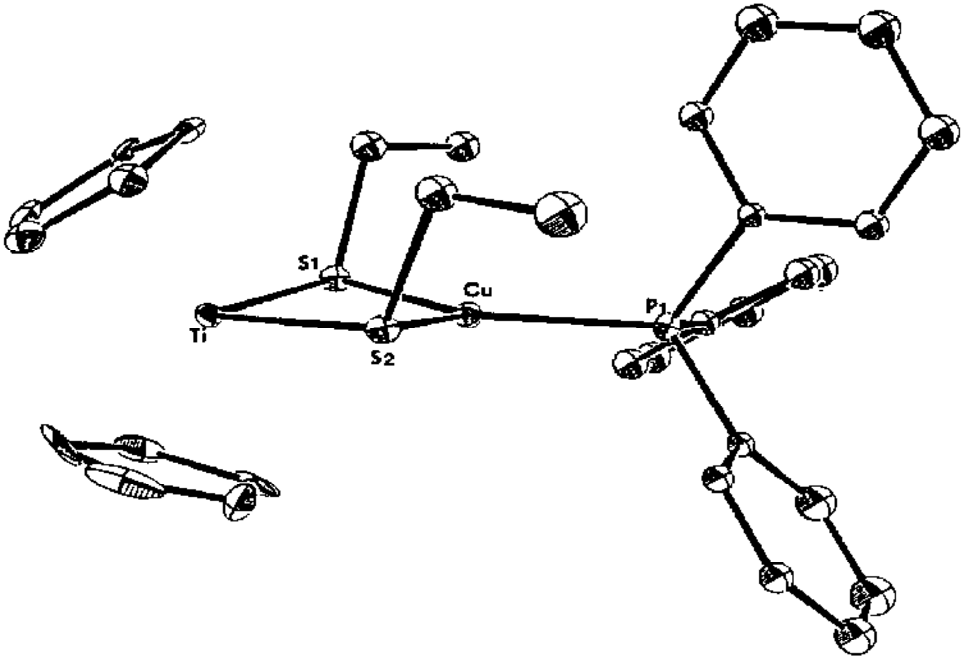

Fig. 31. ORTEP drawing of 7.31. Reproduced with permission from ref. 147. Copyright 1987 American Chemical Society.

tween the ethyl groups of the bridging thiolato groups and the substituents on the phosphine bound to copper. Structural studies of **7.31** (Fig. 31) and **7.32** were reported. Angles at sulfur of 72.9(1)°–74.1(1)°, an S–Ti–S angle of 99.1(1)°, S–Cu–S angles of 110.9(1)° and 114.1(1)° and Ti–Cu separations of 2.803(3) and 2.840(2) Å strongly support the notion of copper-to-titanium dative bonding. Preliminary extended Hückel and Xα molecular orbital calculations are consistent with such a metal–metal interaction. Additional INDO calculations gave a Ti–Cu bond order of 0.2.

The structurally related paramagnetic complexes $[Cp_2V(SEt)_2CuPR_3]^+$ (R = Ph **7.39**, Cy **7.40**) have been prepared by a synthetic route analogous to that used for the Ti–Cu ELHB complexes, employing the vanadocene dithiolate as a metalloligand [148]. The EPR spectra of these species are consistent with coupling of the unpaired electron on vanadium to the nuclear spin of vanadium, as well as both copper and phosphorus nuclei. On the basis of molecular orbital calculations performed for structurally related systems, the *transannular* coupling of the electron to copper is believed to occur through space rather than through the bridging sulfur atoms, thus further supporting the notion of direct electronic communication between the metal centers.

White and Stephan [149,150] have investigated the structures and chem-

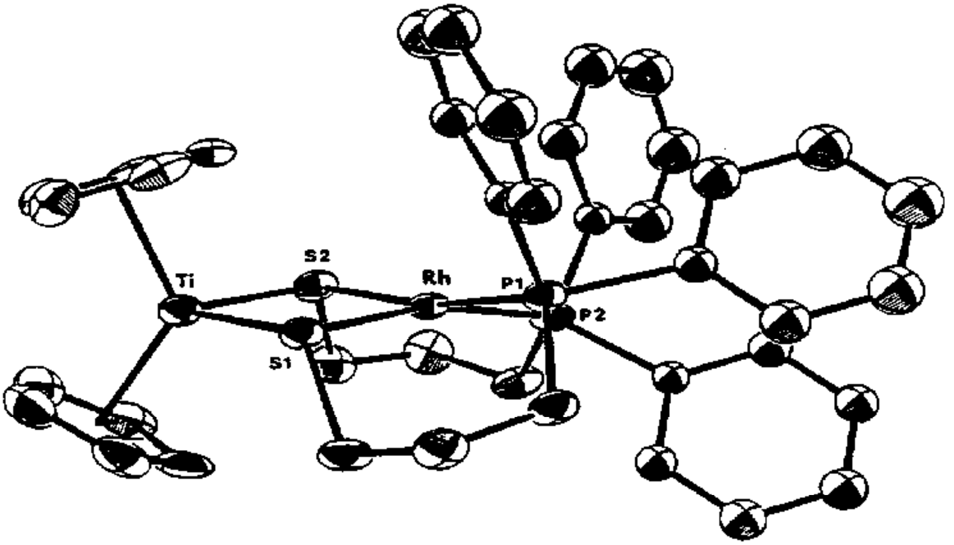

Fig. 32. ORTEP drawing of 7.37. Reproduced with permission from ref. 149. Copyright 1987 American Chemical Society.

istry of the related species $[Cp_2Ti(SCH_2CH_2CH_2PPh_2)_2Ni]$ **7.22** and $[Cp_2Ti(SCH_2CH_2CH_2PPh_2)_2Rh]^+$ **7.37**. Both these species were prepared via a reaction between the titanocene dithiolate metalloligand and a late metal complex containing easily replaceable ligands. Structural characterizations of **7.22** and **7.37** (Fig. 32) show that the metalloligand is capable of accomodating a late metal center in either a pseudotetrahedral or pseudo-square-planar geometry respectively. In **7.22**, the metalloligand wraps about the nickel atom in a manner similar to that seen in **7.30**. The core parameters, and in particular the Ti · · · Ni distance of 2.825(3) Å, suggest a dative $d^{10} \rightarrow d^0$ interaction. The structural data for **7.37** are consistent with a decreased degree of metal–metal interaction, presumably as a result of the poorer donor ability of the d^8 rhodium center compared with the d^{10} Cu(I) and Ni(0) centers in **7.30** and **7.22** respectively.

The complexes **7.22** and **7.37** exhibit reversible waves in the cyclic voltammogram. For **7.22**, two reversible waves attributed to consecutive reversible one-electron oxidations of the Ni(0) to Ni(I) (i.e. **7.23**) and to Ni(II) (i.e. **7.24**) are observed. Attempts to oxidize **7.22** chemically led to degradation of the ELHB complex to $[Ni_3(SCH_2CH_2CH_2PPh_2)_4]^{2+}$. Although the Ni(II) species is apparently thermodynamically unstable, the palladium analog **7.25** can be prepared via direct reaction of the titanocene dithiolate metalloligand with $[Pd(MeCN)_4]^{2+}$. In the case of **7.37**, the reversible electrochemistry is attributed to redox chemistry at the titanium metal center. The reduced Ti–Rh species **7.38** can be generated by reaction

TABLE 6

Selenolato- and thiolato-bridged ELHB complexes

M–M′	Number	Complex	M–M′ distance (Å)	Ref.
Ti–Cr	**7.1**	$Cp_2Ti(\mu\text{-SMe})_2Cr(CO)_4$		131, 132, 136
	7.2	$Cp_2Ti(\mu\text{-SEt})_2Cr(CO)_4$		138
Ti–Mo	**7.3**	$Cp_2Ti(\mu\text{-SMe})_2Mo(CO)_4$	3.321(2)	131, 132 135–137
	7.4	$Cp_2Ti(\mu\text{-SEt})_2Mo(CO)_4$		138
	7.5	$Cp_2Ti(\mu\text{-SPh})_2Mo(CO)_4$		132, 133, 136
	7.6	$Cp_2Ti(\mu\text{-SePh})_2Mo(CO)_4$		132
	7.7	$Cp_2Ti(\mu\text{-SH})_2Mo(CO)_4$		134
	7.8	$[Cp_2Ti(\mu\text{-S})_2Mo(CO)_4]^{2-}$		134
	7.9	$Cp_2Ti(\mu\text{-SCH}_2CH_2CO_2Me)_2Mo(CO)_4$		134
	7.10	$(MeCp)_2Ti(\mu\text{-SPh})_2Mo(CO)_4$		134
Ti–W	**7.11**	$Cp_2Ti(\mu\text{-SMe})_2W(CO)_4$		133, 136
	7.12	$Cp_2Ti(\mu\text{-SEt})_2W(CO)_4$		138
	7.13	$Cp_2Ti(\mu\text{-SPh})_2W(CO)_4$		133, 136
	7.14	$Cp_2Ti(\mu\text{-SH})_2W(CO)_4$		134
	7.15	$Cp_2Ti(\mu\text{-SMe})_2Fe(NO)_2$		143
	7.16	$Cp_2Ti(\mu\text{-SPh})_2Fe(NO)_2$		143
	7.17	$Cp_2Ti(\mu\text{-SeMe})_2Fe(NO)_2$		143
	7.18	$Cp_2Ti(\mu\text{-SePh})_2Fe(NO)_2$		143
	7.19	$Cp_2Ti(\mu\text{-TePh})_2Fe(NO)_2$		143
Ti–Ni	**7.20**	$[Cp_2Ti(\mu\text{-SMe})_2NiCp]^+$		144
	7.21	$[Cp_2Ti(\mu\text{-SPh})_2NiCp]^+$		144
	7.22	$[Cp_2Ti(\mu\text{-SCH}_2CH_2CH_2PPh_2)_2Ni]$	2.825(3)	150
	7.23	$[Cp_2Ti(\mu\text{-SCH}_2CH_2CH_2PPh_2)_2Ni]^+$		150
	7.24	$[Cp_2Ti(\mu\text{-SCH}_2CH_2CH_2PPh_2)_2Ni]^{2+}$		150
Ti–Pd	**7.25**	$[Cp_2Ti(\mu\text{-SCH}_2CH_2CH_2PPh_2)_2Pd]^{2+}$		150
Ti–Cu	**7.26**	$[Cp_2Ti(\mu\text{-SMe})_2CuCl]_2$		131, 145
	7.27	$[Cp_2Ti(\mu\text{-SPh})_2CuCl]_n$		145
	7.28	$[Cp_2Ti(\mu\text{-SMe})_2CuBr]_n$		145
	7.29	$[Cp_2Ti(\mu\text{-SPh})_2CuBr]_n$		145
	7.30	$[Cp_2Ti(\mu\text{-SCH}_2CH_2CH_2PPh_2)_2Cu]^+$	3.024(1)	146
	7.31	$[Cp_2Ti(\mu\text{-SEt})_2CuPPh_3]^+$	2.803(1)	147
	7.32	$[Cp_2Ti(\mu\text{-SEt})_2CuPCy_3]^+$	2.840(1)	147
	7.33	$[Cp_2Ti(\mu\text{-SEt})_2CuPEt_3]^+$		147
	7.34	$[Cp_2Ti(\mu\text{-SEt})_2CuPBz_3]^+$		147
	7.35	$[Cp_2Ti(\mu\text{-SEt})_2CuPPh_2CH_2CH_2PPh_2]^+$		147
	7.36	$[Cp_2Ti(\mu\text{-SEt})_2Cupy]^+$		147
Ti–Rh	**7.37**	$[Cp_2Ti(\mu\text{-SCH}_2CH_2CH_2PPh_2)_2Rh]^+$	3.127(2)	149
	7.38	$[Cp_2Ti(\mu\text{-SCH}_2CH_2CH_2PPh_2)_2Rh]^0$		149
V–Cu	**7.39**	$[Cp_2V(\mu\text{-SEt})_2CuPPh_3]^+$		148
	7.40	$[Cp_2V(\mu\text{-SEt})_2CuPCy_3]^+$		148

TABLE 6 (continued)

M–M′	Number	Complex	M–M′ distance (Å)	Ref.
Nb–Mo	**7.41**	$Cp_2Nb(\mu\text{-}SMe)_2Mo(CO)_4$		139
	7.42	$Cp_2Nb(\mu\text{-}SPh)_2Fe(CO)(NO)$		143
	7.43	$Cp_2Nb(\mu\text{-}SePh)_2Fe(CO)(NO)$		143
	7.44	$Cp_2Nb(\mu\text{-}TePh)_2Fe(CO)(NO)$		143
	7.45	$Cp_2Nb(\mu\text{-}SPh)_2Co(CO)_2$		143
	7.46	$Cp_2Nb(\mu\text{-}SePh)_2Co(CO)_2$		143
	7.47	$Cp_2Nb(\mu\text{-}TePh)_2Co(CO)_2$		143
Nb–Ni	**7.48**	$[(Cp_2Nb(\mu\text{-}SMe)_2)_2Ni]^{2+}$	2.765(5) 2.776(5)	139–141
Nb–Pd	**7.49**	$[(Cp_2Nb(\mu\text{-}SMe)_2)_2Pd]^{2+}$		139
Nb–Pt	**7.50**	$[(Cp_2Nb(\mu\text{-}SMe)_2)_2Pt]^{2+}$		139
Ta–Pt	**7.51**	$[(Cp_2Ta(\mu\text{-}SMe)_2)_2Pt]^{2+}$	2.788(1) 2.809(7)	142

of **7.37** with Cp_2Co. The EPR spectrum of **7.38** shows clearly the presence of coupling of the unpaired electron, centered on titanium, to both rhodium and the two phosphorus atoms. This observation, together with the results of molecular orbital calculations on related systems, suggest direct through-space communication between the metal centers [151].

The relevance of metal–metal interactions in these thiolato-bridged ELHB complexes to SMSI is clear. In particular, it is noteworthy that studies of heterogeneous systems, in which titania is the support, have implied that the SMSI effects may arise via interaction of reduced titanium centers with the later transition metal. Thus Ti(III)–M interactions observed in the homogeneous ELHB complexes may be analogous to those occurring in the heterogeneous catalyst systems.

8. CHALCOGENIDE-ATOM-BRIDGED ELHB COMPLEXES

While the coordination chemistry of thiometallates has been studied extensively [152], few of the known bimetallic derivatives are organometallic ELHB species. Ruffing and Rauchfuss have studied the chemistry of the chalcogenide-bridged ELHB complex $[Cp_2TiS_2Mo(CO)_4]^{2-}$ **7.8** [134] which was described in Section 7. Rauchfuss and coworkers [153–156] have also studied the utility of $(C_5H_4Me)_2V_2S_4$ in the formation of organometallic ELHB complexes. Reaction of this V_2S_4 species with $Fe_3(CO)_{12}$ or $Fe(CO)_5$–Me_3NO gave the cluster $(C_5H_4Me)_2(S_2)V_2(\mu\text{-}S)_2Fe(CO)_3$ **8.6**. In a similar manner, reactions of $(C_5H_4Me)_2V_2S_4$ with $Hg[Fe(CO)_3NO]_2$,

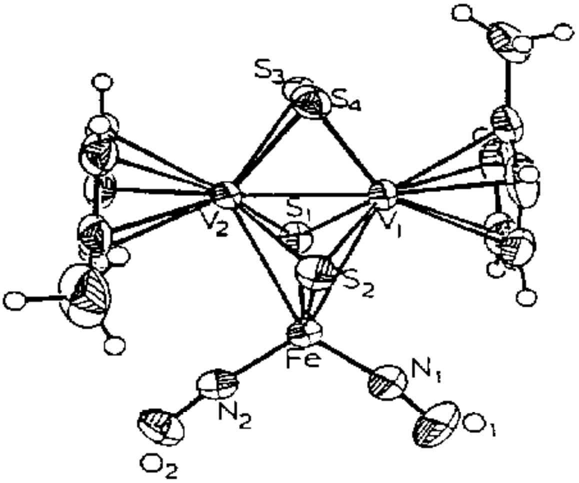

Fig. 33. ORTEP drawing of **8.7**. Reproduced with permission from ref. 154. Copyright 1986 American Chemical Society.

$CpCo(CO)I_2$, $(PPh_3)_2Ir(N_2)Cl$ or $[CpNi(CO)]_2$ yielded the complexes $(C_5H_4Me)_2(S_2)V_2(\mu\text{-}S)_2Fe(NO)_2$ **8.7**, $(C_5H_4Me)_2(S_2)V_2(\mu\text{-}S)_2CoCp$ **8.13**, $(C_5H_4Me)_2(S_2)V_2(\mu\text{-}S)_2Ir(PPh_3)Cl$ **8.16** and $[(C_5H_4Me)_2(S_2)V_2(\mu\text{-}S)_2)_2]Ni$ **8.17** respectively. The structures of **8.6**, **8.7** (Fig. 33) and **8.17** (Fig. 34) were confirmed crystallographically. The V–Fe distances in **8.6** and **8.7** are unusually long (ca. 2.87 Å) owing to the π interactions of vanadium with sulfur being competitive with V–Fe bonding.

The reactivity of these complexes arises due to the presence of the exocyclic disulfide. For example, reaction of **8.6** or **8.7** with PBu_3 afforded

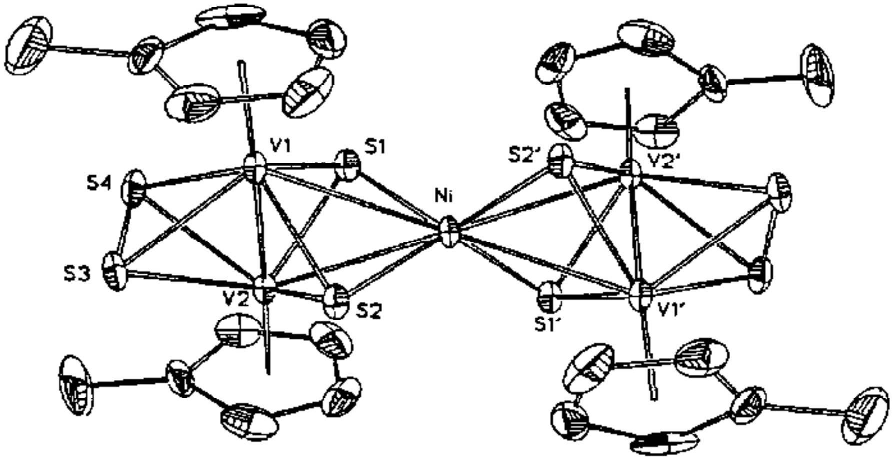

Fig. 34. ORTEP drawing of **8.17**. Reproduced with permission from ref. 154. Copyright 1986 American Chemical Society.

removal of a single sulfur atom, yielding $(C_5H_4Me)_2(S)V_2(\mu\text{-}S)_2FeL_n$ (L_n = $(CO)_3$ **8.8**, $(NO)_2$ **8.9**). Differences in the quadrupole splitting in the Fe Mossbauer spectra are consistent with a higher V–Fe bond order in **8.8** than in **8.6**. This is further supported by the structural studies (**8.8** V–Fe distances: 2.8132(9) and 2.7509(9) Å).

Oxidative addition of the exocyclic disulfide to platinum provides a route to the inclusion of a second late metal center. Thus reaction of **8.6** with $(PPh_3)_2Pt(C_2H_4)$ yielded the heterotrimetallic species $(C_5H_4Me)_2V_2(\mu\text{-}S)_2Fe(CO)_3(\mu\text{-}S)_2Pt(PPh_3)_2$ **8.10**. Similarly, reaction of **8.17** with $(PPh_3)_2Pt(C_2H_4)$ proceeded in a stepwise manner to give $(C_5H_4Me)_4(S_2)V_4(\mu\text{-}S)_6NiPt(PPh_3)_2$ **8.18** and $(C_5H_4Me)_4V_4(\mu\text{-}S)_8Ni(Pt(PPh_3)_2)_2$ **8.19** (eqn. (17)):

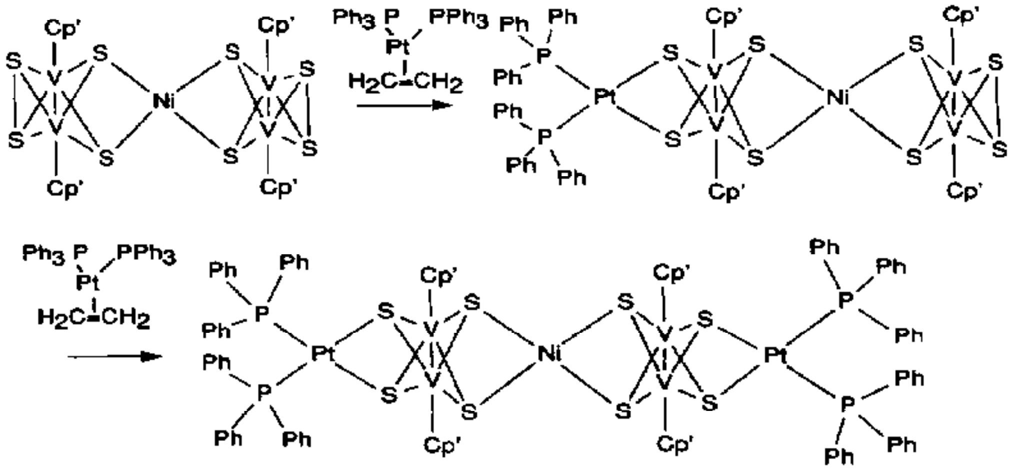

(17)

Reduction of **8.7** with zinc, followed by reaction with $Co(NO)_2I$, gave a product proposed to be $(C_5H_4Me)V(\mu\text{-}S_3)FeCo_2(NO)_6$ **8.11**. The structure of this species has not been confirmed crystallographically.

Reaction of $(C_5H_4Me)_2V_2S_4$ with excess $Hg[Fe(CO)_3(NO)]_2$ yields the tetrametallic cubane, $(C_5H_4Me)_2V_2(\mu\text{-}S)_4Fe_2(NO)_2$ **8.12** [155]. Alternatively, the 58-electron cluster **8.12** can be prepared by reaction of **8.7** with $Hg[Fe(CO)_3(NO)]_2$. Structural studies indicate that the electron deficiency in **8.12** is largely associated with the vanadium centers, giving rise to relatively long V–Fe bonds (2.75 Å) (Fig. 35). In a similar manner, the 60-electron cubane, $(C_5H_4Me)_2V_2(\mu\text{-}S)_4Co_2(NO)_2$ **8.15**, is prepared by reaction of $(C_5H_4Me)_2V_2S_4$ with $Co(CO)_3NO$. Reaction of **8.12** with $Co(CO)_3(NO)$ results in transmetallation yielding $(C_5H_4Me)_2V_2(\mu\text{-}S)_4FeCo(NO)_2$ **8.13**. In the presence of excess $Co(CO)_3(NO)$, **8.12** is converted to **8.15**.

Rauchfuss and coworkers [156] have also studied the related complexes $(C_5H_4Me)_2(PTD)(S)V_2(\mu\text{-}S)_2Pt(PPh_3)_2$ **8.20** and $(C_5H_4Me)_2(PTD)_2V_2(\mu\text{-}$

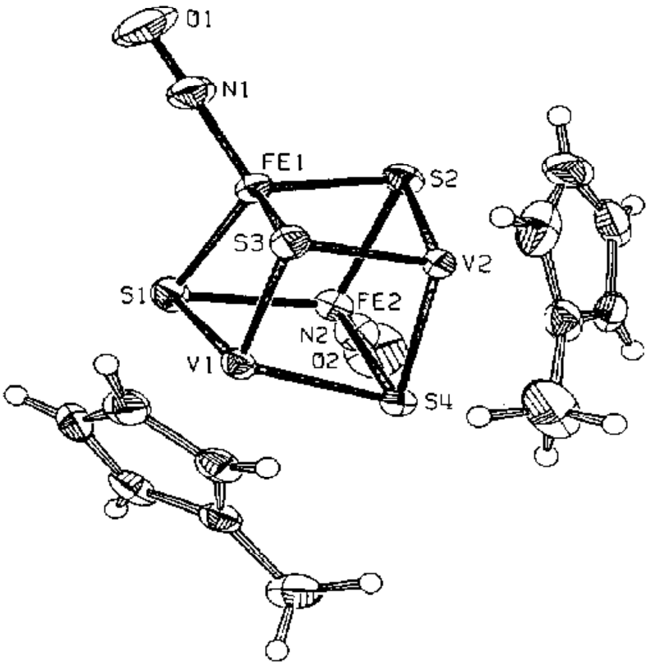

Fig. 35. ORTEP drawing of **8.12**. Reproduced with permission from ref. 155. Copyright 1983 American Chemical Society.

S)$_2$Pt(PPh$_3$)$_2$ **8.21**, in which the diazene, 4-phenyl-1,2,4-triazoline-3,5-dione (PTD), acts as a prosthesis for the μ-S$_2$ moiety. The structure of **8.20** has been confirmed crystallographically.

Oxo-bridged ELHB complexes have been synthesized by Jacobsen et al. [157]. Initially, oxyalkyl complexes of the form Cp$_2$(Cl)Zr(μ-OCHRCHR′)W(CO)$_3$Cp were prepared by reaction of Cp$_2$ZrHCl and Cp(CO)$_3$W(CHRCOR′). Upon irradiation at −50 °C, alkene extrusion occurs with formation of the oxo-bridged complex Cp$_2$(Cl)Zr(μ-O)W(CO)$_3$Cp **8.1**. Structural characterization of **8.1** shows that the W–O–Zr vector is almost linear (175.7 °). Thermal decomposition of **8.1** occurs at 25 °C giving [Cp$_2$ZrCl]$_2$O and [CpW(CO)$_3$]$_2$, while thermal stability is gained by substitution of the CO groups on tungsten. Reaction of **8.1** with alkynes or phosphine yielded Cp$_2$(Cl)Zr(μ-O)W(RCCR′)(CO)Cp (R = CMe$_3$, R′ = H **8.2**; R = R′ = Ph **8.3**) and Cp$_2$(Cl)Zr(μ-O)W(CO)$_2$(PMe$_3$)Cp **8.4** respectively. Further reaction of **8.4** with MeLi gave Cp$_2$(Me)Zr(μ-O)W(CO)$_2$-(PMe$_3$)Cp **8.5**.

TABLE 7

Chalcogenide-atom-bridged ELHB complexes

M–M′	Number	Complex	M–M′ distance (Å)	Ref.
Zr–W	**8.1**	$Cp_2(Cl)Zr(\mu\text{-}O)W(CO)_3Cp$		157
	8.2	$Cp_2(Cl)Zr(\mu\text{-}O)W(CO)(Me_3CC{\equiv}CH)Cp$		157
	8.3	$Cp_2(Cl)Zr(\mu\text{-}O)W(CO)(PhC{\equiv}CPh)Cp$		157
	8.4	$Cp_2(Cl)Zr(\mu\text{-}O)W(CO)_2(PMe_3)Cp$		157
	8.5	$Cp_2(Me)Zr(\mu\text{-}O)W(CO)_2(PMe_3)Cp$		157
V–Fe	**8.6**	$(C_5H_4Me)_2(S_2)V_2(\mu\text{-}S)_2Fe(CO)_3$	2.8956(7)	154
	8.7	$(C_5H_4Me)_2(S_2)V_2(\mu\text{-}S)_2Fe(NO)_2$	2.849(1)	154
	8.8	$(C_5H_4Me)_2(S)V_2(\mu\text{-}S)_2Fe(CO)_3$	2.8132(9) 2.7509(9)	154
	8.9	$(C_5H_4Me)_2(S)V_2(\mu\text{-}S)_2Fe(NO)_2$		154
	8.10	$(C_5H_4Me)_2V_2(\mu\text{-}S)_2Fe(CO)_3(\mu\text{-}S)_2Pt(PPh_3)_2$		154
	8.11	$(C_5H_4Me)V(\mu\text{-}S)_3FeCo_2(NO)_6$		154
	8.12	$(C_5H_4Me)_2V_2(\mu\text{-}S)_4Fe_2(NO)_2$	2.75	155
	8.13	$(C_5H_4Me)_2V_2(\mu\text{-}S)_4FeCo(NO)_2$		155
V–Co	**8.14**	$(C_5H_4Me)_2(S_2)V_2(\mu\text{-}S)_2CoCp$		154
	8.15	$(C_5H_4Me)_2V_2(\mu\text{-}S)_4Co_2(NO)_2$		155
V–Ir	**8.16**	$(C_5H_4Me)_2(S_2)V_2(\mu\text{-}S)_2IrCl(PPh_3)$		154
V–Ni	**8.17**	$(C_5H_4Me)_2(S_2)V_2(\mu\text{-}S)_2)_2Ni$	2.817(2)	154
	8.18	$(C_5H_4Me)_4(S_2)V_4(\mu\text{-}S)_6NiPt(PPh_3)_2$		154
	8.19	$(C_5H_4Me)_4V_4(\mu\text{-}S)_8Ni(Pt(PPh_3)_2)_2$		154
V–Pt	**8.20**	$(C_5H_4Me)_2(PTD)(S)V_2(\mu\text{-}S)_2Pt(PPh_3)_2$		156
	8.21	$(C_5H_4Me)_2(PTD)_2V_2(\mu\text{-}S)_2Pt(PPh_3)_2$		156

9. DISTAL ELHB COMPLEXES

Early reports of ELHB complexes in which the metal atoms are well separated or distal involved the metallation of the Cp rings of ferrocene [158–160]. Reactions of lithiated ferrocenes with amido-titanium halides led to several Ti–Fe complexes such as $(R_2N)_3Ti(\mu\text{-}C_5H_4)FeCp$ (R = Me **9.13**, Et **9.14**), $CpFe(C_5H_4Li)$ and $(R_2N)_3TiBr$. Similarly, the disubstituted species $((Et_2N)_3Ti(\mu\text{-}C_5H_4))_2Fe$ **9.15** and the bridged complex $(Et_2N)_2Ti((\mu\text{-}C_5H_4)FeCp)_2$ **9.16** have been prepared [158]. In the case of **9.15**, the proposed structure has been confirmed by a crystallographic study [161]. These reactions have been extended to yield a number of ELHB species. For example, use of Cp_2Ru in place of Cp_2Fe yielded the analogous ruthenium species $((Et_2N)_3Ti(\mu\text{-}C_5H_4))_2Ru$ **9.19** [159]. Reaction with Cp_2MCl_2 afforded the species $Cp_2M(\mu\text{-}C_5H_4)FeCp)_2$ (M = Ti **9.17**, Zr **9.35**, Hf **9.64**) [160]. Metallation of the reagent $(C_5H_4Cl)_2Fe$ led to the separable *meso* and

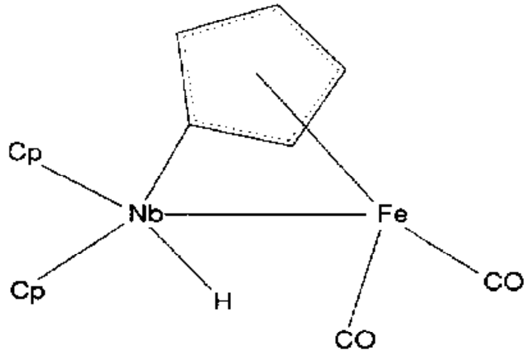

Fig. 36. Structure of **9.66**.

racemic forms of $Cp_2Ti((\mu\text{-}C_5H_3Cl)Fe(C_5H_4Cl))_2$ **9.18** [162].

Metallation of a Cp ring has also been achieved for complexes other than ferrocenes. One such species is prepared by reaction of $Cp_2Nb(BH_4)$ with $CpFe(CO)_2Me$ in the presence of base, giving $Cp_2(H)Nb(\mu\text{-}C_5H_4)Fe(CO)_2$ **9.66** (Fig. 36) [163]. Crystallographic methods were used to confirm the presence of the bridging $\eta^1,\eta^5\text{-}C_5H_4$ group and an Fe–Nb bond (2.968(1) Å).

In a similar manner, reaction of Cp_2TiCl_2 with $Li[CpMn(CO)_3]$ led to the trimetallic species $Cp_2Ti((\mu\text{-}C_5H_4)Mn(CO)_3)_2$ **9.8** [164]. In a structural study of this species, Wilkinson and coworkers confirmed the σ/π nature of the bridging C_5H_4 moieties; however, they noted a significant distortion of these rings from planarity.

Kotz et al. [138] have studied the electrochemical behavior of the very air-sensitive species **9.17** in addition to a number of other bimetallic species. Cyclic voltammetric waves, attributable to irreversible oxidation processes, were interpreted in terms of initial oxidation at iron and subsequent decomposition. Quasi-reversible reduction was observed at -1.53 V(SCE) and was assigned to a Ti(IV)/Ti(III) redox couple.

More recently, Casey and coworkers [77,165] have achieved metallation of a Cp ring via reactions of the M–M′-bonded species $Cp_2Zr(Ru(CO)_2Cp)_2$ **10.7** (see Section 10). Reactions of **10.7** with either CO or PMe_3 led to elimination of $CpRu(CO)_2H$ and formation of $Cp_2(CO)Zr(\mu\text{-}C_5H_4)RuL(CO)$ ($L = CO$ **9.38**, PMe_3 **9.39**). Interestingly, reaction of **10.7** with ethylene afforded the complex $Cp_2Zr(CH_2CH_2C_5H_4)Ru(CO)_2$ **9.40**. The Zr–Ru bond in **9.40** is cleaved by addition of Me_3COH to give the complex $Cp_2(Me_3CO)Zr(\mu\text{-}CH_2CH_2C_5H_4)RuH(CO)_2$ **9.41** in which the substituted Cp group links the two distal metal centers.

The inclusion of a functionalized ligand in an early metal complex is a synthetic route to complexes which has been exploited to prepare many distal ELHB complexes. One approach to the preparation of such complexes has been to functionalize a cyclopentadienyl group of an early metal metallocene. In 1979, Schore described the preparation of the species $Cl_2(Cp)Zr(C_5H_4SiMe_2CH_2PPh_2)$ and its reaction with $Fe_2(CO)_9$, yielding $Cl_2(Cp)Zr(\mu\text{-}C_5H_4SiMe_2CH_2PPh_2)Fe(CO)_4$ **9.31** [166].

More recently, Schore and coworkers [167] have described the use of the metalloligands $Cl_2(Cp)Zr(C_5H_4SiMe_2CH_2CH_2PPh_2)$ and $Cl_2Zr(C_5H_4\text{-}SiMe_2CH_2CH_2PPh_2)_2$ in reaction with cobalt carbonyl species. In these cases, the tetrametallic or polymetallic products, **9.44** and **9.45**, were obtained. Cleavage of the Co–Co bond of **9.44** led to the formation of $[Cl_2(Cp)Zr(\mu\text{-}C_5H_4SiMe_2CH_2CH_2PPh_2)Co(CO)_3]^-$ **9.42** (eqn. (18)):

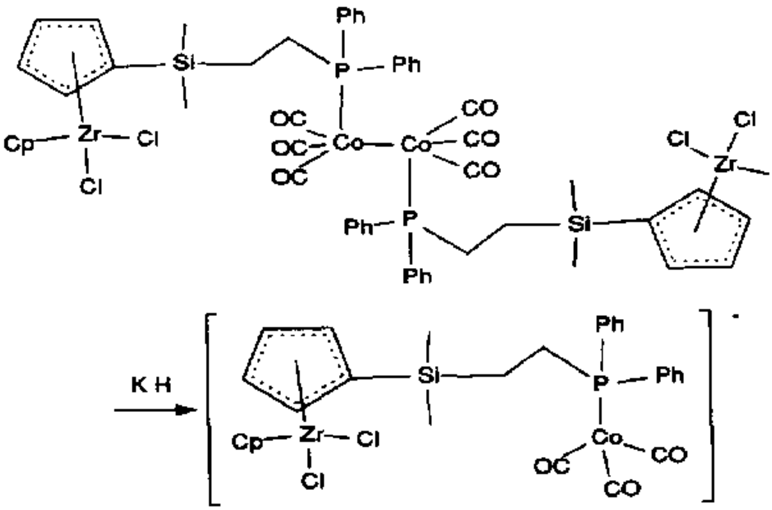

(18)

This compound was also prepared directly from $[Co(CO)_4]^-$. Acetylation of **9.42** with acetyl chloride yielded $Cl_2(Cp)Zr(\mu\text{-}C_5H_4SiMe_2CH_2CH_2\text{-}PPh_2)Co(CO)_3(COMe)$ **9.43**.

Using a related Ti(IV) complex, Leblanc et al. have described the preparation of molybdenum, chromium and iron carbonyl complexes of $Cl_2(Cp)Ti(C_5H_4CH_2CH_2PPh_2)$ [168]. The Ti–Mo complex $Cl_2(Cp)Ti(\mu\text{-}C_5H_4CH_2CH_2PPh_2)Mo(CO)_5$ **9.2** can be reduced with aluminum to the related Ti(III)–Mo(0) complex. Further reduction in the presence of CO affords the Ti(II)–Mo(0) complex $(CO)_2Cp(Ti(\mu\text{-}C_5H_4CH_2CH_2PPh_2)\text{-}Mo(CO)_5$ **9.4**. Employing similar titanium and zirconium complexes, in which both Cp rings on the early metal were functionalized, complexes of the form $Cl_2M(\mu\text{-}C_5H_4CH_2CH_2PPh_2)_2Mo(CO)_4$ (M = Ti **9.5**, Zr **9.28**) were prepared. The NMR and IR spectral data support the formulation of these products as ELHB complexes in which the functionalized early metal complexes act as bidentate ligands. Similar reactions with $[Rh(\mu\text{-}Cl)(C_2H_4)(CO)]_2$ led to the isolation of Ti–Rh and Zr–Rh complexes which

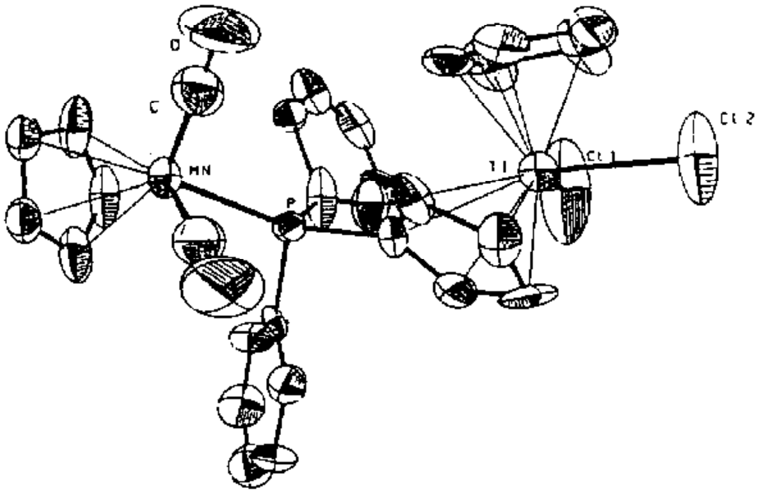

Fig. 37. ORTEP drawing of **9.9**. Reproduced with permission from ref. 169. Copyright 1983 American Chemical Society.

were formulated as $[Cl_2M(\mu\text{-}C_5H_4CH_2CH_2PPh_2)_2Rh(CO)Cl]_n$ (M = Ti **9.20**, Zr **9.58**). On the basis of ^{31}P NMR data, the authors postulated a dimeric ($n = 2$) structure [168].

In 1983, Rausch et al. reported the use of $C_5H_4PPh_2$ as a bridging ligand for the formation of ELHB complexes [169]. Reaction of either of the titanium complexes, $Cl_2(Cp)Ti(C_5H_4PPh_2)$ or $(CO)_2(Cp)Ti(C_5H_4PPh_2)$, with $CpMn(CO)_2(THF)$ led to the formation of $L_2(Cp)Ti(\mu\text{-}C_5H_4PPh_2)\text{-}Mn(CO)_2Cp$ (L = Cl **9.9**, CO **9.10**). The formulations of these compounds were supported by spectral data as well as an X-ray structural study of **9.9** (Fig. 37).

The zirconium species $Cp(OCMe_3)Zr(C_5H_4PPh_2)Cl$ was prepared by Casey and Nief in 1985 [170]. Reaction of this species with $[CpFe(CO)_2]^-$ led to formation of the metal–metal-bonded complex $Cp(OCMe_3)Zr(C_5H_4\text{-}PPh_2)Fe(CO)_2Cp$ **9.33** containing a pendent (i.e. not complexed) phosphine moiety. Photolysis of this complex results in the loss of CO from the iron and binding to the iron of the phosphine group of the $C_5H_4PPh_2$ ligand on the zirconium, thus yielding $Cp(OCMe_3)Zr(\mu\text{-}C_5H_4PPh_2)Fe(CO)Cp$ **9.34** (eqn. (19)):

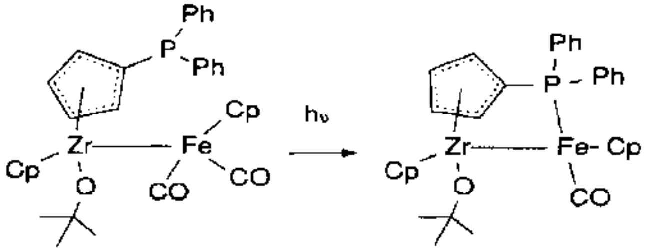

(19)

In a similar reaction, photolysis of $Co(CO)_4^-$ in the presence of the above zirconium species yields $Cp(OCMe_3)Zr(\mu\text{-}C_5H_4PPh_2)Co(CO)_3$ **9.46**. These complexes are the first to contain both a metal–metal bond and a bridging bifunctional ligand.

Tikkanen et al. [171] have reported the reaction of $Cl_2Zr(C_5H_4PPh_2)_2$ with $(NBD)Mo(CO)_4$ giving $Cl_2Zr(\mu\text{-}C_5H_4PPh_2)_2Mo(CO)_4$ **9.29**. Reaction of **9.29** with MeLi led to methylation at zirconium yielding $Me_2Zr(\mu\text{-}C_5H_4PPh_2)_2Mo(CO)_4$ **9.30**. The spectroscopic characterization of these complexes is consistent with linked, yet essentially unperturbed, molybdenum diphosphine and zirconocene dichloride moieties. Structural data for **9.29** are also consistent with this interpretation (Fig. 38). The lack of any interaction between the metals is consistent with the Mo–Zr distance of 4.8524(3) Å.

Ti(II)–M complexes were prepared by reaction of the Ti(II) metalloligand, $CpTi(C_7H_6PPh_2)$, with the appropriate late metal carbonyl [172]. The spectroscopic data suggested no metal–metal interactions, and thus the species $CpTi(\mu\text{-}C_7H_6PPh_2)ML_x$ ($ML_x = Ni(CO)_3$ **9.24**, $Fe(CO)_4$ **9.12**, $Mo(CO)_5$ **9.6**) were formulated as formally Ti(II)–M(0) compounds. In the case of **9.6**, the absence of metal–metal interaction was confirmed by a crystallographic study. The structural data revealed that the titanium and molybdenum fragments of **9.6** were well separated, with a Ti–Mo distance of 5.442(2) Å. The coordination spheres of each metal were very similar to those of their monometallic analogs.

In addition to Cp rings functionalized with phosphine groups, a preliminary report [173] describes the use of $(HSeC_5H_4)_2Fe$ as a metalloligand. Complexes of the form $Cp_2Zr(\mu\text{-}SeC_5H_4)_2Fe$ **9.36** and $(C_5H_4CMe_3)_2M(\mu\text{-}SeC_5H_4)_2Fe$ (M = Zr **9.37**, Hf **9.65**) have been prepared. Solution studies indicated that these complexes are not fluxional but are locked in a staggered conformation of the ferrocene moiety.

In the preparation of distal ELHB complexes, an alternative to functionalizing a Cp ring of an early metal metallocene is to incorporate a

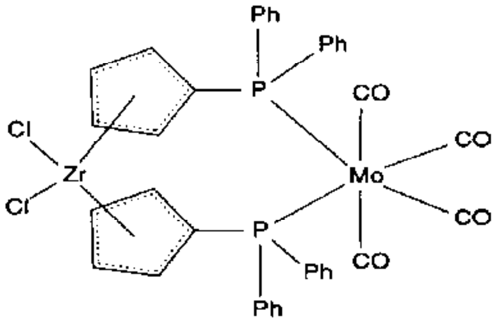

Fig. 38. Structure of **9.29**.

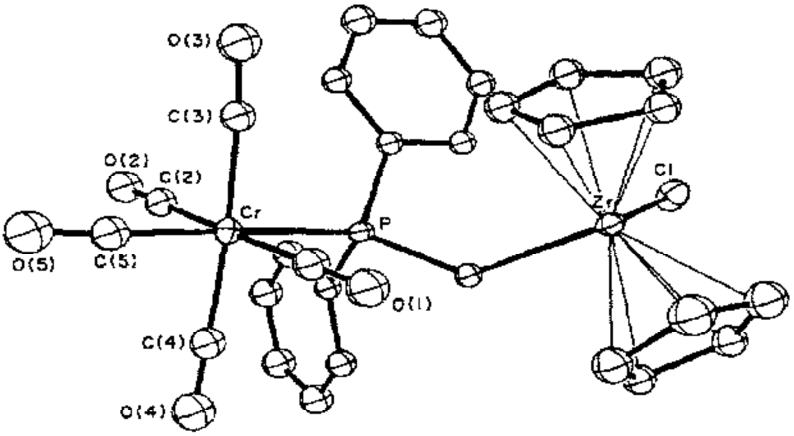

Fig. 39. ORTEP drawing of **9.25**. Reproduced with permission from ref. 174. Copyright 1983 American Chemical Society.

σ-bonded moiety containing a dangling phosphine functionality. Schore and coworkers [174,175] have described the preparation of the metalloligands $Cp_2(Cl)Zr(CH_2PPh_2)$ and $Cp_2Zr(CH_2PPh_2)_2$ via stoichiometric reactions of the alkyl lithium species Ph_2PCH_2Li with Cp_2ZrCl_2. Reaction of the monophosphine derivative with $Cr(CO)_5(THF)$ or $Fe_2(CO)_9$ led to quantitative formation of $Cp_2(Cl)Zr(\mu\text{-}CH_2PPh_2)Cr(CO)_5$ **9.25** and $Cp_2(Cl)Zr(\mu\text{-}CH_2PPh_2)Fe(CO)_4$ **9.32** respectively. The corresponding reaction of the diphosphine metalloligand led to the formation of the analogous trimetallic

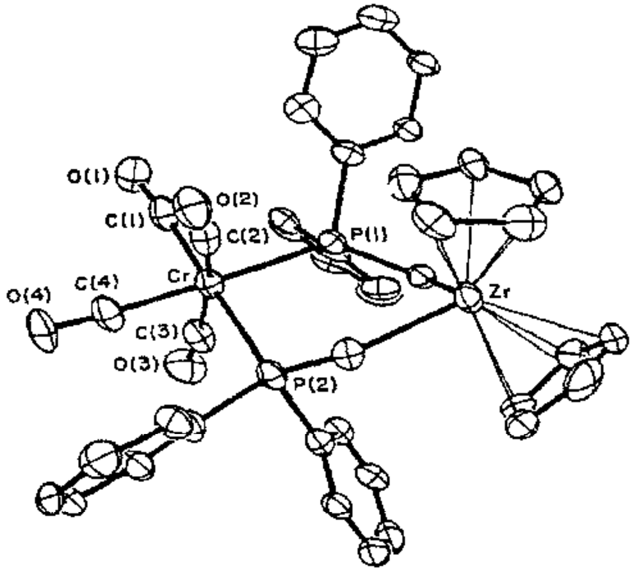

Fig. 40. ORTEP drawing of **9.26**. Reproduced with permission from ref. 174. Copyright 1983 American Chemical Society.

species $Cp_2Zr(\mu\text{-}CH_2PPh_2Cr(CO)_5)_2$ **9.27**. Reaction of the diphosphine species with $(NBD)Cr(CO)_4$ yielded the species $Cp_2Zr(\mu\text{-}CH_2PPh_2)_2\text{-}Cr(CO)_4$ **9.26**. Structural studies of **9.25** (Fig. 39) and **9.26** (Fig. 40) were described. Both complexes contain essentially the expected geometries at both zirconium and chromium; however, steric crowding, which is evident in the structural data for **9.26**, is relieved by slight distortions of the geometries about zirconium and chromium. In addition, the six-membered ring, formed by the chelation of the phosphine moieties to zirconium and chromium, adopts a distorted twist-boat orientation.

Reaction, in the appropriate ratios, of the metalloligands $Cp_2(Cl)Zr(CH_2\text{-}PPh_2)$ and $Cp_2Zr(CH_2PPh_2)_2$ with $[Rh(CO)_2Cl]_2$ gave the products $(Cp_2\text{-}(Cl)Zr(\mu\text{-}CH_2PPh_2))_2Rh(CO)Cl$ **9.53** and $Cp_2Zr(\mu\text{-}CH_2PPh_2)_2Rh(CO)Cl$ **9.54** respectively [176,177]. In both cases, the phosphine groups adopt a *trans* orientation on rhodium. The complexes $O(Cp_2M(\mu\text{-}CH_2PPh_2)_2)_2Rh\text{-}(CO)Cl$ (M = Ti **9.22**, Zr **9.56**) contain extended metalloligands which were also found to adopt *trans* chelation modes [178]. Of particular interest, from the perspective of CO activation, is the observation of a band at 1650 cm^{-1} in the solid state IR spectrum of **9.54**. This was attributed to one of the possible rotamers of **9.54** in which the rhodium-bound CO interacts with the oxophilic zirconium in an η^2 fashion. However, this band was not observed for **9.54** in THF solution [176].

The *trans* orientation of the phosphine groups in **9.54** is a further indication of the significant steric demands of the metalloligand. In the case of the titanium analog of **9.54**, (i.e. $[Cp_2Ti(\mu\text{-}CH_2PPh_2)_2Rh(CO)Cl]_2$ **9.21**) molecular weight determinations were consistent with a dimer. Presumably a

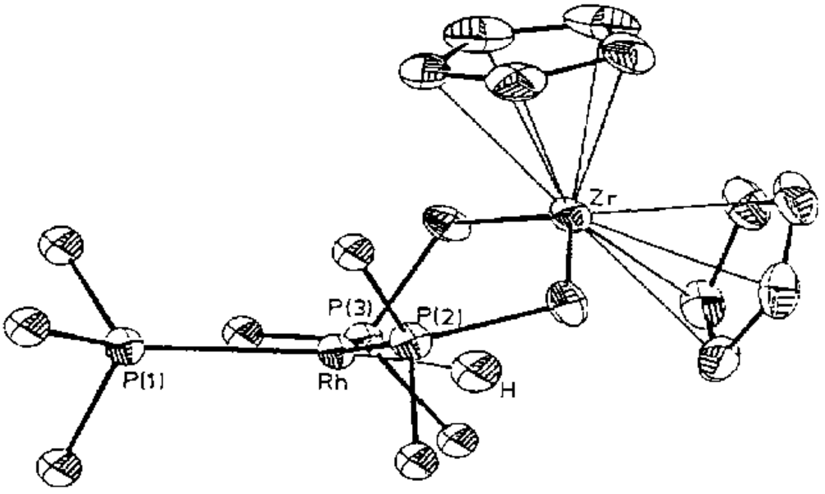

Fig. 41. ORTEP drawing of **9.52**. Reproduced with permission from ref. 182. Copyright 1987 American Chemical Society.

dimeric structure in which the titanium metalloligand moieties bridge two rhodium atoms is a result of even greater steric constraints of the titanium metalloligand [179]. In contrast, the nickel complex, $(Cp_2Zr(\mu\text{-}CH_2PMe_2)_2)_2Ni$ **9.63**, which is easily prepared by reaction of the metalloligand with $(COD)_2Ni$ [180], contains NiP_2C_2Zr rings which adopt pseudochair conformations. These geometries together with C–Zr–C angles of about 99.9° and Zr–Ni distances of 4.319(1)–4.416(1) Å demonstrate the dramatic reduction in the steric demands of the methyl-substituted metalloligand.

Reaction of $Cp_2Zr(CH_2PPh_2)_2$ with $RhH(PPh_3)_4$ yields $Cp_2Zr(\mu\text{-}CH_2PPh_2)_2RhH(PPh_3)$ **9.52** [181,182]. The *trans* chelation of the diphosphine metalloligand, proposed on the basis of the NMR data, was confirmed by X-ray crystallography (Fig. 41) [182]. The geometry about the zirconium is distorted, as shown by the large C–Zr–C angle of 134.3°. This is in contrast to the angle found in the free metalloligand (100.2°) or the angle in the related *cis* bound complex **9.26** (93.5°). This opening of the C–Zr–C angle suggests a pseudopentacoordinate geometry. Two possible explanations were considered: (i) the presence of a rhodium-to-zirconium dative bond or (ii) the presence of a hydride bridging the rhodium and zirconium. The Rh–Zr distance of 3.141 Å and the geometry of the rhodium coordination sphere spoke against the presence of a dative Rh–Zr interaction. The location and refinement of the hydride, in the X-ray study, revealed a Zr–H distance of 2.28 Å, while the Rh–H distance was 1.51 Å. These data clearly support the notion of a semibridging hydride (i.e. Rh–H · · · Zr).

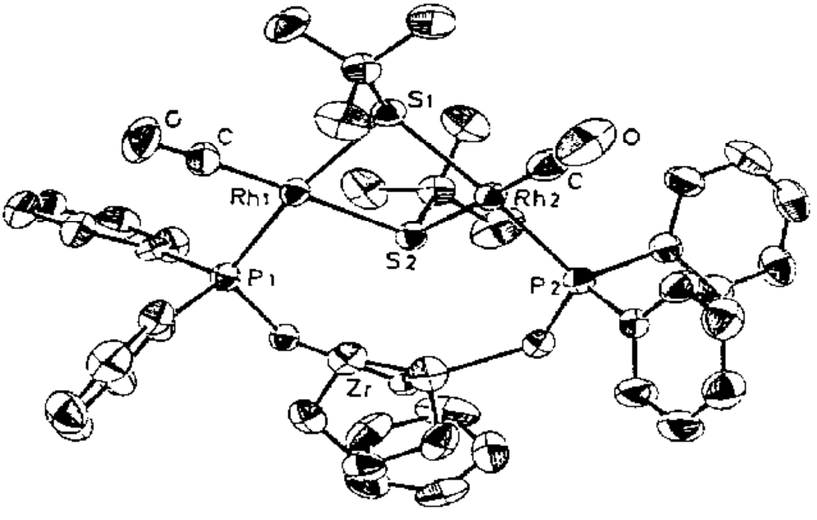

Fig. 42. ORTEP drawing of **9.55**. Reproduced with permission from ref. 184. Copyright 1986 American Chemical Society.

Preliminary reports of the use of **9.52** as a catalyst precursor for the hydroformylation of 1-hexene have been published [181,182]. Increased activity and selectivity for the terminal aldehyde product are observed for this ELHB catalyst. These features were attributed to the polarization of the Rh–H bond by the zirconium moiety.

Kalck and coworkers have reported a related Zr–Rh_2 complex prepared by reaction of $Cp_2Zr(CH_2PPh_2)_2$ and $Rh_2(\mu\text{-}SCMe_3)_2(CO)_4$ [183–185]. The proposed structure of the product, $Cp_2Zr(\mu\text{-}CH_2PPh_2)_2(Rh(CO)(\mu\text{-}SCMe_3))_2$ **9.55**, involved binding of one of the phosphine groups to each of the rhodium atoms which are in turn bridged by the two thiolate groups. The structure was confirmed by a crystallographic study [184]. Further, the X-ray data show that the zirconium is again best described as pseudopentacoordinate as a result of the large C–Zr–C angle (137.5(1)°) and the close approach of one of the sulfur atoms (Zr · · · S 2.995(1) Å) (Fig. 42).

The use of **9.55** in hydroformylation catalysis has also been described [183–185]. Studies have shown that the Zr–Rh_2 species does exhibit enhanced activity compared with related chelated complexes in which no zirconium is present. Although the role of the zirconium moiety is not thoroughly understood, it has been suggested that zirconium acts as an electron buffer to modulate electron density from the rhodium atoms in the successive steps of the catalytic cycle (i.e. oxidative addition of H_2, coordination of 1-hexene, and CO insertion).

Some preliminary investigations of a related Ti(III) metalloligand have

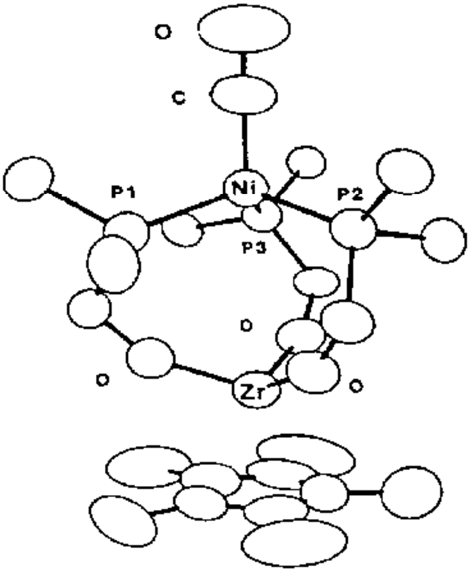

Fig. 43. ORTEP drawing of **9.62**. Reproduced with permission from ref. 187. Copyright 1985 American Chemical Society.

been described [186]. The species $[Cp_2Ti(CH_2PPh_2)_2]^-$ was found to give a characteristic triplet of triplets in its EPR spectrum. Reaction of this reduced metalloligand with $Mo(CO)_6$ resulted in a complex giving an EPR spectrum in which no Ti–P coupling was observed. This was interpreted in terms of a heterobimetallic species $[Cp_2Ti(\mu\text{-}CH_2PPh_2)_2Mo(CO)_4]^-$ **9.7**; however, this species was not isolated.

Ferguson and Wolczanski [187] have prepared ELHB complexes employing the bridging ligand OCH_2PPh_2. This ligand affords the inclusion of an early metal alkoxide moiety which is designed to model the metal oxide supports used in heterogeneous systems. The complex $Cp^*Zr(\mu\text{-}OCH_2PPh_2)_3Ni(PPh_2CH_2OH)$ **9.59** was prepared via the reaction of $(HOCH_2PPh_2)_4Ni$ with Cp^*ZrMe_3. Ligand exchange reactions of **9.59** led to the replacement of the phosphine on nickel, giving $Cp^*Zr(\mu\text{-}OCH_2PPh_2)_3NiL$ ($L = PMe_3$ **9.60**, $P(OMe)_3$ **9.61**, CO **9.62**). A structural study of **9.62** (Fig. 43) revealed that the two metals are well separated (Zr · · · Ni 4.049(1) Å) and possess pseudotetrahedral coordination spheres which are essentially unperturbed by the presence of the other metal atom.

Attempts to remove one of the bridging ligands in **9.59**–**9.62** and thus create a site where one might effect bimetallic chemistry were unsuccessful. However, in a recent communication, Ferguson and Wolczanski have described the synthesis of a related Zr–Rh species where bimetallic activation of a carbon oxide fragment has been achieved [188]. Reaction of the $HOCH_2PPh_2$ with Cp^*ZrMe_3, in the appropriate ratio, led to the formation of the metalloligand $Cp^*(Me)Zr(CH_2PPh_2)_2$. Reaction of this species with $[Rh(CO)_2Cl]_2$ resulted in binding of the phosphine groups to rhodium with subsequent insertion of CO into the Zr–Me bond to yield $Cp^*Zr(\mu\text{-}$

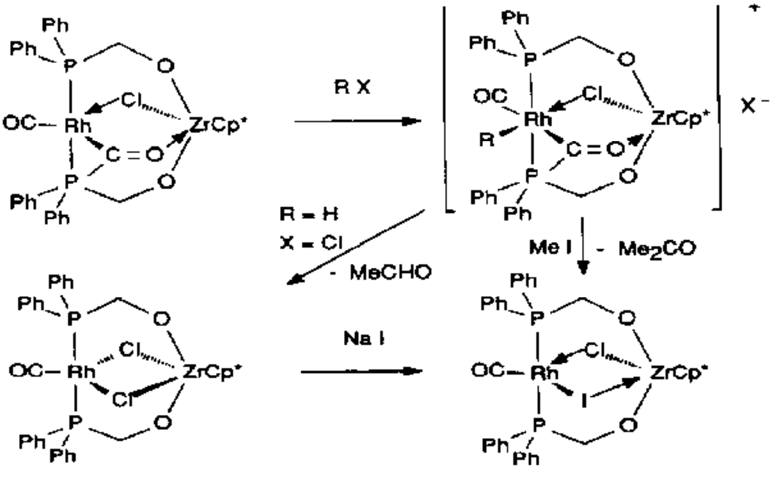

Fig. 44. Structure of **9.62**.

TABLE 8

Distal ELHB complexes

M–M′	Number	Complex	M–M′ distance (Å)	Ref.
Ti–Cr	**9.1**	$Cl_2(Cp)Ti(\mu\text{-}C_5H_4CH_2CH_2PPh_2)Cr(CO)_5$		168
Ti–Mo	**9.2**	$Cl_2(Cp)Ti(\mu\text{-}C_5H_4CH_2CH_2PPh_2)Mo(CO)_5$		168
	9.3	$Cl(Cp)Ti(\mu\text{-}C_5H_4CH_2CH_2PPh_2)Mo(CO)_5$		168
	9.4	$(CO)_2Ti(\mu\text{-}C_5H_4CH_2CH_2PPh_2)Mo(CO)_5$		168
	9.5	$Cl_2Ti(\mu\text{-}C_5H_4CH_2CH_2PPh_2)_2Mo(CO)_4$		168
	9.6	$CpTi(\mu\text{-}C_7H_6PPh_2)_2Mo(CO)_5$	4.442(2)	172
	9.7	$[Cp_2Ti(\mu\text{-}CH_2PPh_2)_2Mo(CO)_4]^-$		186
Ti–Mn	**9.8**	$Cp_2Ti((\mu\text{-}C_5H_4)Mn(CO)_3)_2$		164
	9.9	$Cl_2(Cp)Ti(\mu\text{-}C_5H_4Ph_2)Mn(CO)_2$		169
	9.10	$(CO)_2(Cp)Ti(\mu\text{-}C_5H_4PPh_2)Mn(CO)_2$		169
Ti–Fe	**9.11**	$Cl_2(Cp)Ti(\mu\text{-}C_5H_4CH_2CH_2PPh_2)Fe(CO)_4$		169
	9.12	$CpTi(\mu\text{-}C_7H_6PPh_2)Fe(CO)_4$		172
	9.13	$(Me_2N)_3Ti(\mu\text{-}C_5H_4)FeCp$		158
	9.14	$(Et_2N)_3Ti(\mu\text{-}C_5H_4)FeCp$		158
	9.15	$((Et_2N)_3Ti(\mu\text{-}C_5H_4))_2Fe$		158, 159, 161
	9.16	$(Et_2N)_2Ti((\mu\text{-}C_5H_4)FeCp)_2$		158
	9.17	$Cp_2Ti((\mu\text{-}C_5H_4)FeCp)_2$		160
	9.18	$Cp_2Ti((\mu\text{-}C_5H_3Cl)Fe(C_5H_4Cl))_2$		162
Ti–Ru	**9.19**	$((Et_2N)_3Ti((\mu\text{-}C_5H_4))_2Ru$		159
Ti–Rh	**9.20**	$[Cl_2Ti(\mu\text{-}C_5H_4CH_2CH_2Ph_2)_2Rh(CO)Cl]_n$		168
	9.21	$[Cp_2Ti(\mu\text{-}CH_2Ph_2)_2Rh(CO)Cl]_2$		179
	9.22	$O(Cp_2Ti(\mu\text{-}CH_2Ph_2)_2Rh(CO)Cl$		178
Ti–Ni	**9.23**	$Cp_2Ti(\mu\text{-}SCH_2CH_2CH_2PPh_2)_2Ni(CO)_2$		150
	9.24	$CpTi(\mu\text{-}C_7H_6PPh_2)Ni(CO)_3$		172
Zr–Cr	**9.25**	$Cp_2(Cl)Zr(\mu\text{-}CH_2PPh_2)Cr(CO)_5$		174, 175
	9.26	$Cp_2Zr(\mu\text{-}CH_2PPh_2)_2Cr(CO)_4$		174
	9.27	$Cp_2Zr(\mu\text{-}CH_2PPh_2Cr(CO)_5)_2$		174
Zr–Mo	**9.28**	$Cl_2Zr(\mu\text{-}C_5H_4CH_2CH_2PPh_2)_2Mo(CO)_4$		168
	9.29	$Cl_2Zr(\mu\text{-}C_5H_4PPh_2)_2Mo(CO)_4$	4.8542(3)	171
	9.30	$Me_2Zr(\mu\text{-}C_5H_4PPh_2)_2Mo(CO)_4$		171
Zr–Fe	**9.31**	$Cl_2(Cp)Zr(\mu\text{-}C_5H_4SiMe_2CH_2PPh_2)Fe(CO)_4$		166
	9.32	$Cp_2(Cl)Zr(\mu\text{-}CH_2PPh_2)Fe(CO)_4$		175
	9.33	$Cp(OCMe_3)Zr(C_5H_4PPh_2)Fe(CO)_2Cp$		170
	9.34	$Cp(OCMe_3)Zr(\mu\text{-}C_5H_4PPh_2)Fe(CO)Cp$		170
	9.35	$Cp_2Zr((\mu\text{-}C_5H_4)FeCp)_2$		160
	9.36	$Cp_2Zr(\mu\text{-}SeC_5H_4)_2Fe$		173
	9.37	$(C_5H_4CMe_3)_2Zr(\mu\text{-}SeC_5H_4)_2Fe$		173
Zr–Ru	**9.38**	$Cp_2(CO)Zr(\mu\text{-}C_5H_4)Ru(CO)_2$	3.064(1)	165
	9.39	$Cp_2(CO)Zr(\mu\text{-}C_5H_4)Ru(CO)(PMe_3)$	3.080(1)	165
	9.40	$Cp_2Zr(\mu\text{-}CH_2CH_2C_5H_4)Ru(CO)_2$		165
	9.41	$Cp_2(Me_3CO)Zr(\mu\text{-}CH_2CH_2C_5H_4)RuH(CO)_2$		165

TABLE 8 (continued)

M–M′	Number	Complex	M–M′ distance (Å)	Ref.
Zr–Co	**9.42**	$[Cl_2(Cp)Zr(\mu\text{-}C_5H_4SiMe_2CH_2CH_2PPh_2)Co(CO)_3]^-$		167
	9.43	$Cl_2(Cp)Zr(\mu\text{-}C_5H_44SiMe_2CH_2CH_2PPh_2)\text{-}Co(CO)_3(COMe)$		167
	9.44	$[Cl_2(Cp)Zr(\mu\text{-}C_5H_4SiMe_2CH_2CH_2PPh_2)\text{-}Co(CO)_3]_2$		167
	9.45	$[Cl_2Zr(\mu\text{-}C_5H_4SiMe_2CH_2CH_2PPh_2)_2\text{-}[Co(CO)_3]_2]_n$		167
	9.46	$Cp(OCMe_3)Zr(\mu\text{-}C_5H_4PPh_2)Co(CO)_3$		170
Zr–Rh	**9.47**	$Cp^*Zr(\mu\text{-}OCH_2PPh_2)_2(\mu\text{-}MeCO)\text{-}(\mu\text{-}Cl)Rh(CO)$		188
	9.48	$[Cp^*Zr(\mu\text{-}OCH_2PPh_2)_2(\mu\text{-}MeCO)\text{-}(\mu\text{-}Cl)Rh(CO)H]^+$		188
	9.49	$[Cp^*Zr(\mu\text{-}OCH_2PPh_2)_2(\mu\text{-}MeCO)\text{-}(\mu\text{-}Cl)Rh(CO)Me]^+$		188
	9.50	$Cp^*Zr(\mu\text{-}OCH_2PPh_2)_2(\mu\text{-}Cl)_2Rh(CO)$		188
	9.51	$Cp^*Zr(\mu\text{-}OCH_2PPh_2)_2(\mu\text{-}I)(\mu\text{-}Cl)Rh(CO)$		188
	9.52	$Cp_2Zr(\mu\text{-}CH_2PPh_2)_2RhH(PPh_3)$	3.141	181, 182
	9.53	$(Cp_2ClZr(\mu\text{-}CH_2PPh_2))_2Rh(CO)Cl$		177
	9.54	$Cp_2Zr(\mu\text{-}CH_2Ph_2)_2Rh(CO)Cl$		176
	9.55	$Cp_2Zr(\mu\text{-}CH_2Ph_2)_2(Rh(CO)(\mu\text{-}SCMe_3))_2$		183–185
	9.56	$O(Cp_2Zr(\mu\text{-}CH_2PPh_2)_2)_2Rh(CO)Cl$		178
	9.57	$Cl_2Zr(\mu\text{-}C_5H_4PPh_2)_2Rh(CO)Cl$		168
	9.58	$[Cl_2Zr(\mu\text{-}C_5H_4CH_2CH_2PPh_2)_2Rh(CO)Cl]_n$		168
Zr–Ni	**9.59**	$Cp^*Zr(\mu\text{-}OCH_2PPh_2)_3Ni(PPh_2CH_2OH)$		187
	9.60	$Cp^*Zr(\mu\text{-}OCH_2PPh_2)_3NiPMe_3$		187
	9.61	$Cp^*Zr(\mu\text{-}OCH_2PPh_2)_3NiP(OMe)_3$		187
	9.62	$Cp^*Zr(\mu\text{-}OCH_2PPh_2)_3NiCO$	4.049(1)	187
	9.63	$(Cp_2Zr(\mu\text{-}CH_2PMe_2)_2)_2Ni$	4.367(1) 4.416(1) 3.962(1) 4.319(1)	180
Hf–Fe	**9.64**	$Cp_2Hf((\mu\text{-}C_5H_4)FeCp)_2$		160
	9.65	$(C_5H_4CMe_3)_2Hf(\mu\text{-}SeC_5H_4)_2Fe$		173
Nb–Fe	**9.66**	$Cp_2(H)Nb(\mu\text{-}C_5H_4)Fe(CO)_2$	2.968(1)	163

$OCH_2PPh_2)_2(\mu\text{-}OCMe)(\mu\text{-}Cl)Rh(CO)$ **9.47**. The complex **9.47**, in which rhodium is linked to a zirconium alkoxide fragment, models heterogeneous $Rh\text{–}ZrO_2$ catalyst systems. Reaction of **9.47** with HCl led to the formation of acetaldehyde and the dichloro-bridged species $Cp^*Zr(\mu\text{-}OCH_2PPh_2)_2(\mu\text{-}Cl)_2Rh(CO)$ **9.50**. Reaction with MeI afforded acetone and $Cp^*Zr(\mu\text{-}OCH_2PPh_2)_2(\mu\text{-}I)(\mu\text{-}Cl)Rh(CO)$ **9.51**. In these reactions of **9.47** with elec-

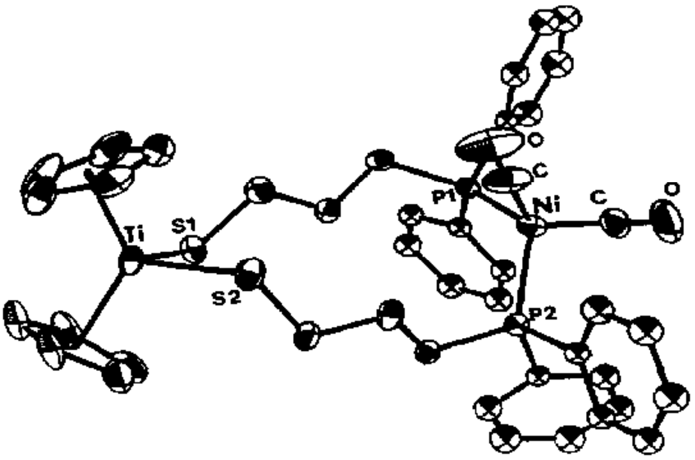

Fig. 45. ORTEP drawing of **9.23**. Reproduced with permission from ref. 150. Copyright 1988 American Chemical Society.

trophiles, spectroscopic evidence suggested an Rh(III) intermediate **9.48** and **9.49** (Fig. 44).

White and Stephan have demonstrated another method for the preparation of a distal ELHB complex involving the reaction of thiolato-bridged species. The compound $[Cp_2Ti(\mu\text{-}SCH_2CH_2CH_2PPh_2)_2Ni]$ **7.22** reacts with CO to give the outside complex $Cp_2Ti(SCH_2CH_2CH_2PPh_2)_2Ni(CO)_2$ **9.23**. A crystallographic study of **9.23** confirmed that the metals are well separated with a Ti · · · Ni distance of 6.9 Å (Fig. 45).

10. METAL–METAL-BONDED ELHB COMPLEXES

ELHB complexes that contain metal–metal bonds have been the subject of interest for some years. A number of synthetic routes have been developed to yield a variety of heterobimetallic bonds. One method for the formation of M–M′ bonds involves the nucleophilic attack of a metal halide by a metal complex anion. In early reports, the complexes $(CO)_6TaHgR$ (R = Me **10.41**, Et **10.42**) [189] and $(CO)_6VAuPPh_3$ **10.19** [190] were prepared via similar reactions of $[Na(C_4H_{10}O_2)_3][Ta(CO)_6]$ or $[Na(diglyme)_2]$-$[V(CO)_6]$ (diglyme = $(MeOCH_2CH_2)_2O$) with the appropriate metal halide. In a similar fashion, Davison and Ellis [191,192] reported the formation of the M–M′-bonded species **10.19** as well as complexes of the form $L(CO)_5MAuPPh_3$ (L = CO, M = Nb **10.24**, Ta **10.39**; L = PPh_3, M = V **10.20**, Nb **10.25**, Ta **10.40**) and $L(CO)_5MHgEt$ (L = CO, M = V **10.22**, Nb **10.31**, Ta **10.42**; L = PPh_3, M = V **10.23**, Nb **10.32**, Ta **10.43**) by reaction of the anions $[M(CO)_5L]^-$ with Ph_3PAuCl or EtHgCl. The complex $(OC)_6VAuPPh_3$ **10.19** was subsequently characterized by ^{51}V NMR [193]

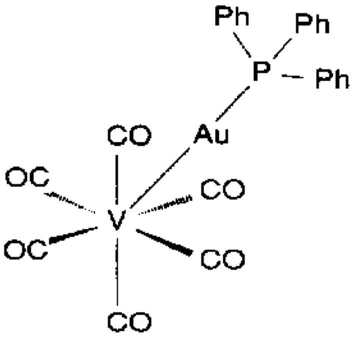

Fig. 46. Structure of **10.19**.

and X-ray crystallographic methods [194]. Both of these techniques provided data consistent with the presence of a V–Au bond. The crystallographic data showed that vanadium is formally seven-coordinate. The capped octahedral coordination sphere of vanadium comprises the six carbonyls and the V–Au bond (2.690(3) Å) (Fig. 46).

Related reactions involving the anion $[CpNbH(CO)_3]^-$ and Ph_3PAuCl have been described [195]. The presence of an M–M′ bond in the resulting complex, $[Cp(CO)_3NbAuPPh_3]^-$ **10.26**, was suggested on the basis of ^{93}Nb NMR data.

In the case of the gold complexes **10.19**, **10.24** and **10.39**, addition of excess phosphine to the hexacarbonyl species did not lead to formation of

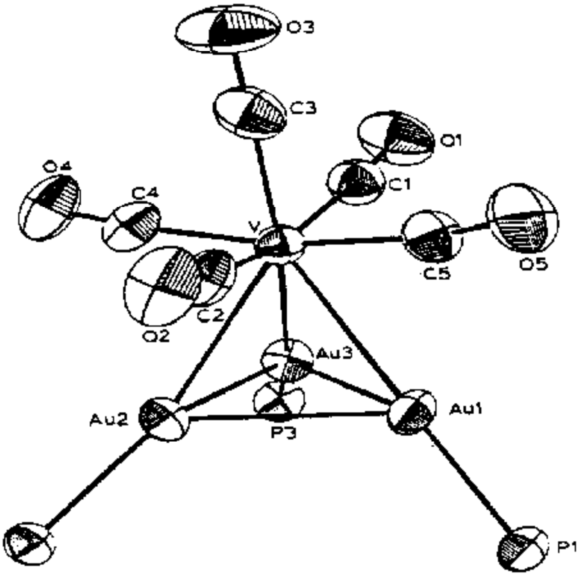

Fig. 47. ORTEP drawing of **10.21**. Reproduced with permission from ref. 197. Copyright 1981 American Chemical Society.

phosphine-substituted products **10.20**, **10.25** or **10.40**. Rather, heterocyclic cleavage of the metal–metal bond resulted, yielding the species $[(Ph_3P)_4Au][M(CO)_6]$ [192]. The analogous copper complex $[(Ph_3P)_3Cu]$-$[V(CO)_6]$ has been studied crystallographically. No metal–metal interaction was observed as the V–Cu separation is almost 7 Å [196].

Ellis [197] has reported that the reaction of the highly reduced species $[V(CO)_5]^{3-}$ with Ph_3PAuCl afforded the V–Au cluster, $(CO)_5V(AuPPh_3)_3$ **10.21**. The formally eight-coordinate vanadium is bound to the trigold fragment via Au–V bonds (2.709(1), 2.736(1), 2.756(1) Å). The four metal atoms form a distorted tetrahedral metal atom core (Fig. 47).

In more recent work involving highly reduced early metal species, Kelsey and Ellis [198] have described the synthesis of $[CpTi(CO)_4]^-$ at low temperature. Reaction of this species with Ph_3PAuCl yielded an isolable purple solid formulated as $Cp^*(CO)_4TiAuPPh_3$ **10.6**. Spectroscopic data support the proposition of a Ti–Au bond, although this was not confirmed crystallographically.

Lappert and Sanger [199] reported a synthesis of $Cp_2TiMo(CO)_3Cp$ **10.2** via reaction of the salt $Na[CpMo(CO)_3]$ with $[Cp_2TiCl]_2$. The reaction of $Na_2Fe(CO)_4$ and Cp_2HfCl_2 led to a dark brown solid, formulated as $[Cp_2HfFe(CO)_4]_2$ **10.11** [200]. The presence of the proposed Hf–Fe bond was supported by Raman data. In solution, spectroscopic evidence suggested isomerization to a related isocarbonyl species.

In another example of the use of a metal anion to form an M–M′-bonded complex, Casey et al. [201] have described reactions of $K[CpRu(CO)_2]$ with Cp_2ZrI_2. The product, $Cp_2Zr(Ru(CO)_2Cp)_2$ **10.7**, was characterized crystallographically, confirming the presence of the Ru–Zr bonds (2.938(1), 2.948(1) Å) (Fig. 48). A related reaction of $[CpFe(CO)_2]^-$ with Cp_2ZrI_2 showed the stepwise substitution of the iron moiety for the iodine on the zirconium;

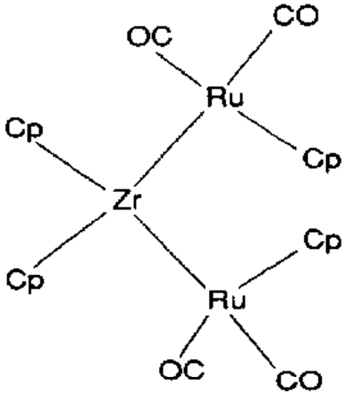

Fig. 48. Structure of **10.7**.

however, the Zr–Fe species was not stable above −20 °C. The reactions of K[CpRu(CO)$_2$] with Cp$_2$ZrCl$_2$, Cp$_2$ZrMeCl and Cp$_2$Zr(OCMe$_3$)Cl have also been described [202]. The products, Cp$_2$(R)ZrRu(CO)$_2$Cp, (R = Cl **10.8**, Me **10.9**, OCMe$_3$, **10.10**) were formulated as containing Zr–Ru bonds. The crystal structure of **10.10** confirmed the presence of the Zr–Ru bond (2.910(1) Å). Molecular orbital calculations [203] performed on the related species Cp$_2$(I)ZrRu(CO)$_2$Cp were consistent with a donor–acceptor description of the Zr–Ru bond. Thus the bond was found to be due to donation from the $4d_{z^2}$ and $4d_{xz}$ orbitals of ruthenium to the corresponding orbitals on zirconium.

A second method for forming M–M′ bonds involves redox reactions in which homobimetallic species are cleaved. In 1969, Miyake et al. [204,205] described the use of this approach in the reactions of Cp$_2$M with (CpCr(CO)$_3$)$_2$. The presence of metal–metal bonds in the air-sensitive products, Cp$_2$MCr(CO)$_3$Cp (M = Ti **10.1**, V **10.12**), was postulated on the basis of spectroscopic data. The related reaction of Cp$'_2$V with Co$_2$(CO)$_8$ has been reported to yield complexes of the form Cp$'_2$VCo(CO)$_4$ (Cp′ = Cp **10.13**, Cp* **10.14**, C$_5$H$_4$CO$_2$Me **10.15**, C$_5$H$_4$CMe$_3$ **10.16**, C$_5$Me$_4$Et **10.17**) [46].

A third approach to the formation of M–M′ bonds is the use of amine elimination reactions, first described by Cardin et al. [206]. Reaction of (iPrO)$_3$TiNMe$_2$ with CpMo(CO)$_3$H yielded the air-sensitive species (iPrO)$_3$TiMo(CO)$_3$Cp **10.3**. In addition, Lappert and Sanger [199] reported the Ti(III) species Cp$_2$TiMo(CO)$_3$Cp **10.2** which could also be formed via an amine elimination reaction involving [Cp$_2$Ti(NMe$_2$)]$_2$ and CpMo(CO)$_3$H. The more recent work of Sartain and Selegue has cast doubt on the presence of metal–metal bonds in these complexes, as isocarbonyl linkages are observed for ELHB complexes containing the CpMo(CO)$_3$ fragment [207].

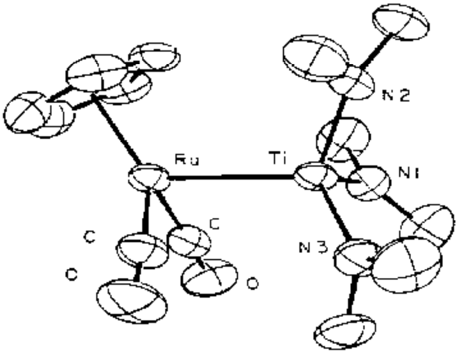

Fig. 49. ORTEP drawing of **10.5**. Reproduced with permission from ref. 207. Copyright 1985 American Chemical Society.

TABLE 9

Metal–metal-bonded ELHB complexes

M–M′	Number	Complex	M–M′ distance (Å)	Ref.
Ti–Cr	**10.1**	$Cp_2TiCr(CO)_3Cp$		204, 205
Ti–Mo	**10.2**	$Cp_2TiMo(CO)_3Cp$		199
	10.3	$(iPrO)_3TiMo(CO)_3Cp$		206
Ti–Fe	**10.4**	$(Me_2N)_3TiFe(CO)_2Cp$	2.567(1) 2.569(1)	208
Ti–Ru	**10.5**	$(Me_2N)_3TiRu(CO)_2Cp$	2.663(1)	207
Ti–Au	**10.6**	$Cp^*(CO)_4TiAuPPh_3$		198
Zr–Ru	**10.7**	$Cp_2Zr(Ru(CO)_2Cp)_2$	2.948(1) 2.938(1)	201
	10.8	$Cp_2(Cl)ZrRu(CO)_2Cp$		202
	10.9	$Cp_2(Me)ZrRu(CO)_2Cp$		201
	10.10	$Cp_2(Me_3CO)ZrRu(CO)_2Cp$	2.910(1)	201
Hf–Fe	**10.11**	$[Cp_2HfFe(CO)_4]_2$		202
V–Cr	**10.12**	$Cp_2V(CO)_3Cp$		204
V–Co	**10.13**	$Cp_2VCo(CO)_4$		46
	10.14	$Cp_2^*VCo(CO)_4$		46
	10.15	$(C_5H_4CO_2Me)_2VCo(CO)_4$		46
	10.16	$(C_5H_4CMe_3)_2VCo(CO)_4$		46
	10.17	$(C_5Me_4Et)_2VCo(CO)_4$		46
V–Cu	**10.18**	$(CO)_6VCu(trias)$ [a]		190
V–Au	**10.19**	$(CO)_6VAuPPh_3$	2.690(3)	190–194
	10.20	$(Ph_3P)(CO)_5VAuPPh_3$		191–193
	10.21	$(CO)_5V(AuPPh_3)_3$	2.736(1) 2.709(1) 2.756(1)	197
V–Hg	**10.22**	$(CO)_6VHgEt$		192
	10.23	$(Ph_3P)(CO)_5VHgEt$		192
Nb–Au	**10.24**	$(CO)_6NbAuPPh_3$		192
	10.25	$(Ph_3P)(CO)_5NbAuPPh_3$		192
	10.26	$[Cp(CO)_3NbAuPPh_3]^-$		195
	10.27	$[(C_5H_4SiMe_3)_2Nb(AuPPh_3)_2]^+$	2.9098(8) 2.9139(8)	212
Nb–Zn	**10.28**	$Cp_2(H)_2NbZnCp$	2.541	209
	10.29	$Cp_2(H)Nb(ZnCp)_2$		209
	10.30	$(Cp_2(H)_2Nb)_2Zn$		209
Nb–Hg	**10.31**	$(CO)_6NbHgEt$		192
	10.32	$(Ph_3P)(CO)_5NbHgEt$		192
	10.33	$Cp_2(H)Nb(HgCl)_2$		211
	10.34	$Cp_2(H)Nb(HgBr)_2$		211
	10.35	$Cp_2(H)Nb(HgI)_2$		211
	10.36	$Cp_2(H)Nb(HgSEt)_2$		211
	10.37	$Cp_2(H)Nb(HgSCMe_3)_2$		211
	10.38	$Cp_2Nb(HgS_2CNEt_2)_3$	2.790(1)	211

TABLE 9 (continued)

M–M′	Number	Complex	M–M′ distance (Å)	Ref.
Ta–Au	**10.39**	$(CO)_6TaAuPPh_3$		191, 192
	10.40	$(Ph_3P)(CO)_5TaAuPPh_3$		191, 192
Ta–Hg	**10.41**	$(CO)_6TaHgMe$		189
	10.42	$(CO)_6TaHgEt$		189, 192
	10.43	$(Ph_3P)(CO)_5TaHgEt$		192
Ta–Zn	**10.44**	$(C_5H_4Me)_2(H)_2TaZnCp$		210
	10.45	$(C_5H_4Me)_2(H)Ta(ZnCp)_2$	2.588 (2) 2.590 (2)	210
	10.46	$((C_5H_4Me)_2(H)_2Ta)_2Zn$		210
	10.47	$Cp_2Ta(ZnCp)_3$		210

[a] trias = $(Me_2AsC_6H_4)_2AsMe$.

However, unambiguous examples of direct metal–metal bonding have been described by Selegue and his coworkers. Reactions of $Ti(NMe_2)_4$ with $CpM(CO)_2H$ led to the complexes $(Me_2N)_3TiM(CO)_2Cp$ (M = Fe **10.4**, Ru **10.5**) [207,208] (Fig. 49). Ti–M bond distances of 2.568(1) and 2.663(1) Å were found for **10.4** and **10.5** respectively. The formation of the direct Ti–M bond rather than an isocarbonyl linkage was rationalized on the basis of both acidity and MO arguments.

A fourth approach to the synthesis of M–M′ bonds involves the use of reactive metal hydrides. The complexes $Cp_2(H)_2NbZnCp$ **10.28**, $Cp_2(H)Nb(ZnCp)_2$ **10.29**, $(Cp_2(H)_2Nb)_2Zn$ **10.30**, $(C_5H_4Me)_2(H)_2TaZnCp$ **10.44**, $(C_5H_4Me)_2(H)Ta(ZnCp)_2$ **10.45** and $(C_5H_4Me)_2(H)_2Ta)_2Zn$ **10.46**, as well as the species $Cp_2Ta(ZnCp)_3$ **10.47** have been prepared by reaction of Cp'_2MH_3 with Cp_2Zn in various stoichiometries [209,210]. Confirmation of the presence of M–Zn bonds was obtained via crystallographic studies of

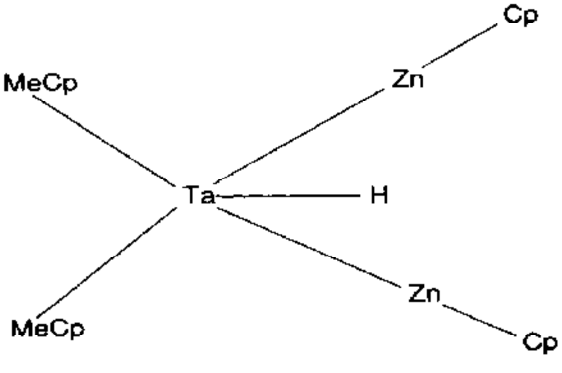

Fig. 50. Structure of **10.44**.

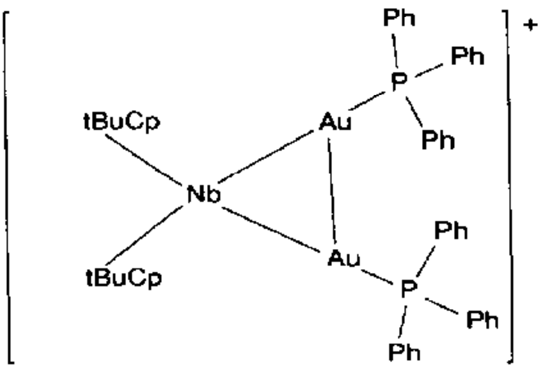

Fig. 51. Structure of **10.27**.

10.28 and **10.44** (Fig. 50). Ta–Zn distances of 2.588(2) and 2.590(2) Å were found in **10.44**, while the Nb–Zn bond length in **10.28** was 2.5407(7) Å. In either complex, the hydrides were considered to be terminal on the early metal with essentially no interaction with zinc.

The Nb–Hg complexes $Cp_2(H)Nb(HgL)_2$ (L = Cl **10.33**, Br **10.34**, I **10.35**, SEt **10.36**, $SCMe_3$ **10.37**) were prepared via reaction of HgL_2 and Cp_2NbH_3 [211]. Employing $Hg(S_2CNEt_2)_2$, trisubstitution was achieved to yield the species $Cp_2Nb(HgS_2CNEt_2)_3$ **10.38**. This tetrametallic compound contains three Nb–Hg bonds with a mean length of 2.790 Å.

Fajardo et al. [212] have reported the formation of $[(C_5H_4SiMe_3)_2Nb(AuPPh_3)_2]^+$ **10.27** via reaction of Cp'_2NbH_3 with $[Ph_3PAu][X]$ (X = ClO_4, PF_6). The crystal structure of **10.27** shows a triangle of metal atoms with Nb–Au bond lengths of 2.9098(8) and 2.9139(8) Å and an Au–Au distance of 2.7359(5) Å (Fig. 51).

11. CONCLUDING REMARKS

This review has described the progress made to date in the area of organometallic ELHB complexes. These studies have achieved several of the initial objectives. Synthetic routes to a variety of ELHB compounds have been established. The chemistry of such mixed-metal species exhibits the ability of Lewis acidic early metals to function with a late metal center in the cooperative activation of small-molecule substrates, in particular CO. Structural, spectroscopic and theoretical studies of ELHB complexes have investigated to some extent the nature and degree of direct electronic interactions between early and late metal centers. Such studies have implications for SMSI effects observed in heterogeneous systems. While much has been achieved, several objectives have yet to be addressed, and thus this area continues to be one of active interest to a number of research groups. The chemistry described herein is the ground work on which further developments will be made. Future studies will undoubtedly focus on the utilization of this chemistry for applications in homogeneous catalysis. The possibility of CO or CO_2 reduction chemistry is of particular interest. Further understanding of the effects of an early metal center on the chemistry of a proximate late metal will also enhance our understanding of heterogeneous catalytic systems.

REFERENCES

1 E.L. Muetterties, T.N. Rhodin, E. Band, C.F. Brucker and W.R. Pretzer, Chem. Rev., 79 (1979) 91.
2 E.L. Muetterties and M.J. Kause, Angew. Chem. Int. Ed. Engl., 22 (1983) 135.
3 W.L. Gladfelter and G.L. Geoffroy, Adv. Organomet. Chem., 18 (1980) 207.
4 M.I. Bruce, J. Organomet. Chem., 242 (1983) 147.
5 M.I. Bruce, J. Organomet. Chem., 283 (1985) 339.
6 D.A. Roberts and G.L. Geoffroy, in G. Wilkinson and F.G.A. Stone (Eds.), Comprehensive Organometallic Chemistry, Vol. 6, Pergamon, Oxford, 1982, Chapt. 40.
7 R.T. Baker, S.J. Tauster and J.A. Dumesic (Eds.), Strong Metal Support Interactions, American Chemical Society, Washington, D.C., 1986.
8 H.T. Evans and M.T. Pope, Inorg. Chem., 23 (1984) 501.
9 Y. Nada, M. Shimada and M. Koizumi, Inorg. Chem., 23 (1984) 629.
10 W.H. Knoth, P.J. Domaille and D.C. Roe, Inorg. Chem., 22 (1983) 198.
11 P.J. Domaille and W.H. Knoth, Inorg. Chem., 22 (1983) 818.
12 D.W. Murphy, J.L. Dye and S.M. Zahurak, Inorg. Chem., 22 (1983) 3679.
13 P.J. Domaille, J. Am. Chem. Soc., 106 (1984) 7677.
14 S.P. Harmalker, M.A. Leparulo and M.T. Pope, J. Am. Chem. Soc., 105 (1983) 4286.
15 V.W. Day, W.G. Klemperer and C. Schwartz, J. Am. Chem. Soc., 109 (1987) 6030.
16 T. Hughbanks, G. Rosenthal and J.D. Corbett, J. Am. Chem. Soc., 108 (1986) 8289.
17 P.J. Domaille and R.L. Harlow, J. Am. Chem. Soc., 108 (1986) 2108.
18 M.H. Alizadeh, S.P. Harmalker, Y. Teaneh, J. Martin Frere and M.T. Pope, J. Am. Chem. Soc., 107 (1985) 2662.
19 J.F.W. Keana and M.D. Organ, J. Am. Chem. Soc., 108 (1986) 7951.
20 R.G. Finke, B. Rapko and P.J. Domaille, Organometallics, 5 (1986) 175.
21 V.W. Day, W.G. Klemperer and D.J. Maltbie, Organometallics, 4 (1985) 104.
22 R.G. Finke and M.W. Droege, J. Am. Chem. Soc., 106 (1984) 7274.
23 C.J. Besecker, V.W. Day, W.G. Klemperer and M.R. Thompson, J. Am. Chem. Soc., 106 (1985) 4125.
24 C.J. Besecker, V.W. Day, W.G. Klemperer and M.R. Thompson, Inorg. Chem., 24 (1985) 44.
25 J.F.W. Keana, M.D. Organ, Y. Lu, M. Beer and J. Varkey, J. Am. Chem. Soc., 107 (1985) 6714.
26 V.W. Day, C.W. Earley, W.G. Klemperer and D.J. Maltbie, J. Am. Chem. Soc., 107 (1985) 8261.
27 J.F.W. Keana, M.D. Organ, Y. Lu, M. Beer and J. Varkey, J. Am. Chem. Soc., 108 (1986) 7957.
28 T. Hughbanks, G. Rosenthal and J.D. Corbett, J. Am. Chem. Soc., 110 (1988) 1511.
29 V.W. Day, M.F. Fredrich and M.R. Thompson, J. Am. Chem. Soc., 103 (1981) 3597.

30 S.A. Sunshine and J.A. Ibers, Inorg. Chem., 24 (1985) 3611.

31 D.A. Keszler, P.J. Squattrito, N.E. Brese, J.A. Ibers, S. Maoytt and L. Tiaxi, Inorg. Chem., 24 (1985) 3063.

32 D.A. Keszler and J.A. Ibers, J. Am. Chem. Soc., 107 (1985) 8119.

33 P.J. Squattrito, P.N. Swepston and J.A. Ibers, Inorg. Chem., 26 (1986) 1187.

34 E. Canadell and M.H. Wangbo, Inorg. Chem., 26 (1987) 3974.

35 S.J. Heyes, N.J. Clayden, C.M. Dobson, M.L.H. Green and P.J. Wiseman, J. Chem. Soc., Chem. Commun., (1987) 1560.

36 C.H. Yang and V.L. Goedken, Inorg. Chim. Acta, 117 (1986) L19.

37 Y. Do, E.D. Simhom and R.H. Holm, J. Am. Chem. Soc., 105 (1983) 6731.

38 Y. Do, E.D. Simhom and R.H. Holm, Inorg. Chem., 24 (1985) 4635.

39 J.A. Kovacs and R.H. Holm, J. Am. Chem. Soc., 108 (1986) 340.

40 J.A. Kovacs and R.H. Holm, Inorg. Chem., 26 (1987) 711.

41 M.J. Carney, J.A. Kovacs, Y.P. Zhang, G.C. Papaefthymiou, K. Spartalian, R.B. Frankel and R.H. Holm, Inorg. Chem., 26 (1987) 719.

42 J.A. Kovacs and R.H. Holm, Inorg.Chem., 26 (1987) 702.

43 C.D. Scattergood, P.G. Bonney, J.M. Slater, C.D. Garner and W. Clegg, J. Chem. Soc., Chem. Commun., 23 (1987) 1749.

44 G. Schmid, V. Batzel and B. Stutte, J. Organomet. Chem., 113 (1976) 67.

45 C. Moise, J.F. Reynoud, J.C. Leblanc and R. Broussier, J. Organomet. Chem., 240 (1982) C15.

46 J. Martin and C. Moise, J. Organomet. Chem., 232 (1982) C55.

47 B. Stutte, V. Batzel, R. Boese and G. Schmid, Chem. Ber., 111 (1978) 1603.

48 G. Schmid, B. Stutte and R. Boese, Chem. Ber., 111 (1978) 1239.

49 S. Gambarotta, S. Stella, C. Floriani, A. Chiesi-Villa and C. Guastini, Angew. Chem., Int. Ed. Engl., 25 (1986) 254.

50 K.S. Wong, R. Scheidt and J.A. Labinger, Inorg. Chem., 18 (1979) 1709.

51 A.A. Pasynskii, A.S. Antsyshkina, Yu.V. Skripkin, V.T. Kalinnikov, M.A. Porai-Koshits, V.N. Ostrikova and G.G. Sadikov, Russ. J. Inorg. Chem., 26 (1981) 1310.

52 A.A. Pasynskii, Yu.V. Skripkin, I.L. Eremenko, V.T. Kalinnikov, G.G. Aleksandrov, V.G. Andrianov and Y.T. Struchkov, J. Organomet. Chem., 165 (1979) 49.

53 D.M. Hamilton, Jr., W.S. Willis and G.D. Stucky, J. Am. Chem. Soc., 103 (1981) 4255.

54 E.J.M. DeBoer and J. DeWith, J. Organomet. Chem., 320 (1987) 289.

55 J.S. Merola, R.A. Gentile, G.B. Ansell, M.A. Modrick and S. Zentz, Organometallics, 1 (1982) 1731.

56 J.S. Merola, K.S. Campo, R.A. Gentile, M.A. Modrick and S. Zentz, Organometallics, 3 (1984) 334.

57 W.J. Sartain and J.P. Selegue, Organometallics, 3 (1984) 1922.

58 E.J.M. DeBoer, J. DeWith and A.G. Orpen, J. Chem. Soc., Chem. Commun., (1985) 1666.

59 P. Renaut, G. Tainturier and B. Gautheron, J. Organomet. Chem., 150 (1976) C9.

60 B. Longato, J.R. Norton, J.C. Huffman, J.A. Marsella and K.G. Caulton, J. Am. Chem. Soc., 103 (1981) 209.

61 B. Longato, B.D. Martin, J.R. Norton and O.P. Anderson, Inorg. Chem., 24 (1985) 1389.

62 J.A. Marsella, J.C. Huffman, K.G. Caulton, B. Longato and J.R. Norton, J. Am. Chem. Soc., 104 (1982) 6360.

63 B.D. Martin, S.A. Matchehett, J.R. Norton and O.P. Anderson, J. Am. Chem. Soc., 105 (1985) 7952.

64 P.T. Barger and J.E. Bercaw, J. Organomet. Chem., 201 (1980) C39.

65 P.T. Barger and J.E. Bercaw, Organometallics, 3 (1984) 278.
66 D.H. Berry and J.E. Bercaw, J. Am. Chem. Soc., 104 (1982) 4712.
67 E.O. Fischer and S. Fontano, J. Organomet. Chem., 40 (1972) 159.
68 H.G. Raubenheimer and E.O. Fischer, J. Organomet. Chem., 91 (1975) C23.
69 W. Petz, J. Organomet. Chem., 72 (1974) 369.
70 G. Erker, U. Dorf, R. Benn, R.D. Rhienhardt and J.L. Petersen, J. Am. Chem. Soc., 106 (1984) 7649.
71 G. Erker and R. Lecht, J. Am. Chem. Soc., 311 (1986) 45.
72 G. Erker and R. Lecht, J. Organomet. Chem., 326 (1987) C75.
73 G. Erker, R. Lecht, J.L. Petersen and H. Bonnemann, Organometallics, 6 (1987) 1962.
74 G. Erker, U. Dorf, R. Mynott, Y.B. Tsay and C. Kruger, Angew. Chem., Int. Ed. Engl., 24 (1985) 584.
75 G. Erker, U. Dorf, C. Kruger and Y.H. Tsay, J. Am. Chem. Soc., 6 (1987) 680.
76 K. Mashima, K. Jyodoi, A. Ohyoshi and H. Takaya, J. Am. Chem. Soc., Chem. Commun., (1986) 1145.
77 C.P. Casey, R.E. Palermo and A.L. Rheingold, J. Am. Chem. Soc., 108 (1986) 549.
78 P.T. Wolczanski, R.S. Threlkel and J.E. Bercaw, J. Am. Chem. Soc., 101 (1979) 218.
79 J.A. Marsella and K.G. Caulton, J. Am. Chem. Soc., 102 (1980) 1747.
80 J.A. Marsella, K. Folting, J.C. Huffman and K.G. Caulton, J. Am. Chem. Soc., 103 (1981) 5596.
81 S.C.H. Ho, D.A. Strauss, J. Armantrout, W.P. Schaefer and R.H. Grubbs, J. Am. Chem. Soc., 106 (1984) 2210.
82 I. Weinstock, C. Floriani, A. Chiesi-Villa and C. Guastini, J. Am. Chem. Soc., 108 (1986) 8298.
83 C.T. Tso and A.R. Cutler, J. Am. Chem. Soc., 108 (1986) 6069.
84 J. Amaudrut, J. Sala-Pala, J. Guerchais, R. Mercier and J. Douglade, J. Organomet. Chem., 235 (1982) 301.
85 J.H. Wengrovius and R.R. Schrock, Organometallics, 1 (1982) 148.
86 G.M. Dawkins, M. Green, K.A. Mead, J.Y. Salaun, F.G.A. Stone and P. Woodward, J. Chem. Soc. D, (1983) 527.
87 U. Behrens and F.G.A. Stone, J. Chem. Soc. D, (1984) 1605.
88 M.R. Awang, R.D. Barr, M. Green, J.A.K. Howard, T.B. Marder and F.G.A. Stone, J. Chem. Soc. D, (1985) 2009.
89 R.D. Barr, M. Green, J.A.K. Howard, T.B. Marder, I. Moore and F.G.A. Stone, J. Chem. Soc., Chem. Commun., (1983) 746.
90 A.W. Gal and H.J. Van der Heijden, J. Chem. Soc., Chem. Commun., (1983) 420.
91 H.J. Van der Heijden, A.W. Gall and P. Pasman, Organometallics, 4 (1985) 1847.
92 P.B. Mackenzie, K.C. Ott and R.H. Grubbs, Pure Appl. Chem., 56 (1984) 59.
93 J.W. Park, P.B. Mackenzie, W.P. Schaefer and R.H. Grubbs, J. Am. Chem. Soc., 108 (1986) 6402.
94 J.A. Labinger, K.S. Wong and W.R. Scheidt, J. Am. Chem. Soc., 100 (1978) 3254.
95 K.S. Wong, W.R. Scheidt and J.A. Labinger, Inorg. Chem., 18 (1979) 136.
96 Y.V. Skripkin, A.A. Pasynskii, V.T. Kalinnikov, M.A. Porai-Koshits, L.K. Minacheva, A.S. Antsyshkina and V.N. Ostrikova, J. Organomet. Chem., 231 (1982) 205.
97 K.S. Wong and J.A. Labinger, J. Am. Chem. Soc., 102 (1980) 3652.
98 B. Balbach, S. Baral, H. Biersack, W.A. Herrmann, J.A. Labinger, W.R. Scheidt, F.J. Timmers and M.L. Ziegler, Organometallics, 7 (1988) 325.
99 S. Baral, J.A. Labinger, W.R. Scheidt and F.J. Timmers, J. Organomet. Chem., 215 (1981) C53.

100 F.J. Timmers, W.R. Scheidt, J.A. Labinger and S. Baral, J. Organomet. Chem., 240 (1982) 153.
101 J.F. Reynoud, J.C. Leblanc and C. Moise, J. Organomet. Chem., 296 (1985) 377.
102 P. Oltmanns and D. Rehder, J. Organomet. Chem., 345 (1988) 87.
103 F.N. Tebbe, J. Am. Chem. Soc., 95 (1973) 5412.
104 A.A. Porai-Koshits, A.S. Antsyshkina, A.A. Pasynskii, G.G. Sadikov, Y.V. Skripkin and A.N. Ostrikova, Inorg. Chim. Acta, 34 (1979) L285.
105 R.L. Bansemer, J.C. Huffman and K.G. Caulton, J. Am. Chem. Soc., 105 (1983) 6163.
106 J.W. Bruno, J.C. Huffman, M.A. Green and K.G. Caulton, J. Am. Chem. Soc., 106 (1984) 8310.
107 C.G. Vonk, J. Cryst. Mol. Struct., 3 (1973) 201.
108 D.G. Sekutowski and G. Stucky, Inorg. Chem., 14 (1975) 2192.
109 H.A. Martin and F. Jellinek, J. Organomet. Chem., 8 (1967) 115.
110 R. Jungst, D. Sekutowski and G. Stucky, J. Am. Chem. Soc., 96 (1974) 8108.
111 D. Sekutowski, R. Jungst and G. Stucky, Inorg. Chem., 17 (1978) 1848.
112 D. Gourier, D. Vivien and E. Samuel, J. Am. Chem. Soc., 107 (1985) 7418.
113 P.D. Smith, J.L. Martin, J.C. Huffman, R.L. Bansemer and K.G. Caulton, Inorg. Chem., 24 (1985) 2997.
114 G. Johannsen and O. Stelzer, Chem. Ber., 110 (1977) 3448.
115 O. Stelzer, E. Unger and V. Wray, Chem. Ber., 110 (1977) 3430.
116 D.C. Bradley and A.S. Kasenally, J. Chem. Soc., Chem. Commun., (1968) 1430.
117 T.S. Targos, R.P. Rosen, R.R. Whittle and G.L. Geoffroy, Inorg. Chem., 24 (1985) 1375.
118 R.T. Baker, T.H. Tulip and S.S. Wreford, Inorg. Chem., 24 (1985) 1379.
119 L. Gelmini, L.C. Matassa and D.W. Stephan, Inorg. Chem., 24 (1985) 2585.
120 M.G.B. Drew, S.R. Wade, M.G.H. Wailbridge and G.R. Willey, J. Chem. Soc. D., (1986) 714.
121 D.W. Stephan and P.Y. Zheng, unpublished results, 1988.
122 R.T. Baker and T.H. Tulip, Organometallics, 5 (1986) 839.
123 L. Gelmini and D.W. Stephan, Inorg. Chim. Acta, 111 (1986) L17.
124 L. Gelmini and D.W. Stephan, Inorg. Chem., 25 (1986) 1222.
125 R.T. Baker, personal communication, 1987.
126 L. Gelmini and D.W. Stephan, unpublished results, 126.
127 L. Gelmini and D.W. Stephan, Organometallics, 7 (1988) 849.
128 J.M. Ritchey, A.J. Zozulin, D.A. Wrobleski, R.R. Ryan, H.J. Wasserman, D.C. Moody and R.T. Paine, J. Am. Chem. Soc., 107 (1985) 501.
129 J.N. Ortiz, J. Am. Chem. Soc., 108 (1986) 550.
130 P.J. Hay, R.R. Ryan, K.V. Salazar, D.A. Wrobleski and A.P. Sattelberger, J. Am. Chem. Soc., 108 (1986) 313.
131 K.K. Joshi, R. Wardle and V.A. Wilson, Inorg. Nucl. Chem. Lett., 6 (1970) 49.
132 H. Kopf and K.H. Rathlein, Angew. Chem., Int. Ed. Engl., 8 (1969) 980.
133 P.S. Braterman, V.A. Wilson and K.K. Joshi, J. Chem. Soc. A, (1971) 191.
134 C.J. Ruffing and T.B. Rauchfuss, Organometallics, 4 (1985) 524.
135 T.S. Cameron, C.K. Prout, G.V. Rees, M.L.H. Green, K.K. Joshi, G.R. Davies and B.T. Kilbourn, J. Chem. Soc., Chem. Commun., (1971) 14.
136 P.S. Braterman, V.A. Wilson and K.K. Joshi, J. Organomet. Chem., 31 (1971) 123.
137 G.R. Davies and B.T. Kilbourn, J. Chem. Soc. A, (1971) 87.
138 J.C. Kotz, W. Vining, W. Coco, R. Rosen, A.R. Dias and M.H. Garcia, Organometallics, 2 (1983) 68.
139 W.E. Douglas and M.L.H. Green, J. Chem. Soc. D, (1972) 1796.

140 W.E. Douglas, M.L.H. Green, C.K. Prout and G.V. Rees, J. Chem. Soc., Chem. Commun., (1971) 896.
141 K. Prout, S.R. Critchley and G.V. Rees, Acta Crystallogr., Sect. B., 30 (1974) 2305.
142 J.C. Daran, B. Meunier and K. Prout, Acta Crystallogr., Sect. B, 35 (1979) 1709.
143 M. Sato and T. Yoshida, J. Organomet. Chem., 94 (1975) 403.
144 H. Werner, B. Ulrich, U. Schubert, P. Hofmann and B. Zimmer-gasser, J. Organomet. Chem., 297 (1985) 27.
145 P.S. Braterman and V.A. Wilson, J. Organomet. Chem., 31 (1971) 131.
146 G.S. White and D.W. Stephan, Inorg. Chem., 24 (1985) 1499.
147 T.A. Wark and D.W. Stephan, Inorg. Chem., 26 (1987) 363.
148 T.A. Wark and D.W. Stephan, unpublished results, 1988.
149 G.S. White and D.W. Stephan, Organometallics, 6 (1987) 2169.
150 G.S. White and D.W. Stephan, Organometallics, 7 (1988) 903.
151 G.S. White, T.A. Wark, D.W. Stephan and J.S. Tse, unpublished results, 1988.
152 A. Muller and E. Diemann (Eds.), Transition Metal Chemistry, Verlag Chemie, Weinheim, 1981.
153 C.M. Bolinger, T.B. Rauchfuss and S.R. Wilson, J. Am. Chem. Soc., 104 (1982) 7313.
154 C.M. Bolinger, T.D. Weatherill, T.B. Rauchfuss, A.L. Rheingold, C.S. Day and S.R. Wilson, Inorg. Chem., 25 (1986) 634.
155 T.B. Rauchfuss, T.D. Weatherill, S.R. Wilson and J.P. Zebrowski, J. Am. Chem. Soc., 105 (1983) 6508.
156 C.M. Bolinger, T.B. Rauchfuss and S.R. Wilson, J. Am. Chem. Soc., 106 (1984) 7800.
157 E.N. Jacobsen, M.K. Trost and R.C. Bergman, J. Am. Chem. Soc., 108 (1986) 8092.
158 H. Burger and C. Kluess, J. Organomet. Chem., 56 (1973) 269.
159 H. Burger and C. Kluess, Z. Anorg. Allg. Chem., 423 (1976) 112.
160 G.A. Razuvaev, G.A. Domrachev, V.V. Sharutin and O.N. Suvorova, J. Organomet. Chem., 141 (1977) 313.
161 U. Thewalt and D. Schomberg, Z. Naturforsch., Teil B, 30 (1975) 636.
162 A.G. Osborne and R.H. Whiteley, J. Organomet. Chem., 181 (1979) 425.
163 A.A. Pasynskii, Y.V. Skripkin, V.T. Kalinnikov, M.A. Porai-Koshits, A.S. Antsyshkina, G.G. Sadikov and V.N. Ostrikova, J. Organomet. Chem., 201 (1980) 269.
164 R.J. Doroda, G. Wilkinson, M.B. Hursthouse, K.M.A. Malik and M. Thornton-Pett, J. Chem. Soc. D, (1980) 2315.
165 C.P. Casey, R.E. Palermo, R.F. Jordan and A.L. Rheingold, J. Am. Chem. Soc., 107 (1985) 4597.
166 N.E. Schore, J. Am. Chem. Soc., 101 (1979) 7410.
167 D.R. Tueting, S.R. Iyer and N.E. Schore, J. Organomet. Chem., 320 (1987) 349.
168 J.C. Leblanc, C. Moise, A. Maisonnat, R. Poilblanc, C. Charrier and F. Mathey, J. Organomet. Chem., 231 (1982) C43.
169 M.D. Rausch, B.H. Edwards, R.D. Rogers and J.L. Atwood, J. Am. Chem. Soc., 105 (1983) 3882.
170 C.P. Casey and F. Nief, Organometallics, 4 (1985) 1219.
171 W. Tikkanen, Y. Fujita and J.L. Petersen, Organometallics, 5 (1986) 888.
172 B. Demerseman, P.H. Dixneuf, J. Douglade, R. Mercier, Inorg. Chem., 21 (1982) 3942.
173 B. Gautheron and G. Tainturier, J. Organomet. Chem., 262 (1984) C30.
174 N.E. Schore, S.J. Young, M.M. Olmstead and P. Hofmann, Organometallics, 2 (1983) 1769.
175 N.E. Schore and H. Hope, J. Am. Chem. Soc., 102 (1980) 4251.
176 R. Choukroun and D. Gervais, J. Organomet. Chem., 266 (1984) C37.

177 R. Choukroun and D. Gervais, J. Chem. Soc., Chem. Commun., (1982) 1300.

178 F. Senocq, M. Basso-Bert, R. Choukroun and D. Gervais, J. Organomet. Chem., 297 (1985) 155.

179 M. Etienne, R. Choukroun, M. Basso-Bert, F. Dahan, and D. Gervais, Nouveau J. Chim., 8 (1984) 531.

180 H.H. Karsch, G. Muller and C. Kruger, J. Organomet. Chem., 273 (1984) 195.

181 R. Choukroun, A. Iraqi and D. Gervais, J. Organomet. Chem., 311 (1986) C60.

182 R. Choukroun, A. Iraqi, D. Gervais, J.C. Daran and Y. Jeannin, Organometallics, 6 (1987) 1197.

183 F. Senocq, C. Randrianlimanana, A. Thorez, P. Kalck, R. Choukroun and D. Gervais, J. Chem. Soc., Chem. Commun., (1984) 1376.

184 R. Choukroun, D. Gervais, J. Jaud, P. Kalck and F. Senocq, Organometallics, 5 (1986) 67.

185 F. Senocq, C. Randrianlimanana, A. Thorez and P. Kalck, J. Mol. Catal., 35 (1986) 213.

186 M. Etienne, R. Choukroun and D. Gervais, J. Chem. Soc. D, (1984) 915.

187 G.S. Ferguson and P.T. Wolczanski, Organometallics, 4 (1985) 1601.

188 G.S. Ferguson and P.T. Wolczanski, J. Am. Chem. Soc., 108 (1986) 8293.

189 K.A. Keblys and M. Dubeck, Inorg. Chem., 3 (1964) 1646.

190 A.S. Kasenally, R.S. Nyholm, R.J. O'Brien and M.H.B. Stiddard, Nature, 204 (1964) 871.

191 A. Davison and J.E. Ellis, J. Organomet. Chem., 23 (1970) 1.

192 A. Davison and J.E. Ellis, J. Organomet. Chem., 36 (1972) 113.

193 E. Talay and D. Rehder, J. Organomet. Chem., 262 (1984) 25.

194 M.G.B. Drew, Acta Crystallogr. Sect. B, 38 (1982) 254.

195 I.P.F. Naumann and D. Rehder, J. Organomet. Chem., 258 (1983) 189.

196 G. Doyle and K.A. Erikson, Organometallics, 4 (1985) 2201.

197 J.E. Ellis, J. Am. Chem. Soc., 103 (1981) 6106.

198 B.E. Kelsey and J.E. Ellis, J. Chem. Soc., Chem. Commun., 1521 (1986) 331.

199 M.F. Lappert and A.R. Sanger, J. Chem. Soc. A, (1971) 1314.

200 J. Abys and W.M. Risen, Jr., J. Organomet. Chem., 204 (1981) C5.

201 C.P. Casey, R.F. Jordan and A.L. Rheingold, Organometallics, 3 (1984) 504.

202 C.P. Casey, R.F. Jordan and A.L. Rheingold, J. Am. Chem. Soc., 105 (1983) 665.

203 B.E. Bursten and K.J. Novo-Gradac, J. Am. Chem. Soc., 109 (1987) 904.

204 A. Miyake, H. Kondo and M. Aoyama, Angew. Chem., Int. Ed. Engl., 8 (1969) 520.

205 Jpn. Patent, 32 (1969) 773.

206 D.J. Cardin, S.A. Keppie and M.F. Lappert, J. Chem. Soc. A, (1970) 2594.

207 W.J. Sartain and J.P. Selegue, J. Am. Chem. Soc., 107 (1985) 5818.

208 W.J. Sartain and J.P. Selegue, Organometallics, 6 (1987) 1812.

209 P.H.M. Budzelaar, K.H. den Haan, J. Boersma, G.J.M. van der Kerk and A.L. Spek, Organometallics, 3 (1984) 156.

210 P.H.M. Budzelaar, A.A.H. van der Zeijden, J. Boersma, G.J.M. van der Kerk, A.L. Spek and A.J.M. Duisenberg, Organometallics, 3 (1984) 159.

211 R. Kergoat, M.M. Kubicki, J.E. Guerchais, N.C. Norman and A.G. Orpen, J. Chem. Soc. D, (1982) 633.

212 M. Fajardo, M.P. Gomez-Sal, P. Royo, S.M. Carrera and S.G. Blanco, J. Organomet. Chem., 312 (1986) C44.